COMPARTMENTALIZATION AND OVERPRESSURING OF THE OLIGOCENE VICKSBURG SANDSTONE, TCB FIELD, KLEBERG COUNTY, TEXAS

By

PHEBE MARIE DEYHIM

Bachelor of Science in Arts and Science

Oklahoma State University

Stillwater, Oklahoma

1997

Submitted to the Faculty of the
Graduate College of the
Oklahoma State University
in partial fulfillment of
the requirements for
the Degree of
MASTER OF SCIENCE
December, 2000

COMPARTMENTALIZATION AND OVERPRESSURING

OF THE OLIGOCENE VICKSBURG

SANDSTONE, TCB FIELD,

KLEBERG COUNTY,

TEXAS

Thesis Approved:

Zuhair al-Shaieb

Thesis Adviser

Darwin Boardman

Robin Gomez

Dean of the Graduate College

ACKNOWLEDGMENTS

I would like to express sincere appreciation to my thesis advisor, Dr. Al, for his support, guidance and most of all his friendship. His has been a great inspiration throughout this study and my graduate career. In addition, his assistance and direction in the completion of this research has been invaluable. I wish to thank my advisory committee, Dr. Ibrahim Cemen and Dr. Darwin Boardman, for suggestions and advice during the preparation of this thesis.

I would like to acknowledge the Gas Research Institute for funding this research. I am very appreciative to Kerr-McGee Corporation and in particular Paul Chandler, for the help and support in providing cores, well-logs, seismic and other information pertinent to this study. I would like to thank James Howard and Phillips Petroleum for graciously measuring capillary pressure. Greg Flournoy and John Hubbard from Schlumberger are appreciated for their technical advice and supplying FMI digital data. Special thanks are extend to Heinz Hall for taking the core photographs and Dr. James Puckette for all his work for the Gas Research Institute study on the Vicksburg.

I would like to thank my fellow graduate students, Jason Nord, Amy Close and Li Han for their advice and support. Finally, I wish like to thank my parents and husband for their continued support throughout my education.

TABLE OF CONTENTS

Chapter Page

LIST OF FIGURES

Figure Page

Figure Page

Figure Page

CHAPTER I

INTRODUCTION

General Statement

Characterization of compartmentalized natural gas reservoirs in the Vicksburg Formation is the primary objective of this study. The overpressured low-contrast/low resistivity (LR/LC) reservoirs were often bypassed because their detection and evaluation were difficult with existing wire-line logging technology. The difficulty of identifying reservoir and seal facies is further compounded in LR/LC intervals. These intervals are becoming increasingly important exploration targets in mature basins.

This analysis of low-contrast Gulf Coast reservoirs focuses on a comprehensive and integrated evaluation of "shaly" intervals in the Oligocene Vicksburg Formation. These intervals are problematic to operators in that their suppressed wire-line log signatures make net-pay and water saturation calculations difficult to obtain. Furthermore, these "shaly" reservoirs may have unpredictable productivity and recoverable reserves and even recognition where production is coming from within the borehole. These problems are expanded by a lack of rock data. As an example, the primary productive low-contrast reservoir in the study area was only recently cored and is not described in the literature.

Improved reservoir characterization and petrophysical evaluation are dependent on understanding rock properties. This comprehension is essential for predicting the interactions between reservoir rocks and petrophysical. It provides the foundation for the series of studies related to the development of improved evaluation techniques for these complex reservoirs.

The 9900-ft sandstone of the Vicksburg Formation was selected for this investigation. It is composed of thinly bedded and interlaminated sandstone and shale and is considered as an example of a low resistivity/low-contrast (LR/LC) sandstone reservoir. Conventional wire-line signatures are usually suppressed, and therefore their utilization as interpretation tools becomes less effective. Reserve calculations and economic evaluation are usually based on net-pay calculations derived from wire-line log measurements. In many instances, wire-line logs are the only tool available to perform this essential task. The availability of high-resolution resistivity and porosity tools and formation micro-imaging logs has greatly improved interpretation of these rocks.

The cores used in this project were calibrated to high resolution and micro-imaging logs. Micro imaging is used to identify sedimentary bedding and diagenetic banding less than one inch thick. Chromatic variations which reflect resistivities of the formation can be attributed to changes of lithofacies and diagenetic patterns. Accurate measuring of the relative thickness of cemented and porous beds in LR/LC zones can improve net-reservoir/net pay calculations and economic evaluation.

In addition to formation micro-imaging, various methods and techniques were used in the identification and characterization of compartments and seals. They are fluid

inclusion stratigraphy (FIS), formation pressure data, and capillary pressure measurements. The emphasis on characterization processes was two fold:

a. To examine the spatial relationship between reservoir and seal intervals within overpressured compartments, and

b. To provide a specific petrophysical and capillary pressure sealing capacity parameter for intra-compartment seals.

Objectives

The primary objective of this study is to provide a detailed petrographic analysis of the Vicksburg Sandstone in the TCB field from the subsurface of Texas. More specifically, the 9900-ft sandstone was of interest to the operators in the field since it had not been studied. This zone is unpredictable since it is very difficult to interpret using conventional petrophysical techniques and its production characteristics and reserve estimates are difficult to estimate. The primary objectives of this investigation are:

1) Examination of cores, wire-line logs, maps and cross sections pertaining to the Vicksburg reservoirs.
2) Detailed core descriptions including lithology, grain size, sedimentary structures, constituents, porosity, and bedding contacts.
3) Correlation high-resolution resistivity images to core for determination of specific features.
4) Preparation of thin sections, x-ray diffraction analyses, and examination of selected samples with the SEM.
5) Characterization of porosity types and quantities

6) Describe the composition and occurrence of cements and their relative timing to porosity reduction and/or enhancement.

7) Verification of seal intervals using log signature and FMI (Formation Micro-Imaging)

Study Area

A LR/LC gas-producing interval was examined in the TCB field in Kleberg County, Texas (Figure 1). This interval was chosen because of data availability and its economic significance. TCB field has produced in excess of 172 billion cubic feet (BCF) gas and 4 million barrels of liquids (MBL) from the Vicksburg formation since 1942 (Petroleum Information/Dwights, 1999; International Oil Scouts Association, 1997; and Taylor and Al-Shaieb, 1986). LR/LC Vicksburg reservoirs within TCB field had a cumulative production in excess of 20.4 BCF and 451 thousand barrels of liquids, before field consolidation in 1993 (P.I./Dwights and Int. Oil Scouts Assoc.). TCB field is part of the greater Vicksburg trend (Figure 2) that has a cumulative production of over 5.0 trillion cubic feet (TCF) gas and 320 MBL (Combes, 1993). LR/LC reservoirs are a significant contributor to this production and are becoming increasingly important as exploration targets. As a result of the difficulty interpreting these economically important reservoirs, Oryx Energy Company provided various data including cores, wire-line logs, and core analyses of the LR/LC "9900-ft" sandstone for this study. While this study focuses on the TCB field, the results may improve evaluation strategies of LR/LC reservoirs along the Vicksburg trend and elsewhere.

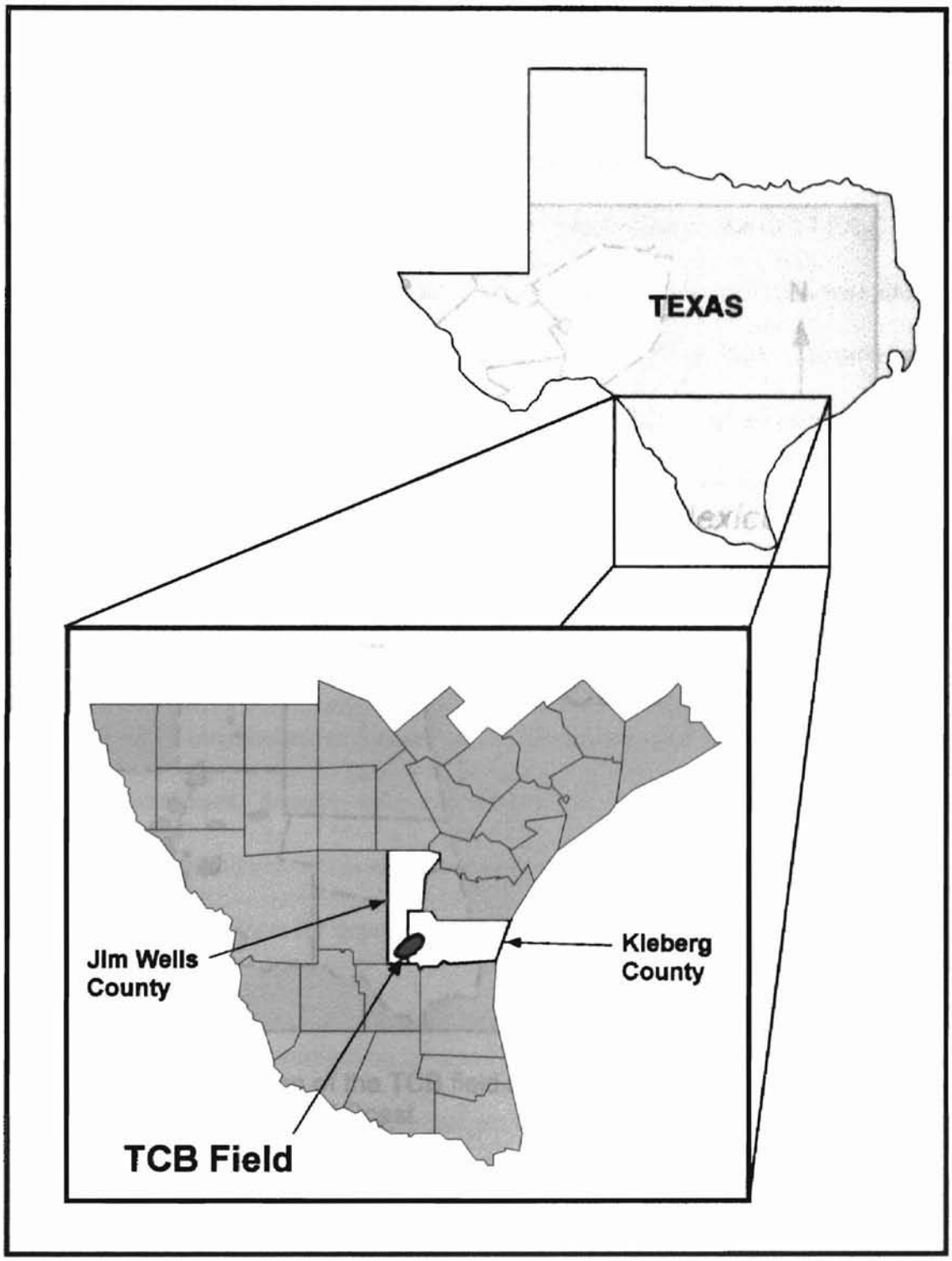

Figure 1. Location of TCB Field in Kleberg and Jim Wells Counties, Texas.

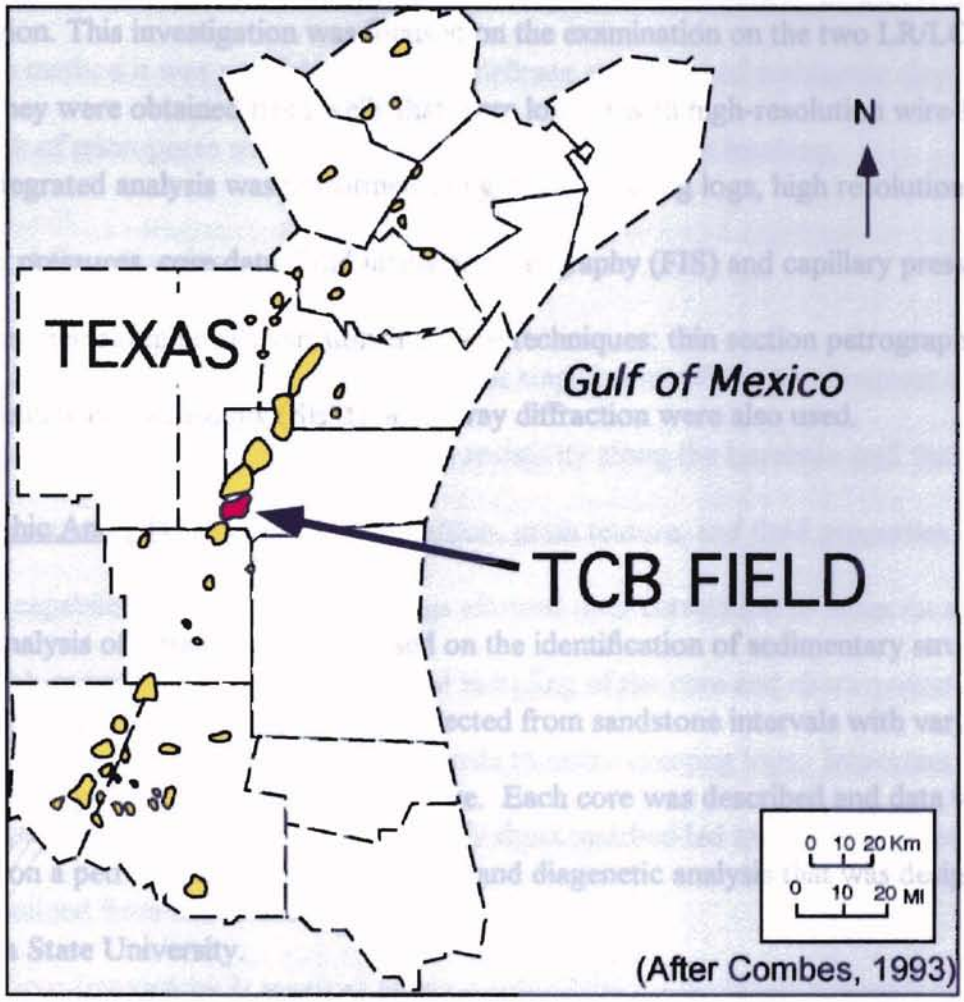

Figure 2. Location of the TCB field and Vicksburg production trend, Texas Gulf Coast.

Methods of Investigation

Two cores provided by Kerr-McGee from the Vicksburg sandstone located in the T.C.B. field were examined. A literature search regarding the geology of the Gulf Coast was conducted to provide information regarding the tectonic and depositional framework of the region. This investigation was focused on the examination on the two LR/LC cores because they were obtained from wells that were logged with high-resolution wire-line tools. Integrated analysis was performed using micro-imaging logs, high resolution logs, formation pressures, core data, fluid inclusion stratigraphy (FIS) and capillary pressures. In addition, petrographic analysis utilizing these techniques: thin section petrography, scanning electron microscopy (SEM), and x-ray diffraction were also used.

Petrographic Analysis

Analysis of obtained cores focused on the identification of sedimentary structures, textures, and lithofacies. Samples were selected from sandstone intervals with varying porosities and permeabilities within each core. Each core was described and data were recorded on a petrolog form for depositional and diagenetic analysis that was designed at Oklahoma State University.

The petrographic investigation involved the examination of 27 thin sections under the polarizing microscope. Thin section analysis concentrated on the identification and characterization of detrital constituents, diagenetic imprints and porosity. Each sample was impregnated with blue epoxy to assist in the identification of porosity. Quantitative

measurements of the petrofabric were obtained through point-counting (10 points per sample).

Samples were prepared for x-ray diffraction for mineralogic and petrographic description. Scanning electron microscopy was used to determine the fabrics and clay minerals, as well as secondary porosity features not visible in petrographic thin sections. Using this method it was possible to observe delicate structures of authigenic clays, framework of micropores and abundance of grain dissolution or leaching.

Formation Micro-Imaging

Micro–imaging tool is designed to focus small beams of electrical current into subsurface formation to measure changes in resistivity along the borehole wall that coincide to subtle changes in rock composition, grain texture, and fluid properties. The resolving capabilities of micro-imaging logs allowed their correlation to cores on an inch scale. High-accuracy correlation facilitated sampling of the core and characterization of the rocks representing various chromatic bands to micro-imaging logs. Important information needed to understand and identify these interbedded and laminated reservoirs can be obtained from this instrument.

Micro-imaging tools measure micro-conductivity using closely spaced button electrodes mounted on pads. Each pad contains 24 sensor electrodes, resulting in measurement resolution of 0.2 to 0.3 inches. These tools typically have 6-8 articulating pads mounted on independent arms. This design allows relatively free movement to improve electrode to formation contact (Halliburton, 1997 and Schlumberger, 1992). Like other micro-resistivity tools, micro-imaging tools are designed to be run in

conductive, water based mud. The depth of investigation for micro-imaging tools is up to 30 inches. When used as dipmeters or high-resolution tools for sedimentological, vug, or fracture analysis, their normal investigation depths are typically a few inches. This shallow depth of investigation limits the resistivity measurements to the flushed zone (Rxo). As a result, formation fluids have minor affect micro-imaging tools and the recorded resistivity measurements reflect only rock properties. Variations in current recorded by micro-imaging tools are converted to synthetic color images. Dark colors reflect high micro-conductivity (low resistivity), while light colors reflect low micro-conductivity (high resistivity) zones.

Most micro-images are viewed in two forms, static and dynamic. The static view has a fixed resistivity scale over the logged interval so that beds with the same color shade have the same resistivity. The dynamic view presentation uses a sliding resistivity scale that is applied at 1-ft intervals. This view enhances the visibility of small details by maximizing the contrast between features. The static view allows the comparison of resistivity over depth. When these resistivity values are core-calibrated, the micro-imager becomes a powerful tool for estimating rock properties.

Pressure Data

Pressure data obtained from scout tickets were used to calculate pressure gradients within the study area. These sources include calculated pressure data from initial well-head shut-in pressures, wire-line bottom hole pressure tests, wire-line formation tests and repeat formation tests.

Fluid Inclusion Stratigraphy

Fluid inclusion stratigraphy involves the complete analysis of volatiles trapped in fluid inclusions using a quadrapole mass spectrometer. Samples of rock cuttings were obtained and sorted into appropriate bottles. Cleaned samples are loaded, together with appropriate standards, into 630-hole trays, covered with a metal impact slug and placed into a vacuum oven at an elevated temperature. This is done to remove remaining adsorbed organic and inorganic volatile material up to C_{13}. Sample trays are then placed into an ultra-high vacuum chamber and evacuated for approximately 8 hours. Bulk fluid inclusion volatiles are afterwards instantaneously released from each sample in a sequential manner by automated mechanical crushing. Volatile organic and inorganic species are dynamically pumped through four quadrupale mass analyzers where molecular species are ionized by electron bombardment. The species are then separated according to their mass to charge ratio (m/z) where millivolts are approximately proportional to concentration in the ionized flow (Hall, 1999).

Fluid Inclusion Stratigraphy (FIS) analysis was carried out on a total of 403 cuttings and core samples from several wells to produce a nearly continuous section from the lower part of the Frio Formation, through the Vicksburg and into the Jackson shale. Samples span from depth intervals 5990-11616 feet.

High-Resolution Logs

Array induction, gamma ray and neutron-density logs were correlated to cores. The measurement accuracy of these tools in thinly bedded and laminated reservoirs was

determined. The presence of thin highly cemented sandstone and shale beds in the cored intervals permitted a close correlation (within 1 ft.) of cores to the high-resolution logs.

Array induction logs provide resistivity measurements of five different depths of investigation: 10, 20, 30, 60, and 90 inches. These tools can resolve beds down to one foot thickness (Sneider and Kulha, 1995). Shallow investigation curves (10" and 20") effectively defined boundaries for beds greater than 1.5 ft. thick, but the thin beds limit the effectiveness of the deeper curves in measuring beds less than three feet thick.

High-resolution gamma ray logs can resole beds thicker than 2 to 3 feet (Sneider and Kulha, 1995). In the Vicksburg interval, gamma ray responses identified sandstones greater than 3 feet thick and detected thinner shales (approximately 1.5 feet thick). In the Vicksburg interval, many beds are less than one foot thick indicated by the cores and FMI logs.

High-resolution neutron and density porosity logs efficiently to changing rock properties. Density porosity correlates well with core-plug porosity measurements for beds thicker than one foot. Neutron values are consistently higher than density porosity values. In addition, core plug data on porosity, permeability, grain density and fluid saturation were also available. These data were augmented with additional core plug samples that were selected on the basis of wire-line log to core correlation.

Capillary Pressure

Capillary pressure data were obtained through mercury injection of rock chips. Injected mercury volume as a function of pressure is then attained. Mercury injection pressure in mercury/air system is converted to capillary pressure in gas/water system.

CHAPTER II

GEOLOGIC SETTING

Stratigraphy and Depositional Setting

The Tijernia-Canalas-Blucher (T.C.B.) field area in Kleberg and Jim Wells counties has produced significant volumes of hydrocarbons from the Oligocene Frio and Vicksburg (Taylor and Al-Shaieb, 1986). The Vicksburg Formation was deposited during the Early Oligocene and consists of sandstone, siltstone and shale. The Vicksburg Formation conformably overlies the Eocene Jackson shale and is overlain by the Oligocene Frio sandstone.

The Oligocene-age Vicksburg Formation (Figure 3) is interpreted as a series of prograding deltas that are separated by marine transgressions (Combes, 1993; Combes-Coleman, 1990; and Taylor and Al-Shaieb, 1986). The Vicksburg is overlain by the Frio Formation, which was deposited in a fluvial environment (Nanz, 1954; Shelton, 1973). The Vicksburg overlies the Eocene-age Jackson Shale that provided an unstable shelf margin for Vicksburg deposition. Sediment loading on the undercompacted Jackson mud caused large-scale slope failure along listric glide planes. Deformation of the Jackson into ridges and diapirs, along with regional extension generated accommodation space for Vicksburg sediment accumulation. Rollover anticlines were generated and segmented by

	TCB FIELD		LOCAL SUBSURFACE NAMES
OLIGOCENE	Frio Fm		Frio
	Vicksburg Fm	Upper	Nowacek Sandstone Wilson Sandstone 7900-ft Sandstone 8500-ft Sandstone 8650-ft Sandstone 8800-ft Sandstone
		Lower	9000-ft Sandstone 9400-ft Sandstone 9550-ft Sandstone 9900-ft Sandstone 10250-ft Sandstone 10500-ft Sandstone 10600-ft Sandstone 11000-ft Sandstone 11800-ft Sandstone
EOCENE	Jackson Group		Jackson Shale

(After Taylor and Al-Shaieb, 1986)

Figure 3. Stratigraphic nomenclature in the TCB field, Kleberg County, Texas.

synthetic and antithetic faults (Figure 4). Vicksburg depositional style was influenced by structure as thicker sand sequences accumulated on the downthrown side of faults. These sequences thinned over the crest of the anticlines and distally into the basin (Figure 4).

Major sand accumulations in the lower and upper Vicksburg reservoirs (Figure 5) represent fluvial-deltaic progradation depositional facies. Analysis of cores and electric logs from the TCB field indicate that the sandstones were deposited in shallow water. The 9900-ft intervals show abundant evidence of marine influence such as fossils, trace fossils and glauconite. This interval represents the transgressive phase of the Vicksburg and interpreted to have been deposited in a shallow marine shoreface environment (Figures 6 and 7).

Generalized seismic stratigraphy indicates the Lower Vicksburg section (10250 – 11800 ft sandstone zones) represents a progradational wedge deposited in a lowstand systems tract (Combes, 1990 and 1993; Al-Shaieb et al., 2000). Basic structural timing of the movement along the growth fault can be determined from seismic data. A visible thickening of sandstone and shale interbeds is evident in the Vicksburg 9400 – 9900-ft intervals, suggesting that movement along the fault was the greatest during this time (Figure 8). The 9400 - 9900 ft. interval is interpreted as a transgressive systems tract (Al-Shaieb et al., 2000). The Upper Vicksburg Wilson – 9000-ft sandstones are interpreted as sheet sands deposited in a prograding highstand systems tract. They are represented by continuous high amplitude beds on the seismic cross section (Figure 9).

Thick shale intervals separating sandstones are interpreted as flooding events. The intensity of progradation, subsidence and marine reworking influenced sediment accumulation and ultimately reservoir geometry and distribution. LR/LC intervals such as

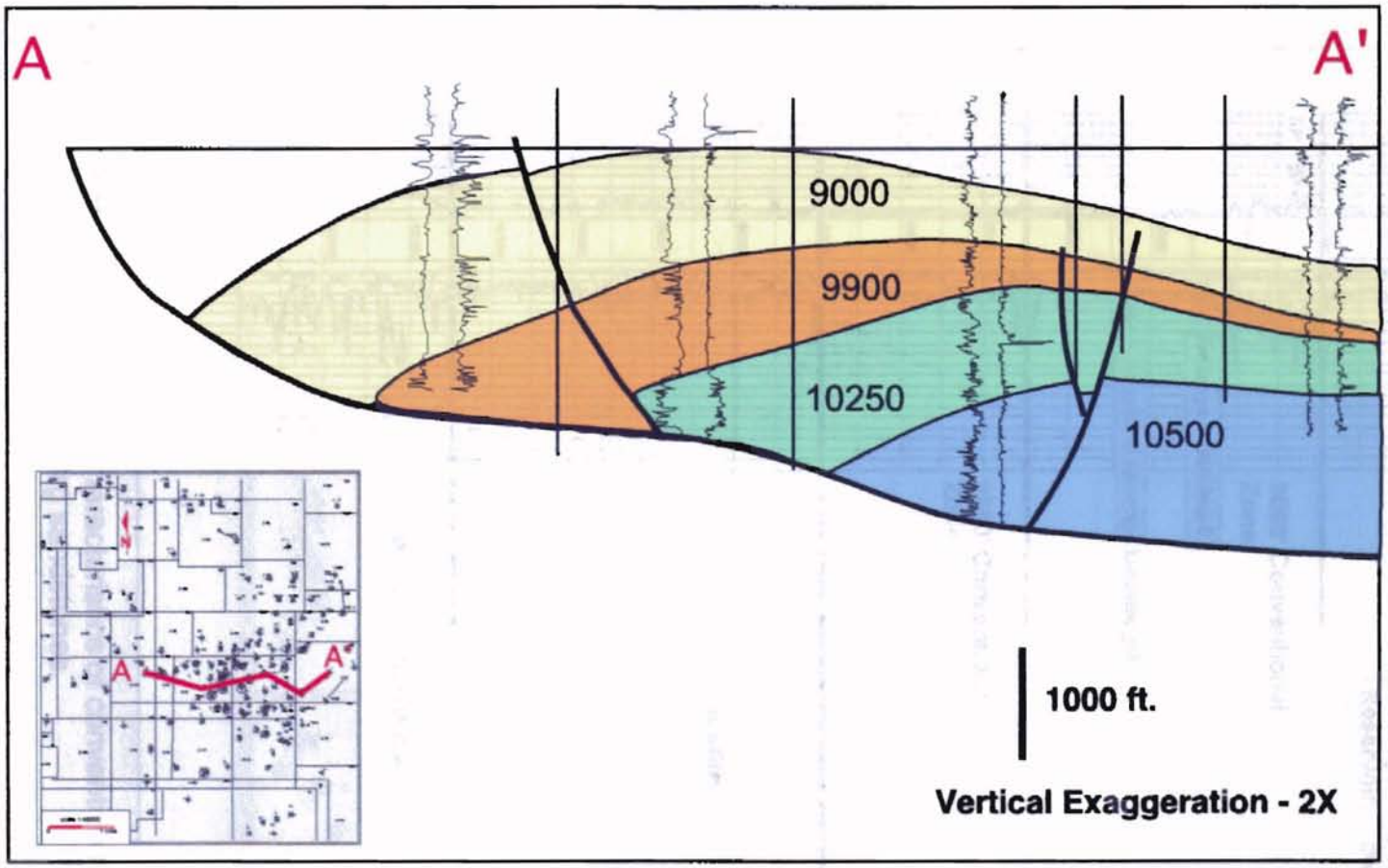

Figure 4. Structural cross section showing the influence of structure on depositional style. Sediment accumulation is thicker on the downthrown sides of faults and thins over the crest of the rollover anticline. Colors separate depositional intervals, which show similar patterns of thickening toward the fault. Numbers identify the upper most sandstone unit (local subsurface names) in each interval.

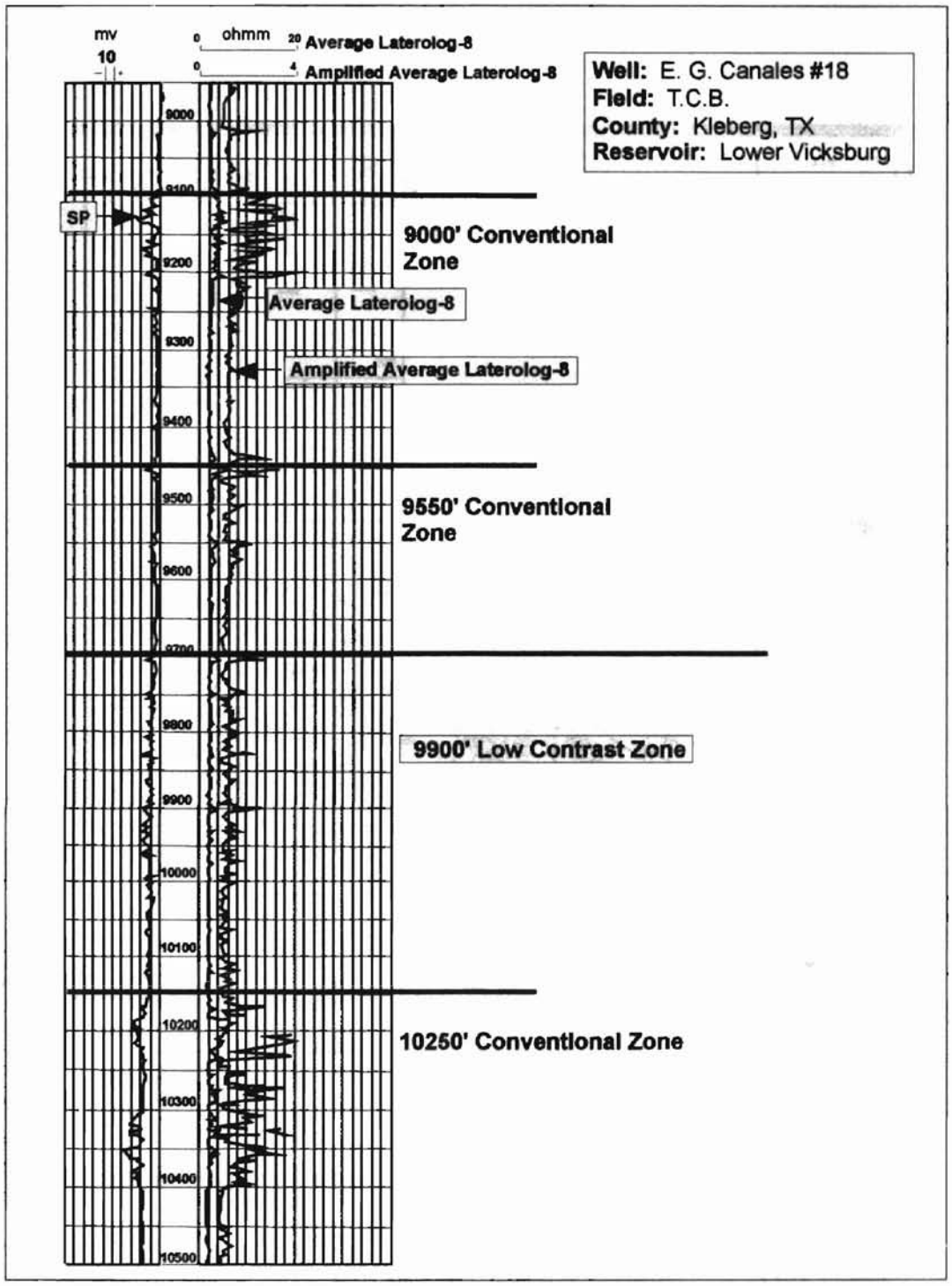

Figure 5. Type log showing log characteristics of conventional and low contrast Lower Vicksburg sandstones.

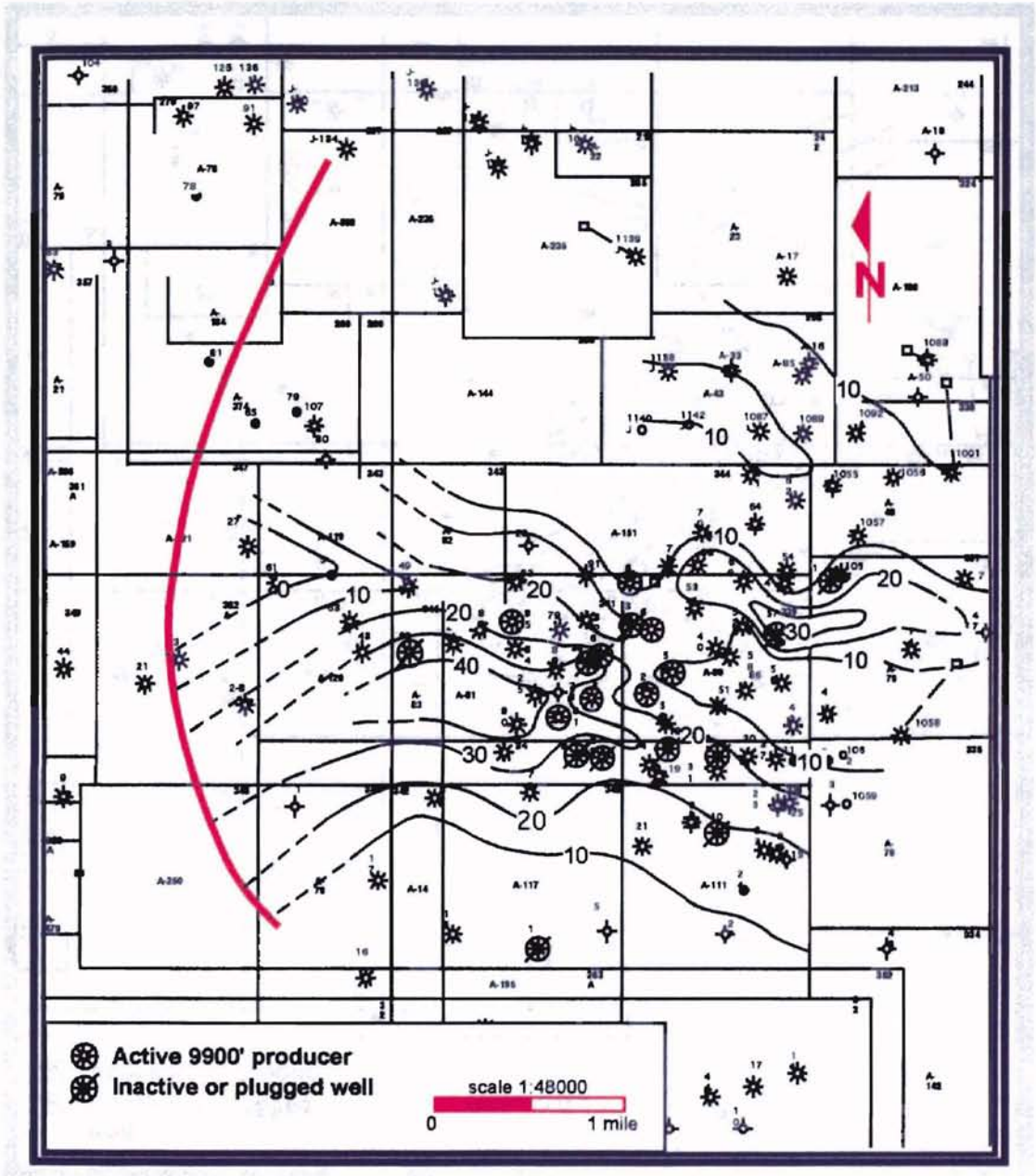

Figure 6. Thickness map of the 9000-ft Vicksburg sandstone. This distribution pattern suggests deposition occurred in a progradational deltaic setting.

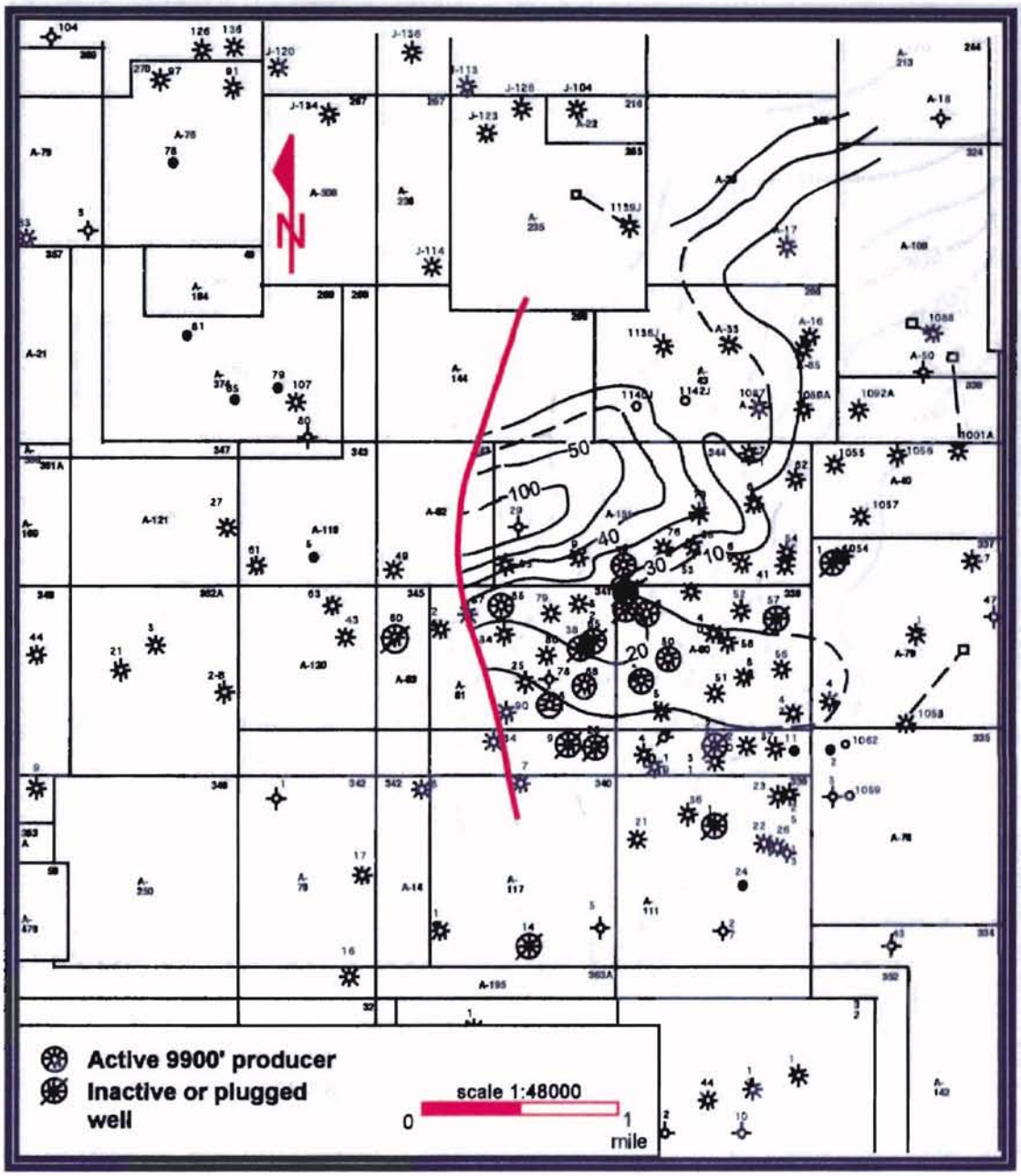

Figure 7. Thickness map showing distribution of net channel sandstone in the lower 10250-ft Vicksburg zone.

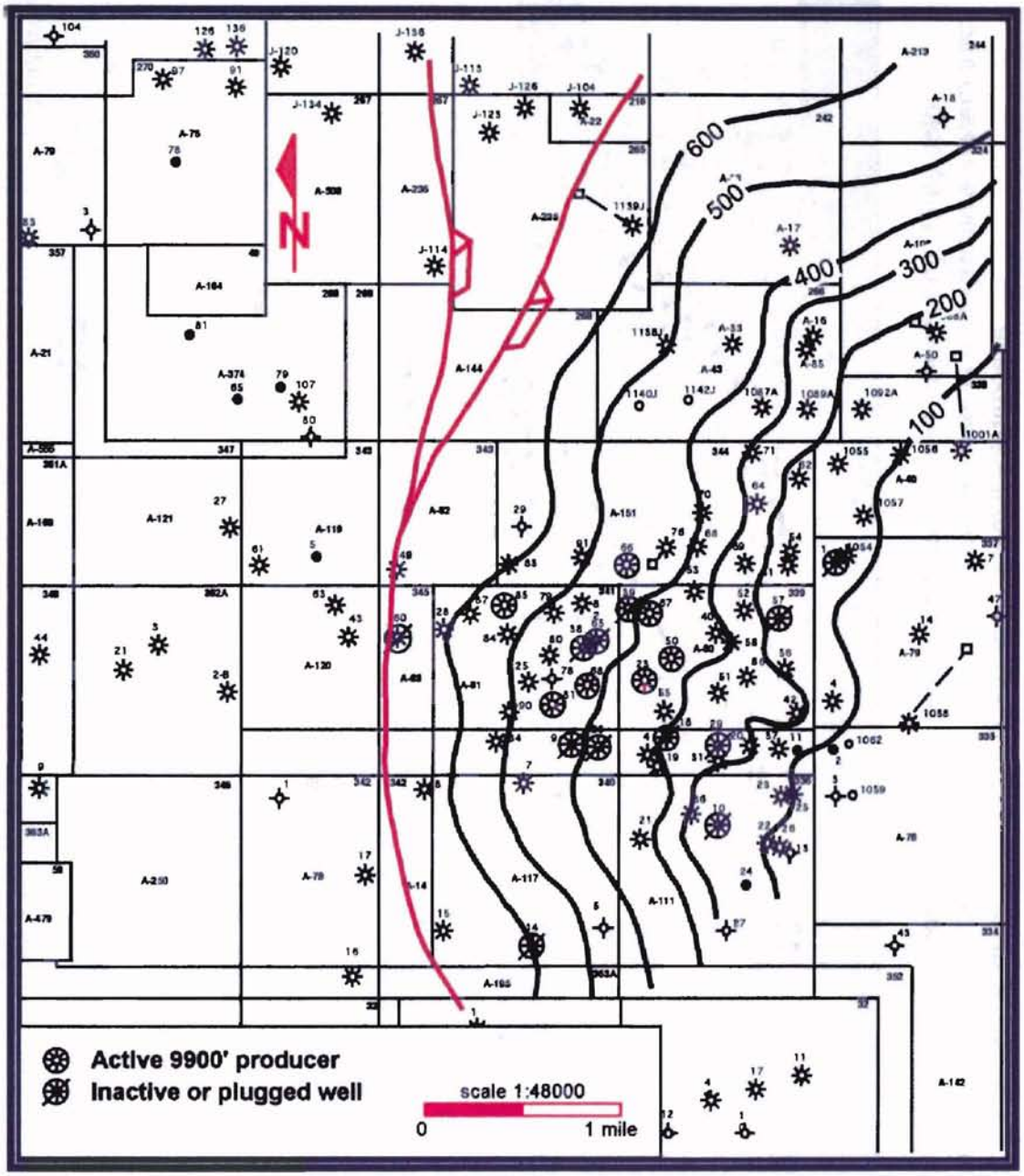

Figure 8. Thickness of the 9900-ft sandstone interval showing thickening of the sandstone toward the fault and thinning basinward across the crest of the rollover anticline in the TCB field.

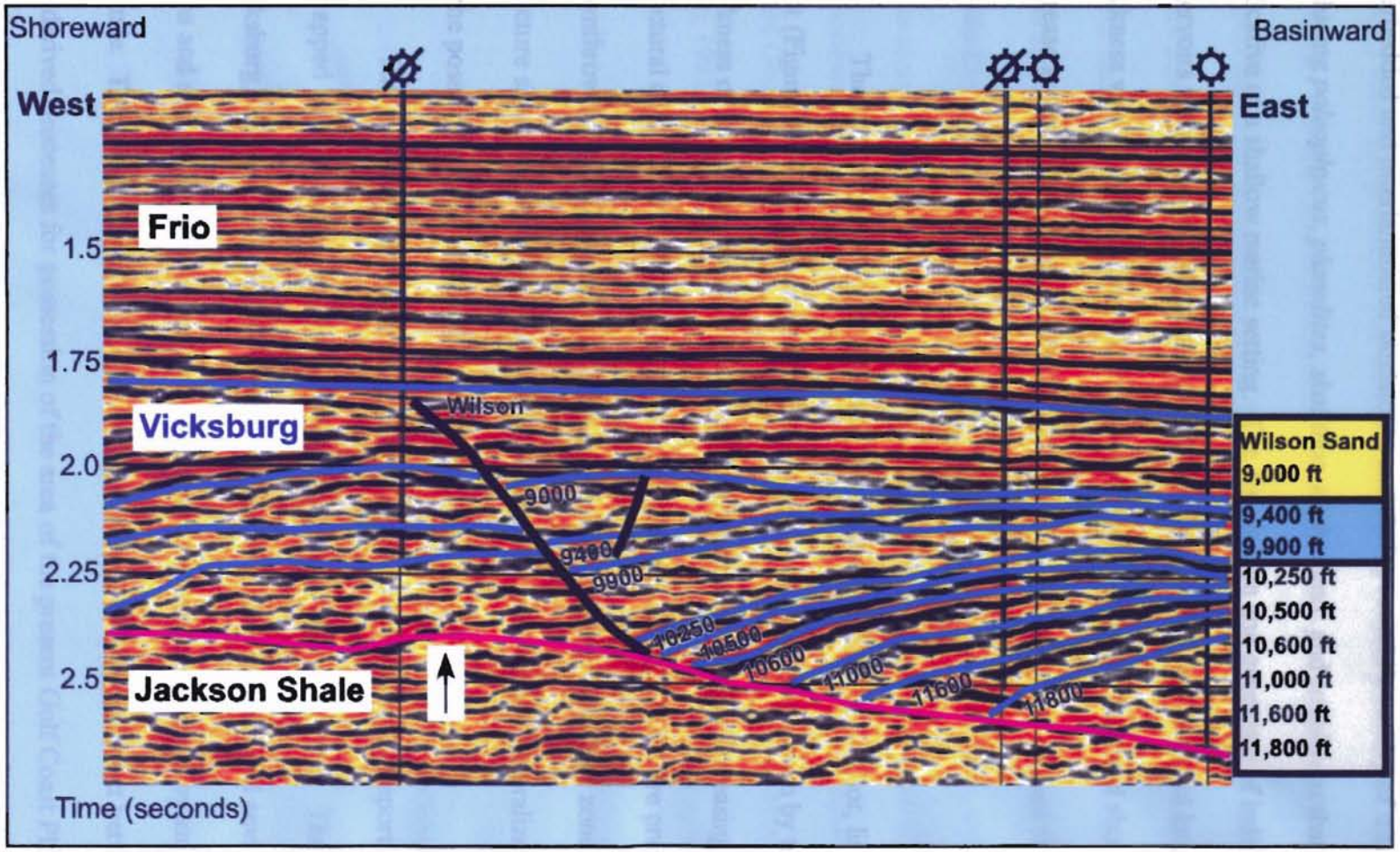

Figure 9. Dip oriented seismic cross section interpreted for structure and stratigraphy. Gray color represents intervals of the lowstand system tract. Blue represents transgressive system tract rocks. The yellow interval consist of highstand system tract deposits.

the 9900-ft sandstone may be interpreted as transgressive lower shoreface deposits. These interbedded and interlaminated sandstones and shales contain a variety of trace fossils including *paleophycus*, *planolites*, *skolithos*, *teichichnus*, and *zoophycos* that are indicative of a shallow marine setting. The distribution and geometry of individual reservoirs within the 9900-ft zone were difficult to establish, but the total interval thickness was mapped (Figure 9). It also thickened toward the fault and showed a marked increase in sandstone along the fault trend.

Structural Features

The local structure at T.C.B. field area is characterized by a major, listric normal fault (Figure 3). The Vicksburg fault has a continuous growth as shown by the increased thickness of lower Vicksburg intervals on the downdip side and by increasing dip and structural complexity in deeper horizons. Numerous subsidiary faults are present, also downthrown to the east and convergent downward with the major fault zone. The structure shown by the cross section (Figure 4) and maps is highly generalized, and not all of the possible faulting is shown.

The structural-tectonic features of South Texas are extremely important in defining entrapped Vicksburg hydrocarbons such as those found in T.C.B. Field. The South Texas Vicksburg, Frio and Wilcox depocenters are similar in their depositional environment types and simply represent an infilling of sediments into the Gulf Basin by an ancestral Rio Grande. The Cenozoic History of the Gulf Coast is essentially a conflict between land and sea derived processes for possession of the area of the present Gulf Coast Plain (Williamson, 1959). This describes what was happening at the various sediment input of

the rivers that were confronting the Gulf of Mexico, but on the much grander plate tectonics scale, the processes that were controlling the overall picture were not nearly as simplified. The Rio Grande Embayment is the main feature, which contains the bulk of hydrocarbon-laden sediments in south Texas. Next in importance are the major fault-flexure zones which were generated contemporaneous with sediment loading. The major growth fault zones and structural features are the main trapping mechanisms in the South Texas subsurface. The general package of growth faulted sediments within the Rio Grande Embayment is bounded to the northeast by the San Marcos Arch; the southwest by the Sierra Madre Oriental, Sierra Madre Occidental and the Laramide fold shear belt; to the northwest by the Trans-Pecos volcanic Field, Southern Rockies and again the Sierra Madre Occidental; and finally to the south and south east by the Gulf of Mexico Basin (Han, 1981).

CHAPTER III

PETROLOGY

Introduction

The Vicksburg sandstone 9900-ft zone studied consists of both detrital constituents and diagenetic products. The sedimentary rock in the Vicksburg Formation can be best named according to the classification cited by Folk's (1974) QRF ternary diagram. Sublitharenite, feldspathic litharenite, subarkose and lithic arkose were the lithologies present in the thin sections examined. The mean rock type of both logged cores intervals plotted as feldspathic litharenite. The average grain size of the samples studied varies from coarse siltstone to very fine sandstone. The majority of the samples are medium sorted, subangular to subrounded and submature to immature in structural maturity. The major detrital constituents in the 9900-ft Vicksburg sandstones are quartz, feldspar, chert and volcanic and metamorphic rock fragments.

Detrital Constituents

Quartz is the most abundant mineral which was chiefly monocrystalline. The feldspar is 5.3% in average, with plagioclase being the most abundant feldspar found more prominent. Feldspar grains commonly show dissolution and alteration in thin section. Due to the high degree of dissolution, potassium-feldspar only occurs in trace content in the 27

samples studied. Secondary porosity created the leaching of potassium-feldspar grains contributed to a great amount of porosity in the studied wells.

Volcanic rock fragments are abundant, being 6.4% in average and up to 10% in some samples. Volcanic textures are well preserved in some volcanic rock fragments, with feldspar laths easily identified. Dissolution of volcanic rock fragments is also commonly encountered. Therefore, it is somewhat difficult to identify extremely to slightly altered grains. Argillaceous rock fragments are the next important rock fragments, taking up 2.7% in average. Chert and metamorphic rock fragments are relatively less important, but also commonly exist in the sample studied. The content of minor detrital constituents ranges from 0.3%-2.4%, with an average of 1.2 %, including glauconite, muscovite, biotite, pyrite, zircon, tourmaline and fossils.

Diagenetic Constituents

Cements. Calcite is the major cement, with an average content of 11.8%. Carbonate cement profoundly affects the reservoir quality, commonly occluding primary and secondary pores. Siderite, quartz overgrowth and anhydrite are a minor component.

Authigenic Clay. The authigenic clays observed in samples studied include illite-smectite mixed layered clay, illite, kaolinite and chlorite.

Porosity

The porosity of the thin section analysis ranges from 0.3%-15.8%, with an average of 7.1%. Most of the pores are secondary, including both intergranular and intragranular.

Pore systems are complex and variable, consisting of a mixture of severely reduced intergranular pores, leached-grain pores, and a large amount of micropores among clays.

Mechanical deformation, leaching of detrital grains and calcite cement, precipitation of calcite cement, authigenic clays greatly altered the original depositional fabric.

Compaction and Mechanical Deformation

Vicksburg sandstones have undergone moderate to strong degrees of compaction. Deformation of ductile components such as argillaceous rocks, volcanic rock fragments, mica, and glauconite are one of the main diagenetic features. Under compaction, they are crushed and squeezed between quartz and feldspar and other hard grains, increasing the compaction and in response decreasing porosity.

Chemically Unstable Constituents

In all samples studied, the majority of the macroporosity comes from the partially to completely dissolution of detrital grains. Quartz, feldspar, argillaceous rock fragments, volcanic rock fragments and cement exhibit moderate to high degree of dissolution. The leaching of feldspar and volcanic rock fragments are especially important. This is a predominant factor for the formation of secondary pore system. In addition, dissolution may also have provided the source material for the precipitation of the late stage cement and authigenic clays.

Cement and Authigenic Clay

Major precipitation features consist of formation of quartz overgrowth, calcite and siderite. Generally, carbonate cements are formed in two stages. In several samples, carbonate cement, which nearly occludes all the primary pores, is believed to precipitate in early stage. Those ductile grains show little to no mechanical deformation. Late stage carbonate cement also commonly exists in samples studied. They can refill the pores produced by the dissolution of feldspar and volcanic rock fragments and other detrital grains. In addition, calcite cements tend to concentrate along bends or in patchy pattern radiating outward.

Authigenic clays are abundant in most of the samples, including pore-lining illite-smectite mixed layered clay, illite, chlorite and pore-filling kaolinite. The formation of authigenic clay mainly plays a destructive role for the establishment of connective pore system, although abundant micropores exist among authigenic clay. Micropores generally have a pore throat radius less than 0.5 microns and primarily occur as intercrystalline pores within the clay. In addition, the formation of abundant authigenic clay is also related to the originally chemically unstable feature of Vicksburg sandstones. Most of the authigenic clay found in the samples appears to have crystallized from pore fluids, since they occur in the form of well-developed crystals. The potassium necessary for the formation of kaolinite may comes form the dissolution of K-feldspar.

Other minor diagenesis processes include: 1) replacement of detrital grains by calcite and dolomite; 2) replacement of feldspars and volcanic rock fragments by authigenic clays;

4) Devitrification of volcanic rock fragments; 5) shrinkage of glauconite, forming some shrinkage pores around the glauconite; 6) precipitation of pyrite from organic matter.

There appears to be a correlation between grain size and visible porosity. Finer grained sandstones have lower average visible porosities, whereas the relatively coarser grained samples are higher in average visible porosities. At the same time, a greater degree of diagenesis alteration is typically predominant in coarser, mores porous rocks. According to thin section observation, several coarser grained samples are completely cemented by calcite. The grains are floating in the carbonate cement. Therefore, this type of carbonate cements is formed in early stage before severe compaction. Subsurface water rich in carbonate first entered the coarser grained and more porous part of the sandstone, occluding nearly all of the primary pores. With deep burial, the leaching of unstable detrital grains (feldspar, volcanic rock fragments, etc.) and carbonate cement will form some secondary pores. But, porosity of this type of samples is relatively low because the early stage carbonate may be a factor occluding the subsurface water flowing in early stage of dissolution, slowing down the leaching speed of unstable constituents. Other diagenetic processes, such as seritization and precipitation of authigenic clays are also slowed down. Volcanic fragments and feldspar show relatively less degree of alteration, with fresh surfaces.

The ductile flowing of the argillaceous and volcanic rock fragments between hard detrital grains further decreases the primary and secondary pores. The dissolution of grains, such as quartz, feldspar and volcanic rock fragments, especially the dissolution of feldspar and volcanic rock fragments provide almost all of the secondary visible pores.

Petrology and Petrography of Reservoir and Seal Facies

Kerr-McGee Company cored the 9900-ft zone in two wells: A.T. Canales #81 and A.T. Canales #85. The cores were correlated and calibrated to Schlumberger Formation Micro-Imager (FMI) logs and High Resolution Array Induction, Density-Neutron Gamma-Ray and Spontaneous Potential logs. Geologic features such as bedding planes, flowage structures, burrows and cross beds were identified in the core and on the FMI images. Chromatic changes associated with these features allowed an inch-scale calibration of the core to the FMI. Calcite and silica-cemented zones identified on the FMI were correlated to clean, low porosity zones on the High Resolution Gamma-Ray and Density-Neutron logs.

The cores were described, and sampled for thin-section, x-ray and SEM analyses. Thin-section porosity was correlated to porosity measurements from logs. Detrital and diagenetic constituents determined by thin section analysis. These sections provided data to augment the macroscopic examination of the cores. Clay minerals were identified using powder X-ray diffraction and SEM analysis.

Classification

The major detrital constituents in the 9900-ft Vicksburg sandtones are quartz, feldspar, chert, and volcanic and metamorphic rock fragments. The sandstones were classified on the basis of the relative percentages of these grains using the Folk (1974) (QRF) ternary diagram (Figure 10). In general, sublitharenite, feldspathic litharenite, subarkose and lithic arkose were the major lithologies determined from individual thin sections. The average compositions for both cores plotted as feldspathic litharenites.

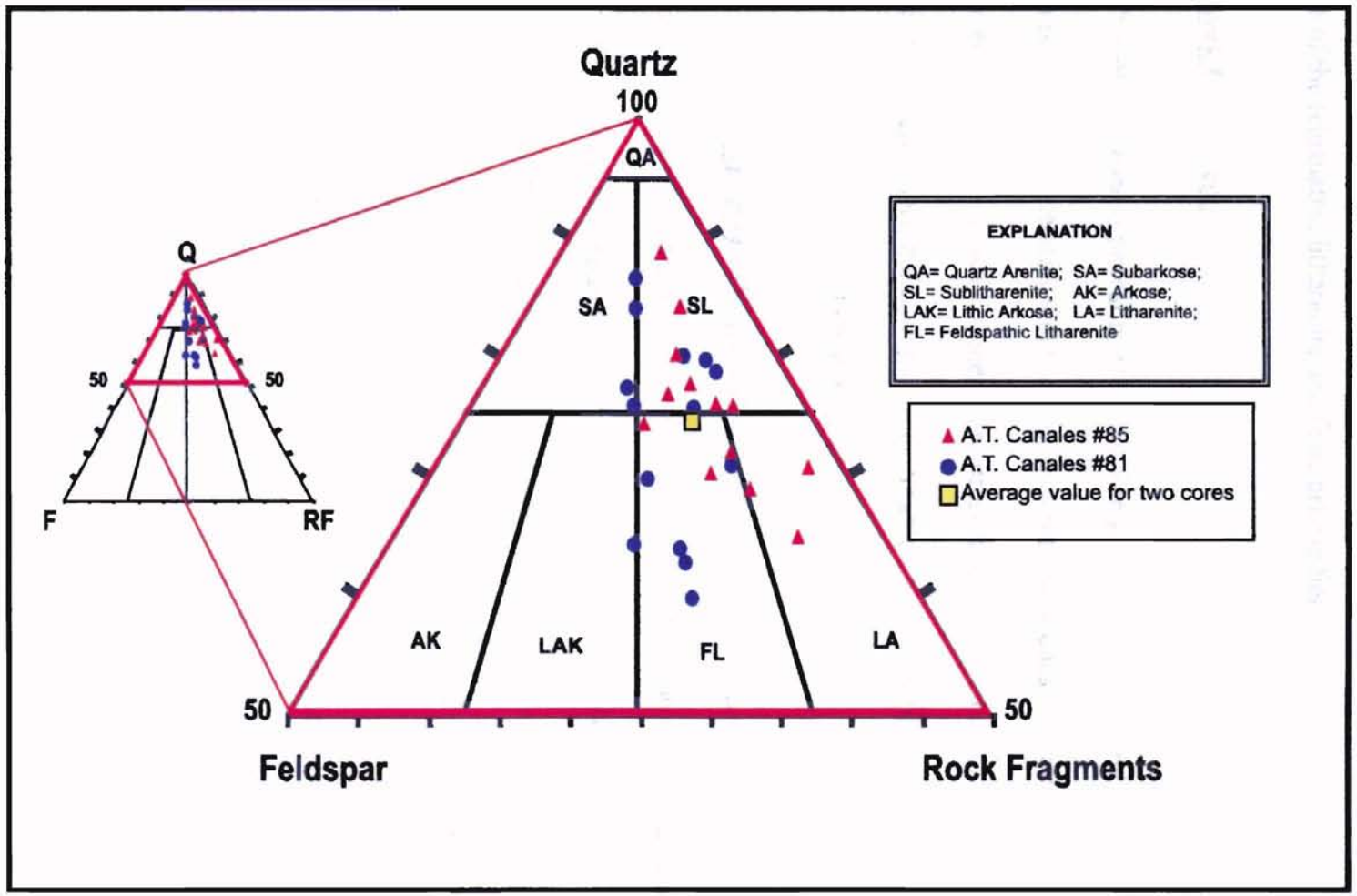

Figure 10. Composition of the 9900-ft sandstone plotted on QRF diagrams (Folk, 1974).

These lithologies represent the present (post-dissolution) composition. Restoring dissolved feldspar and rock fragments would shift the original composition plots toward the base of the feldspathic litharenite and lithic arkose fields.

Framework Constituents

The 9900-ft zone is primarily silty very-fine grained sandstone and shale. The sandstones are moderately sorted. Quartz is the major constituent, while feldspar and sedimentary and volcanic rock fragments are present in various amounts. Minor constituents include chert, metamorphic rock fragments, muscovite, biotite, glauconite, zircon, pyrite, tourmaline and skeletal fragments.

Major Constituents. The most abundant detrital grain in the Vicksburg sandstones is quartz (Figure 11). Most grains are monocrystalline and exhibit uniform extinction. Polycrystalline quartz is present in minor amounts and likely represents a metamorphic source. Fluid and mineral inclusions are present in some monocrystalline grains.

Plagioclase feldspar is the second most abundant detrital grain. Plagioclase grains are easily identified by their albite twinning (Figure 11).

Rock fragments are a common constituent in the Vicksburg sandstones. Volcanic fragments are abundant (6-10% of the total rock) and easily identified by the randomly oriented plagioclase phenocrysts of their microphyric texture (Figure 12). Seritization and devitrification of these grains are common, making grain identification more difficult. Sedimentary rock fragments are present in various amounts. Argillaceous fragments are

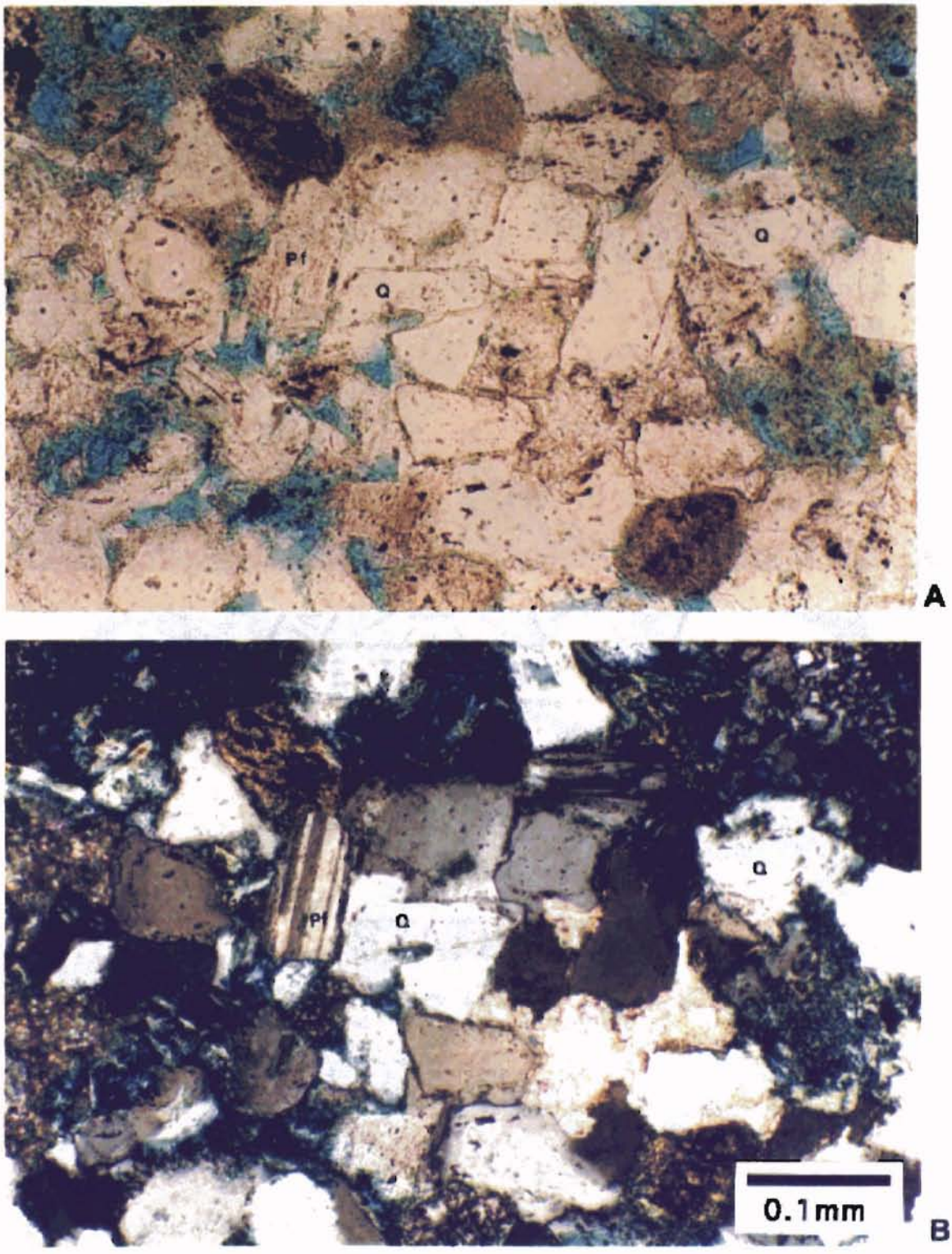

Figure 11. Quartz (Q) and plagioclase feldspar (Pf) are major framework grains i the 9900-ft sandstone. Albite twinning is characteristic of plagioclase.
A. Plane-polarized light (PPL).
B. Cross-polarized light (CPL).

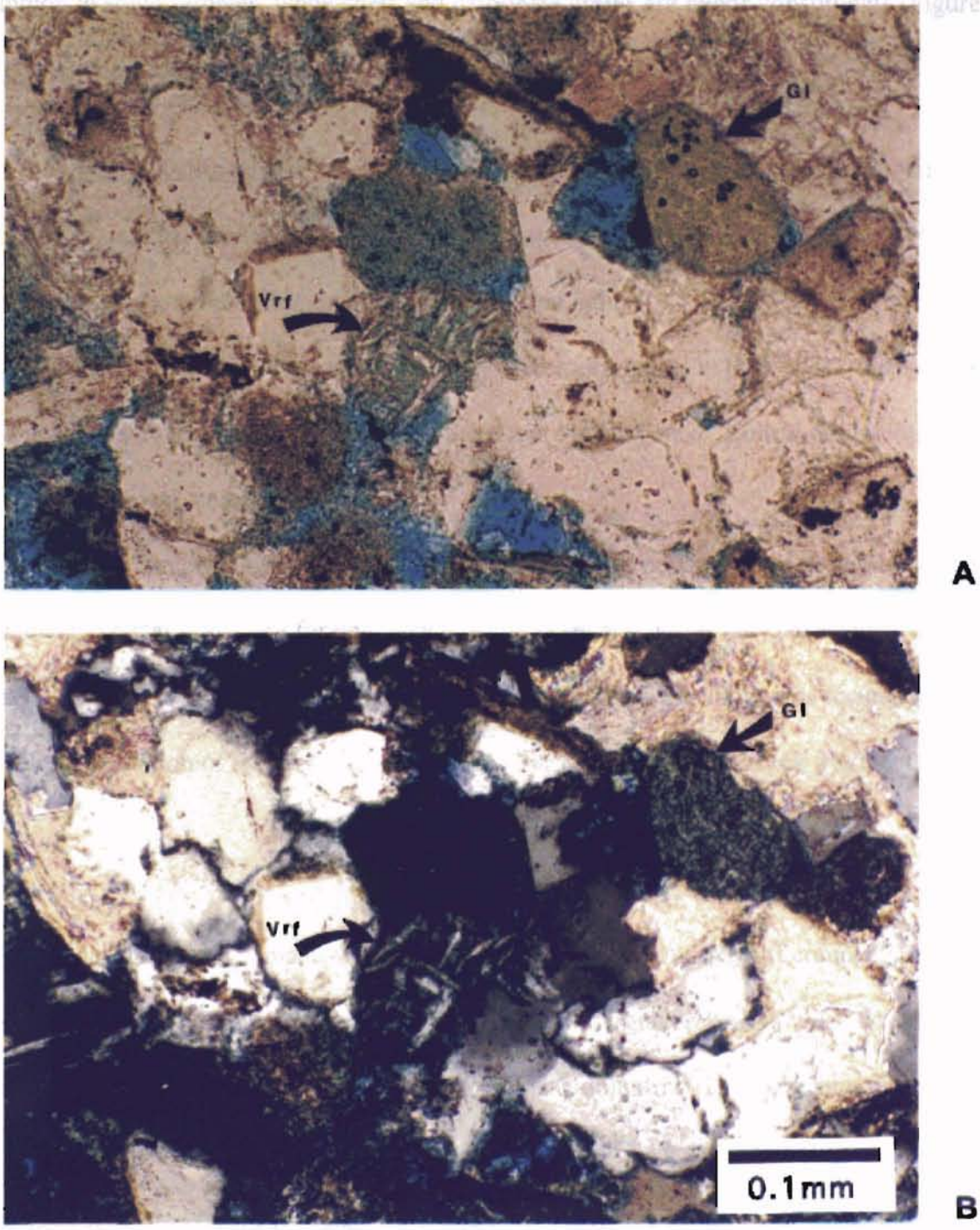

Figure 12. Volcanic rock fragment (Vrf) with randomly oriented phenocrysts of plagioclase feldspar. Glauconite (Gl) is a common constituent. Oxidation of ferrous iron changes green glauconite to brown. A. PPL B. CPL

common in some samples, while chert and carbonate grains are minor constituents (Figure 13). Metamorphic rock fragments occur as a minor constituent.

Other Constituents. Glauconite is a common secondary constituent. It occurs as rounded grains that are typically green color in plane-polarized light (Figure 12). It is green with moderate birefringence in cross-polarized light.

Muscovite and biotite were widespread accessory grains in both cores. Muscovite was identified by its distinct morphology, color and birefringence. Biotite was recognized by its pleochroism, color and extinction.

Pyrite, zircon, tourmaline and skeletal grains are all present in minor amounts. The dominant skeletal grains are forams, which occur as several grains per thin section. Detrital clay is present as true or pseudomatrix (Figure 14). The latter was formed by ductile deformation of softer grains such as argillaceous and volcanic rock fragments.

Diagenetic Constituents and Features

Sandstones not cemented in early diagenesis often show signs of compaction. Flexible and soft components were ductilly deformed. Argillaceous and volcanic rock fragments flowed between quartz grains forming pseudomatrix. Elongate muscovite and biotite grains were bent or fractured by harder quartz and feldspar grains (Figure 15). Chemical diagenesis has significantly modified the Vicksburg sandstones, which have experienced several episodes of cementation and dissolution. Calcite is the dominant cement, but silica cement is significant in some areas.

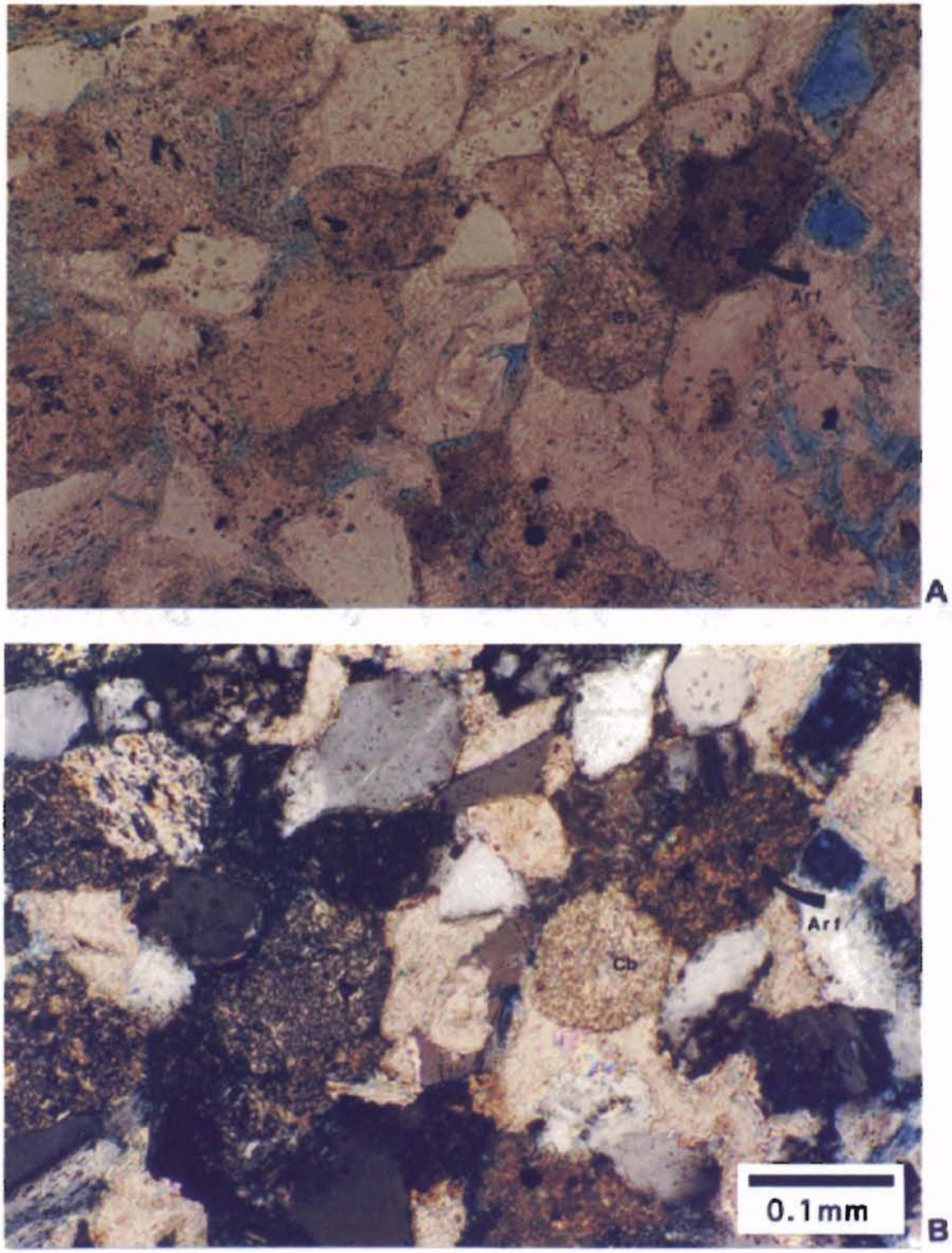

Figure 13. Carbonate grains (Cb), and argillaceous rock fragments (Arf) are common in the Vicksburg sandstone.
A. PPL B. CPL

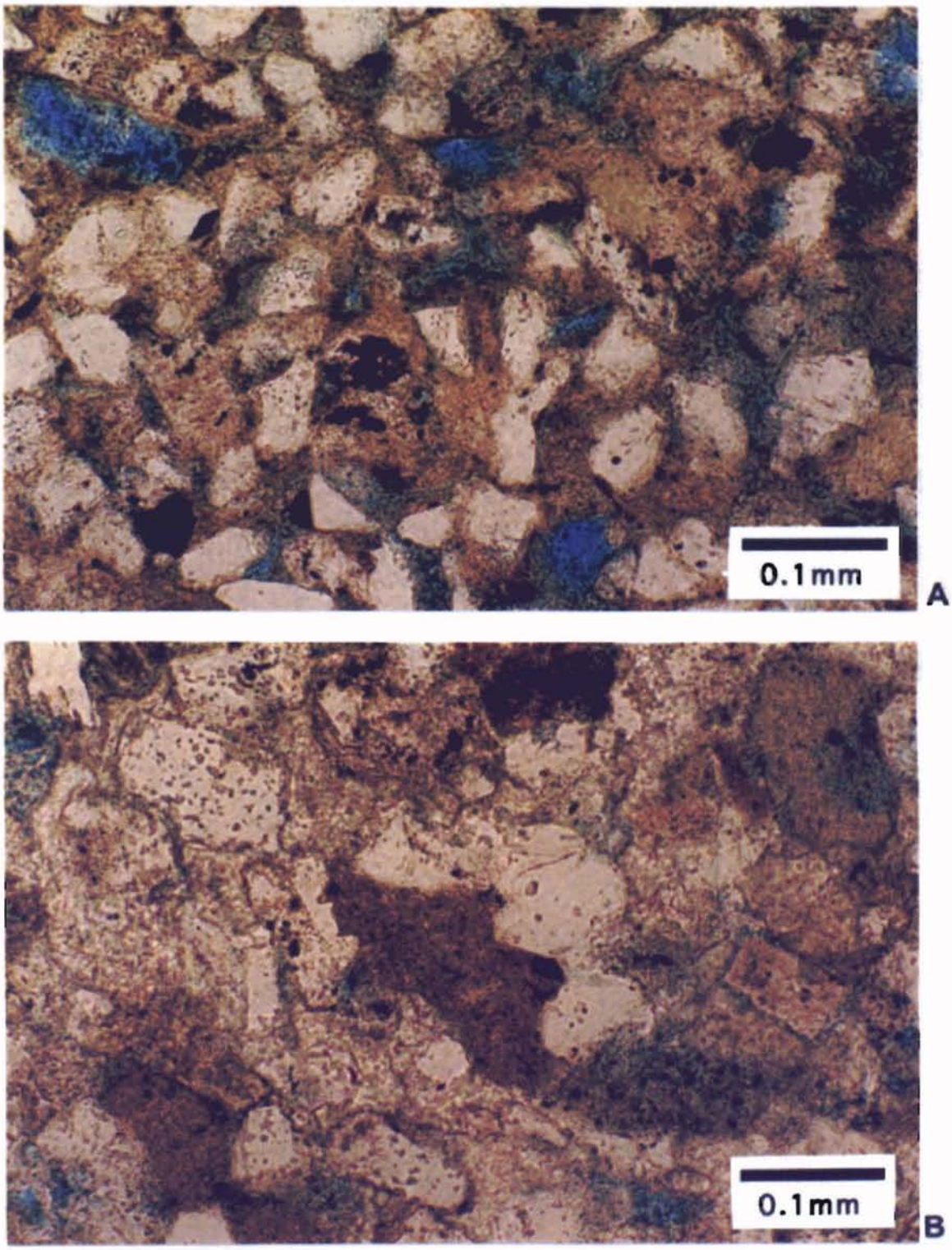

Figure 14. A. Detrital clay matrix that impeded fluid movement and reduced grain dissolution. PPL

B. Pseudomatrix formed by the ductile deformation of argillaceous rock fragments. PPL

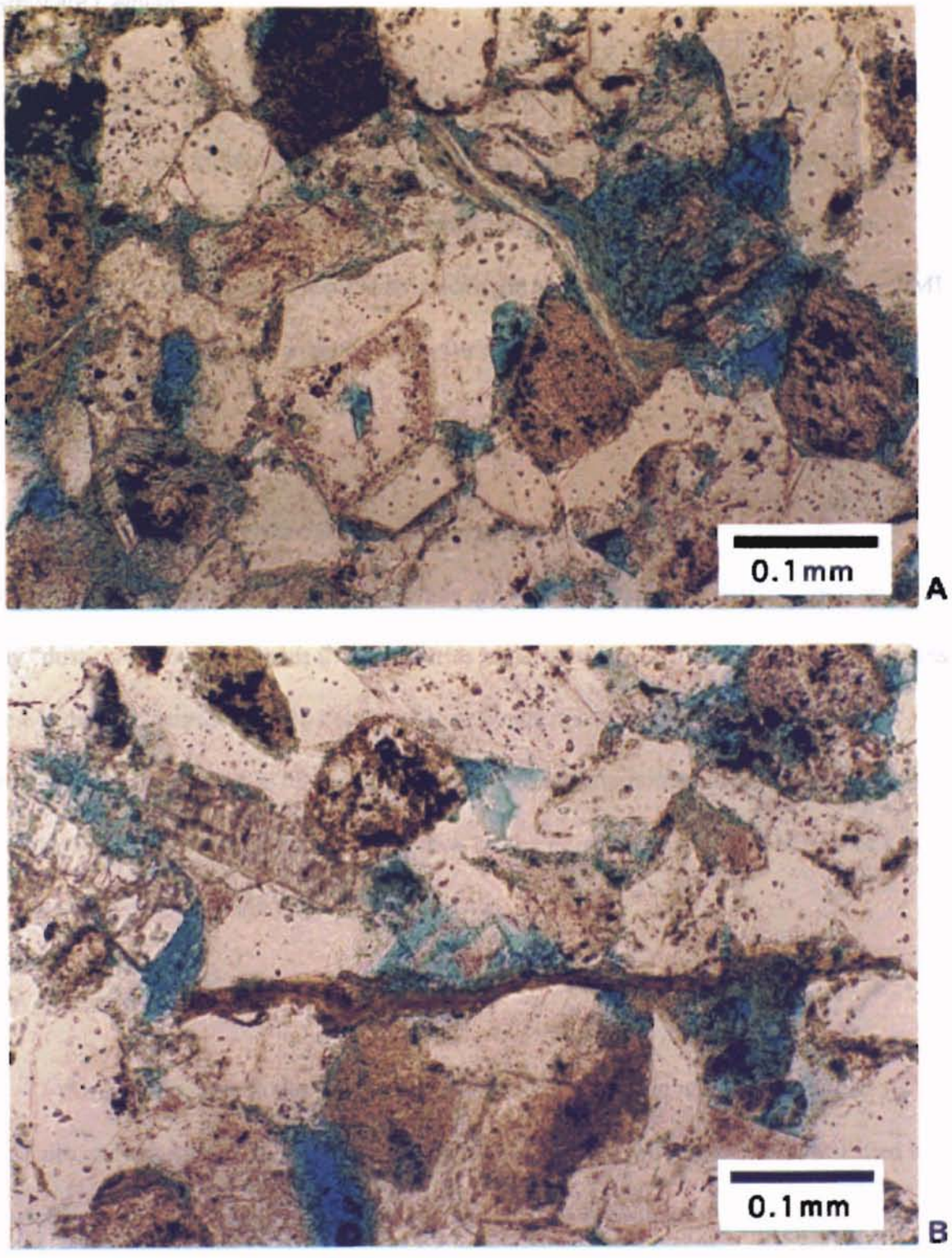

Figure 15. Compaction deformation of muscovite (A) and biotite (B) between harder quartz and feldspar grains.
A. PPL B. PPL

Carbonate Cement

Calcite is the major cement and completely occludes porosity in some sandstones. It varies from being isolated patches to widespread zones. Calcite replaces quartz grains in the latter area and forms poikilotopic texture where quartz grains "float" in calcite cement (Figure 16). Zones cemented by calcite are identified as white color bands on FMI logs (Figure 17). Siderite is a minor constituent and occurs as subhedral crystals.

Silica Cement

Silica cement as syntaxial quartz overgrowth is common (Figure 18). The overgrowths are easily recognized when they are separated from the detrital grain by a clay "dust rim." In some cases the boundaries between the overgrowths and detrital grains are not distinct, but the cement contains fewer inclusions than the detrital grain. Silica cement is more prevalent in cleaner sandstones with lesser amounts of clays. Here, advanced stages of overgrowth occur. Silica-cemented zones appear as white color bands on the micro-resistivity imaging logs (Figure 17).

Clay Minerals

Authigenic clays in the 9900-ft interval are smectite-illite mixed layer, illite, kaolinite and chlorite. Mixed layer smectite-illite is the most abundant. It is identified by its characteristic peaks on X-ray diffractograms.. SEM photomicrographs reveal mixed-layer smectite-illite is pore lining and bridging. Kaolinite is the second most abundant clay. It is identified in thin-section by its crystal morphology, color and low birefringence. Kaolinite was also identified using X-ray diffraction and SEM (Figure 19). Authigenic

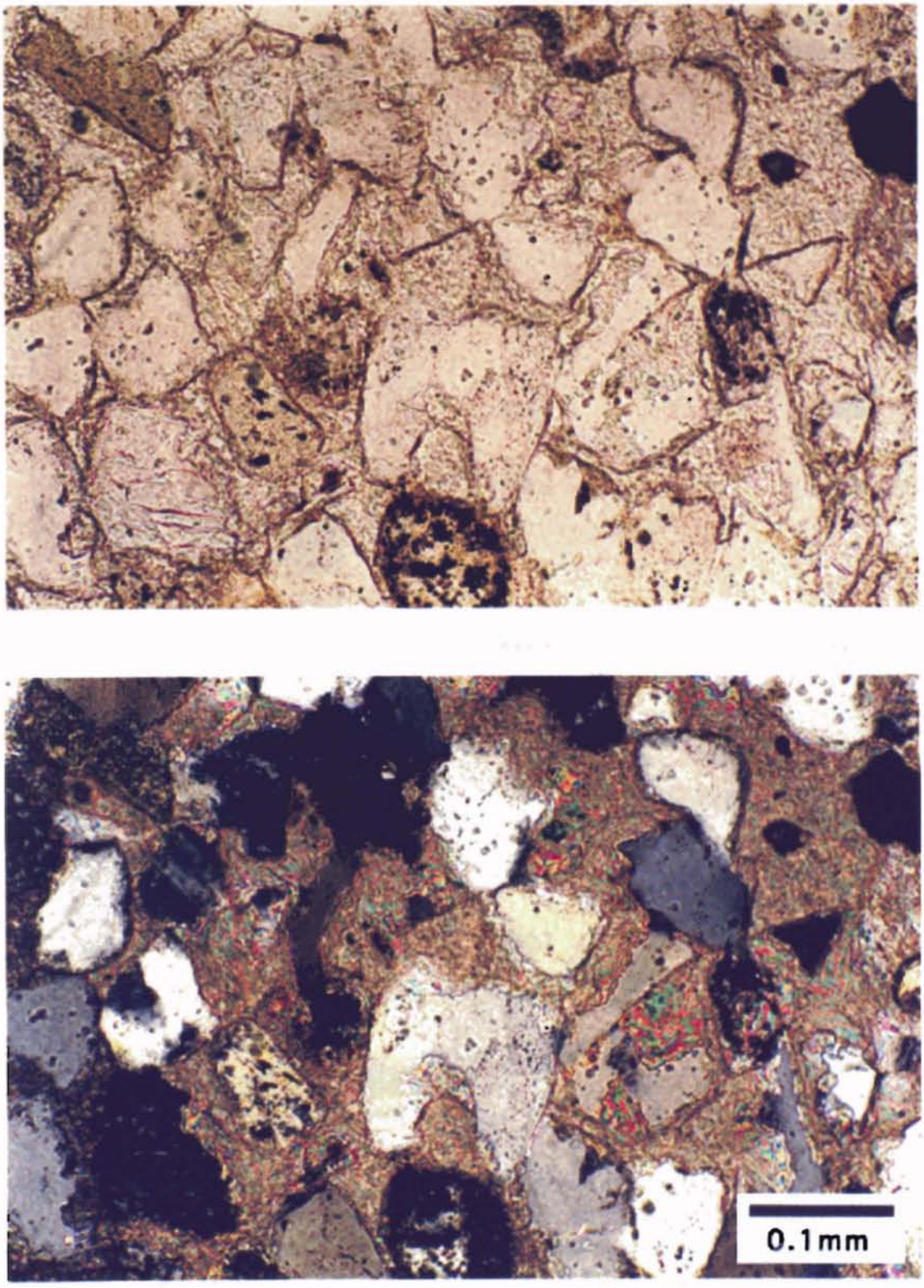

Figure 16. Poikilotopic texture formed by the replacement of quartz and other framework grains by calcite cement.
A. PPL B. CPL

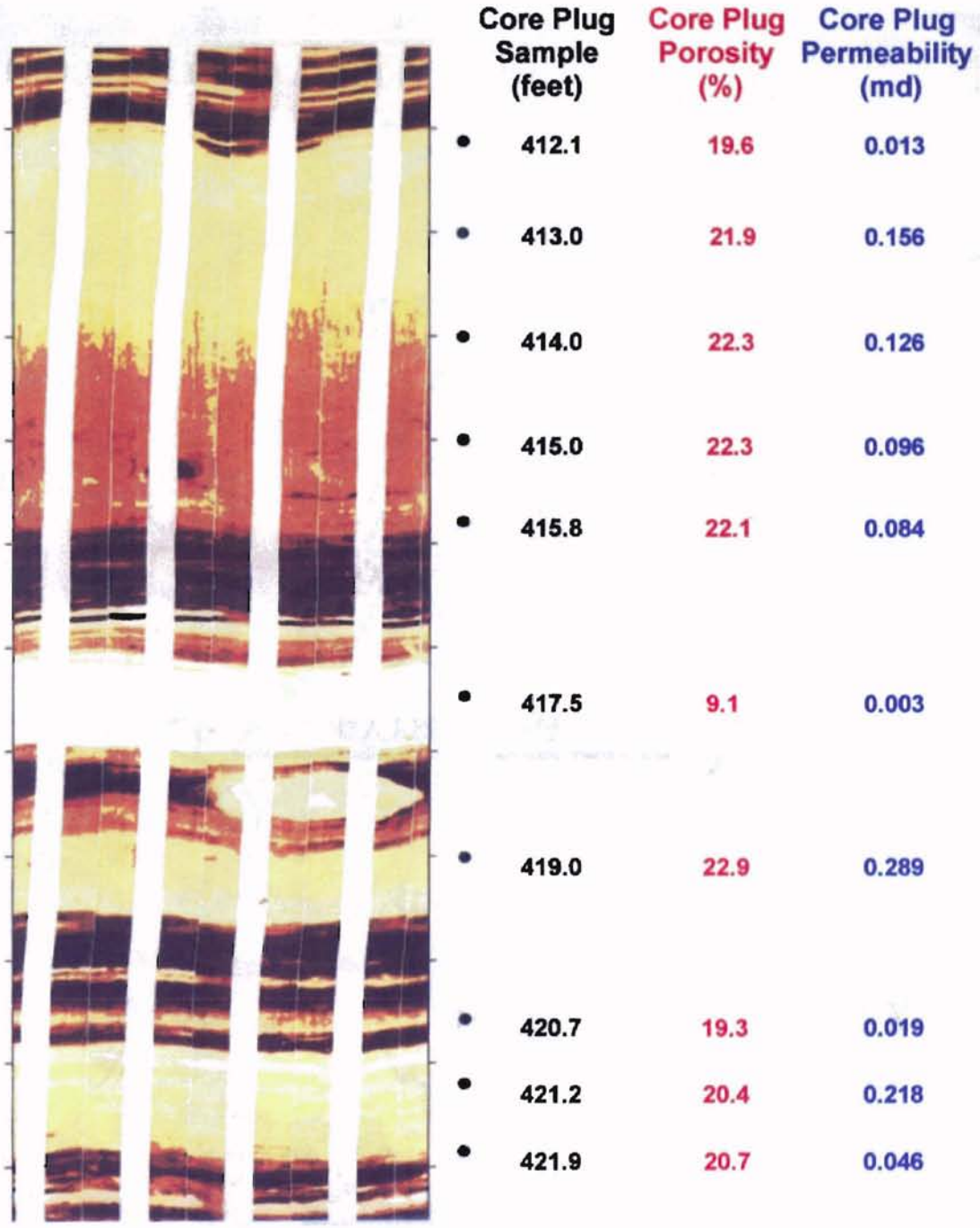

Figure 17. A comparison of FMI colors and porosity and permeability measurement from core plugs. White zones are calcite and/or silica cemented and low porosity and permeability. Yellow zones are typically high porosity and permeability. Orange zones are clay rich and high porosity, but low permeability. Gray color represents claystone or shale. (From Al-Shaieb et al., 1998.)

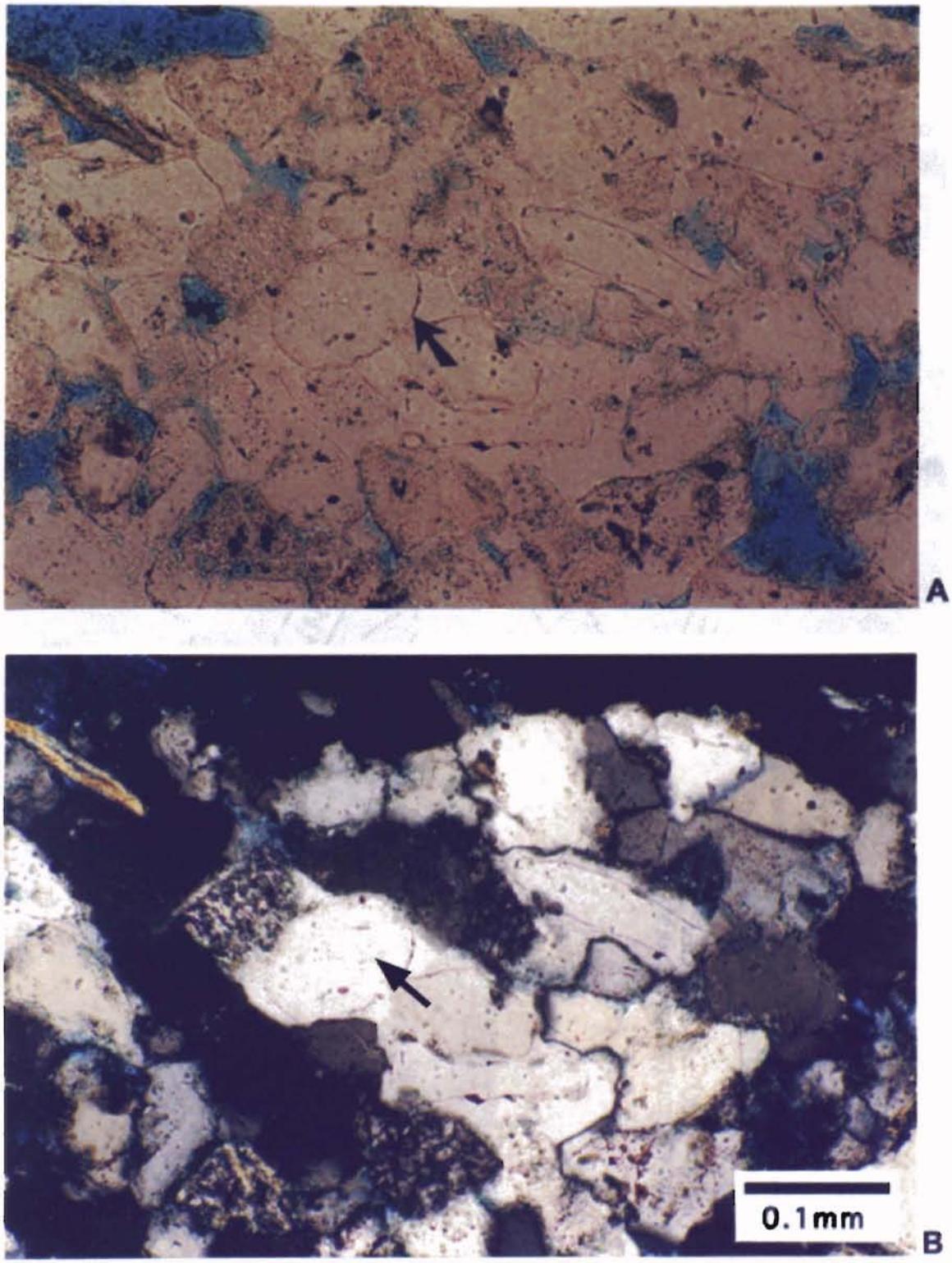

Figure 18. Silica cement in the form of syntaxial quartz overgrowths. Clay dust rims (arrows) separate cement from detrital grains.
A. PPL B. CPL

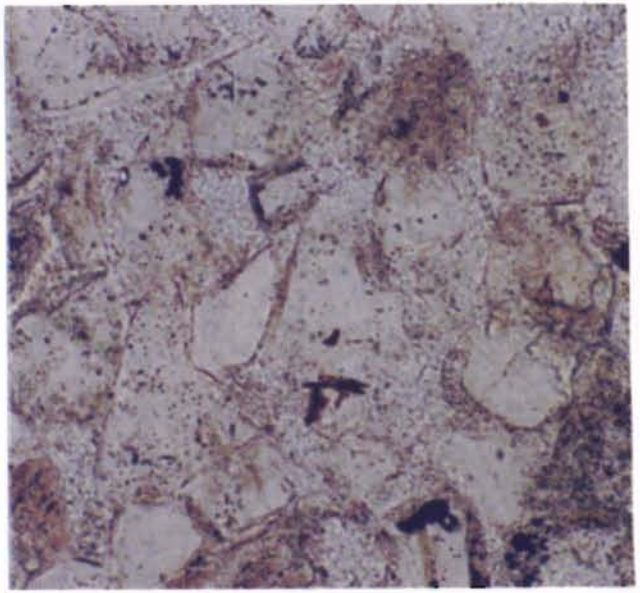

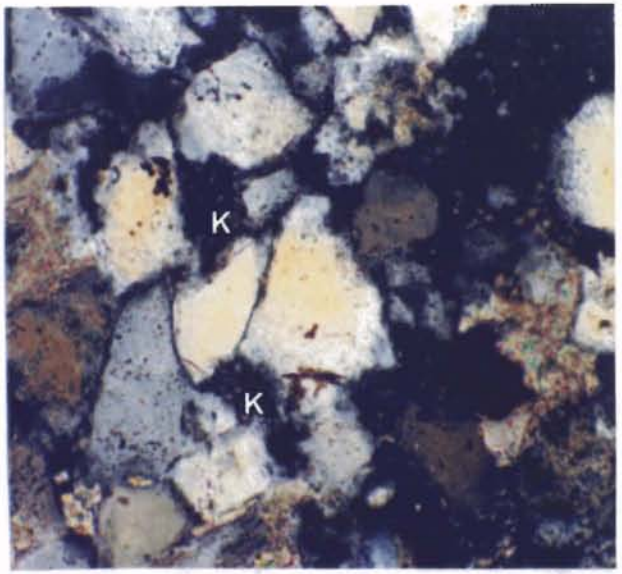

A

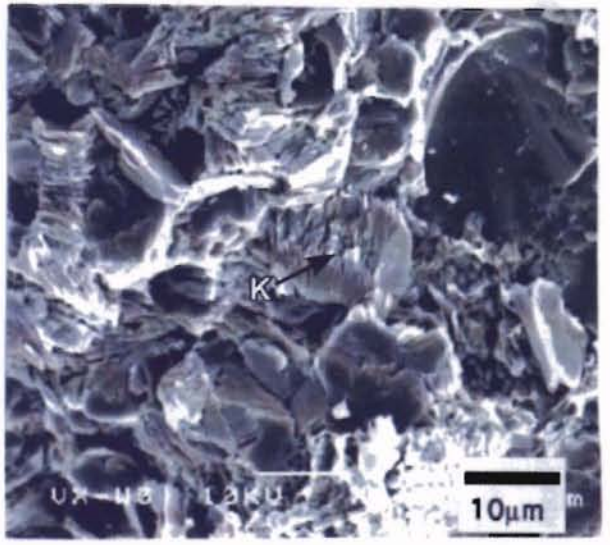

B

Figure 19. A. Thin-section photomicrograph of pore-filling kaolinite (K). PPL and CPL

B. SEM micrograph of pore-occluding kaolinite (K) from a seal zone in the Vicksburg sandstone.

illite occurs as highly birefringent crystals that line pores. It is identified throughout the core, but is not readily abundant. Chlorite is a minor authigenic constituent that was identified by X-ray and SEM (Figure 20). Intervals with abundant clay minerals and lower resistivity are identified as darker yellow and orange bands on the micro-resistivity imaging logs (Figure 17).

Porosity

Both primary and secondary porosities are preserved in the 9900-ft sandstone. Volumetrically, secondary porosity is much more significant than primary. Primary porosity is believed to have provided the avenues for pore-fluid migration, which resulted in partial or complete dissolution of metastable constituents to generate secondary porosity. Porosity estimated from thin section was consistently lower than porosity measured by core plug analyses. This discrepancy may be due in part to underestimating microporosity between clays or in partially dissolved grains. Core plug porosity was consistent with density porosity measurements in zones within the logging tool's resolution capability (Al-Shaieb et al., 1998).

Color variation in the micro-resistivity log indicates porosity range on less than one-inch scale. Yellow and orange color bands consistently indicated porosity exceeding 18%. White band porosity values are less than 10% (Figure 17).

Primary Porosity Intergranular porosity is the form of primary porosity preserved in these rocks. As a result of compaction and cementing, primary porosity is present in only trace amounts. It typically occurs as small (.01-.03 mm diameter) planar-sided pores

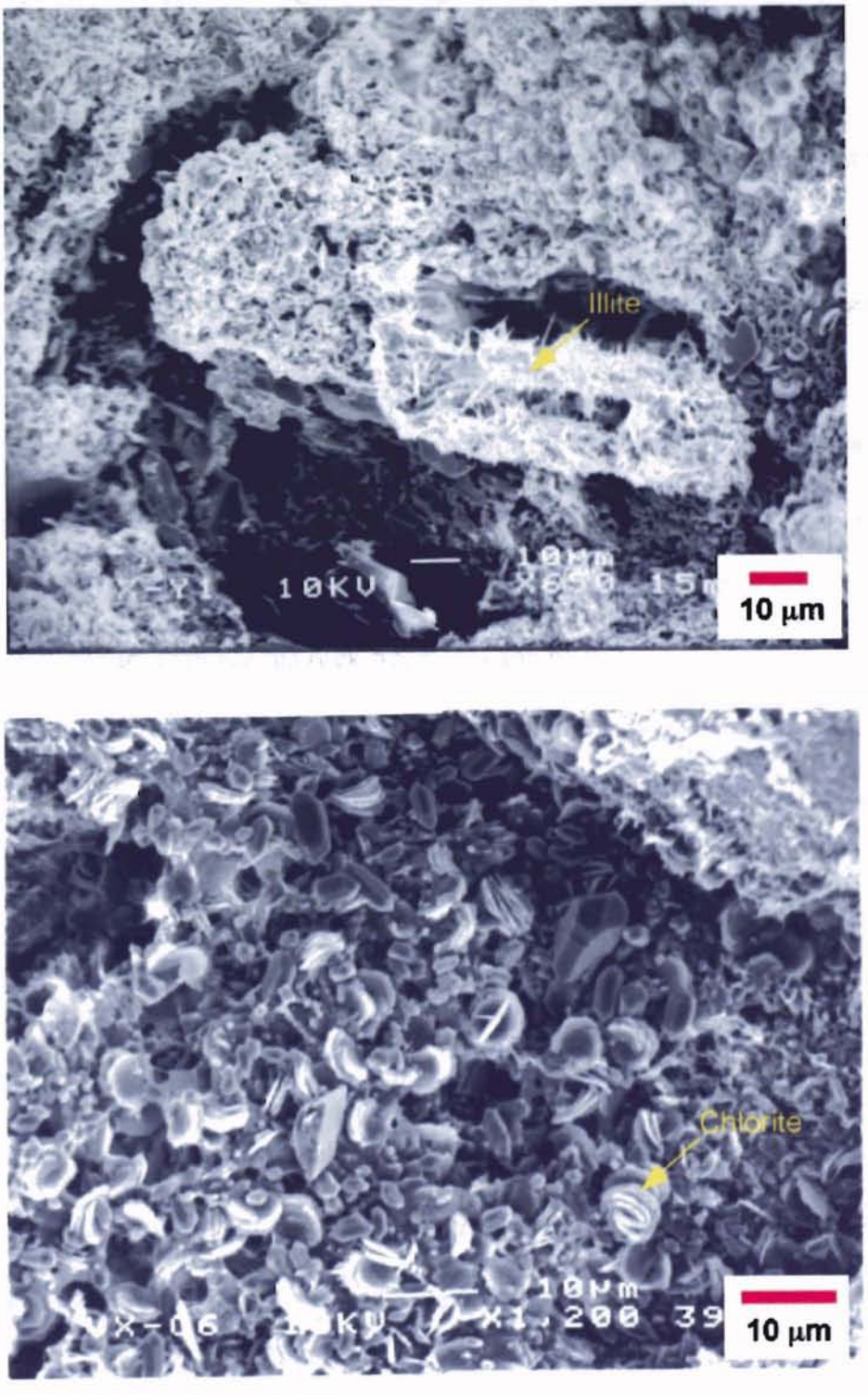

Figure 20. SEM micrograph of authigenic illite and chlorite, Vicksburg sandstone, TCB field.

bordered by syntaxial quartz overgrowths (Figure 21). In cleaner sandstones, near-total destruction of primary porosity is common.

Secondary Porosity. Secondary porosity is the volumetrically significant porosity in the 9900-ft sandstone. It can be attributed to the partial and/or complete dissolution of metastable siliceous grains. Pore morphologies range from partial leaching of grains to total grain dissolution and oversized intergranular porosity (Figure 22).

Plagioclase feldspar dissolution accounts for the largest share of secondary porosity. Leaching of volcanic rock fragments also generated significant secondary porosity. Lesser amounts of porosity were formed by the dissolution of other constituents including glauconite, argillaceous rock fragments and matrix.

Feldspar and volcanic rock fragments exhibit various stages of dissolution. Initially, leaching formed intragranular microporosity. As dissolution progressed, the grains were skeletonized and finally totally consumed.

Moldic porosity with near-circular shape suggests the total dissolution of rounded rock fragments or glauconite grains. Shrinkage porosity around glauconite may represent the initial stage of the latter form of moldic porosity. Infrequent oversized pores appear to be the result of multiple grain dissolution.

Microporosity is an important feature in the 9900-ft sandstone. It developed within partially dissolved grains and/or when available pore space was filled with authigenic clays. These intercrystalline micropores generally have small pore throat radii (less than 0.5 microns) and significantly reduce permeability (Al-Shaieb, et al., 1998).

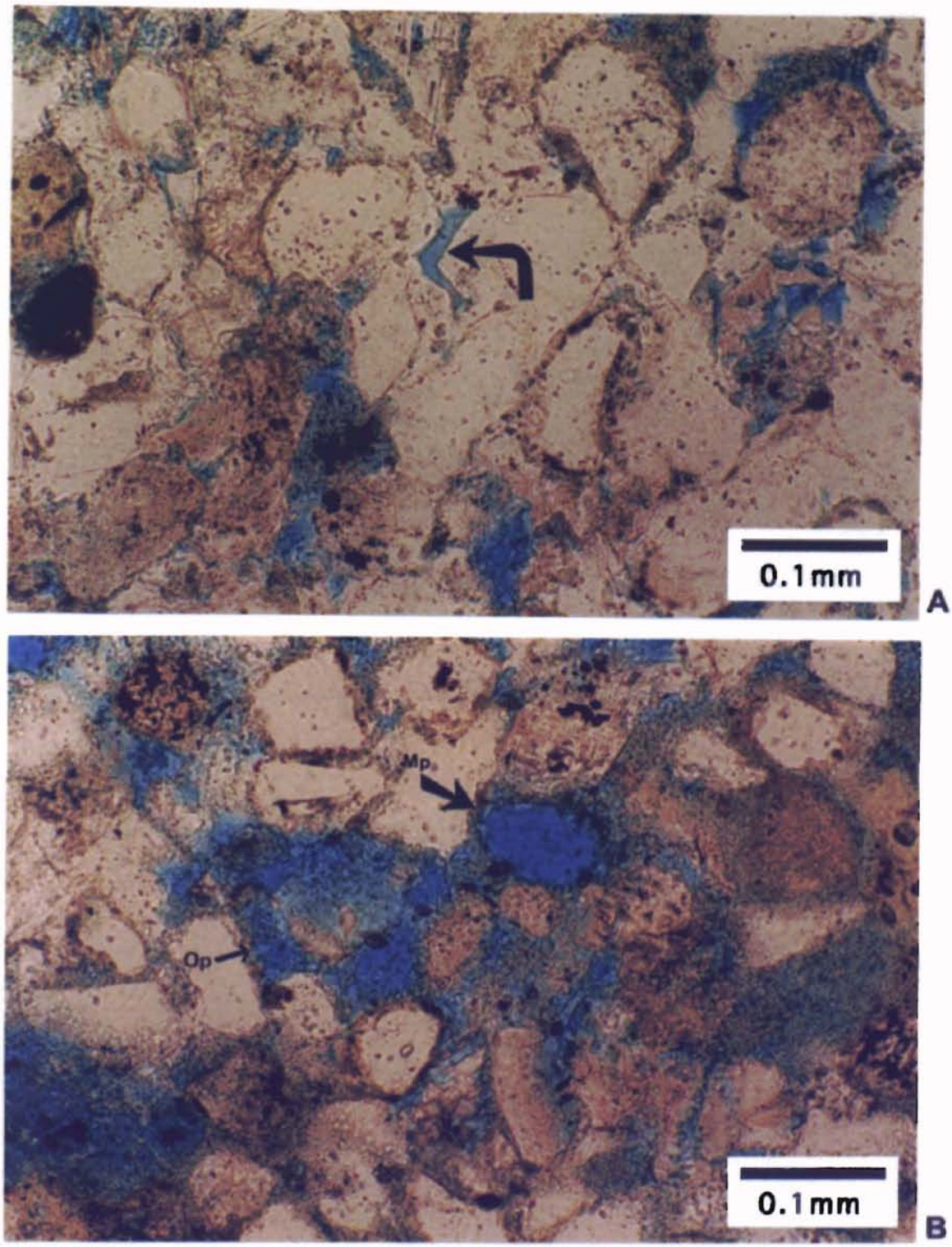

Figure 21. A. Primary porosity (arrow) rimmed by planar crystal faces.
B. Secondary porosity: Oversized pores (Op) resulted from multiple grain dissolution. Authigenic clays precipitated prior to grain dissolution ring late-stage moldic pore (Mp). Mainstage secondary porosity is commonly filled with authigenic clay (green).

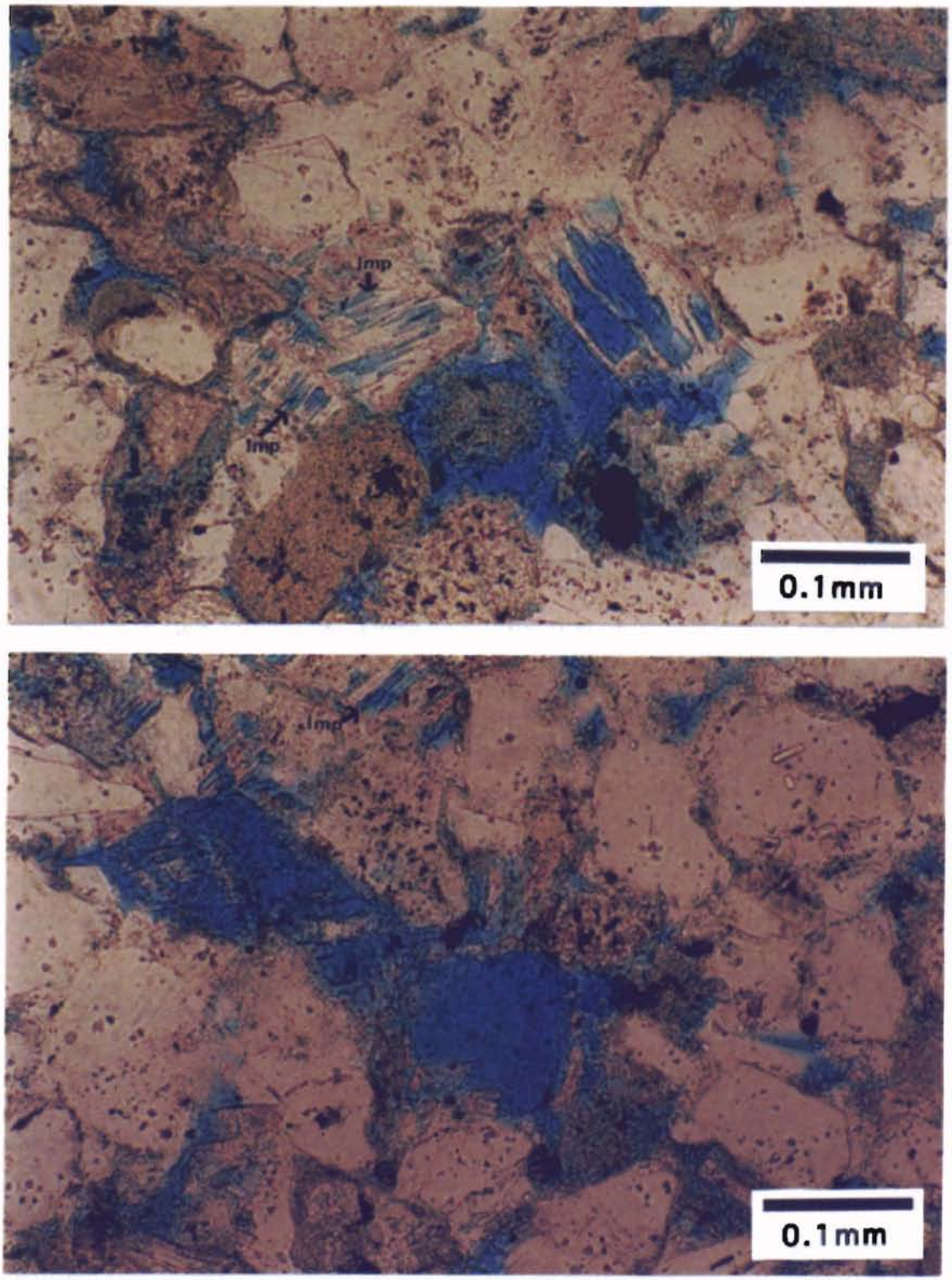

Figure 22. Dissolution stages of siliceous grains. Partial leaching of feldspar and volcanic rock fragments generated intragranular microporosity (Imp). As dissolution progressed, grains were consumed and finally completely dissolved.

CHAPTER IV

FORMATION MICRO-IMAGING AND CHROMATIC ZONE IDENTIFICATION

Introduction

One of the primary goals in wire-line logging is to identify reservoirs and seals. High-resolution logging technology has greatly enhanced this process. Borehole micro-imaging has added a new dimension to wire-line logging by providing an outstanding visualization of rock properties. These high-resolution resistivity images when integrated with core analysis aids in locating and identifying potential low contrast/low resistivity reservoirs. FMI provides the resolution of bed thickness and other lithogical features such as sedimentary structures, burrows and trace fossils and fault zones to name a few.

Micro-imaging Tools

The introduction of micro-imaging tools in the mid-1980's has benefited the petroleum industry. These tools are designed to focus small beams of electrical current into subsurface formation to measure changes in resistivity along the borehole wall that coincide to subtle changes in rock composition, grain texture, and fluid properties. Important information needed to understand and identify these thinly laminated and bedded reservoirs can be obtained from this instrument.

Micro-imaging tools measure micro-conductivity using closely spaced button electrodes mounted on pads. Each pad contains 24 sensor electrodes, resulting in measurement resolution of 0.2 to 0.3 inches. These tools typically have 6-8 articulating pads mounted on independent arms (Figure 23). This design allows relatively free movement to improve electrode to formation contact (Halliburton, 1997 and Schlumberger, 1992). Like other micro-resistivity tools, micro-imaging tools are designed to be run in conductive, water based mud. The depth of investigation for micro-imaging tools is up to 30 inches. When used as dipmeters or high-resolution tools for sedimentological, vug, or fracture analysis, their normal investigation depths are typically a few inches. This shallow depth of investigation limits the resistivity measurements to the flushed zone (R_{xo}). As a result, formation fluids have minor affect micro-imaging tools and the recorded resistivity measurements reflect only rock properties. Variations in current recorded by micro-imaging tools are converted to synthetic color images. Dark colors reflect high micro-conductivity (low resistivity), while light colors reflect low micro-conductivity (high resistivity) zones.

Most micro-images are viewed in two forms, static and dynamic. The static view has a fixed resistivity scale over the logged interval so that beds with the same color shade have the same resistivity. The dynamic view presentation uses a sliding resistivity scale that is applied at 1-ft intervals. This view enhances the visibility of small details by maximizing the contrast between features. The static view allows the comparison of resistivity over depth. When these resistivity values are core-calibrated, the micro-imager becomes a powerful tool for estimating rock properties.

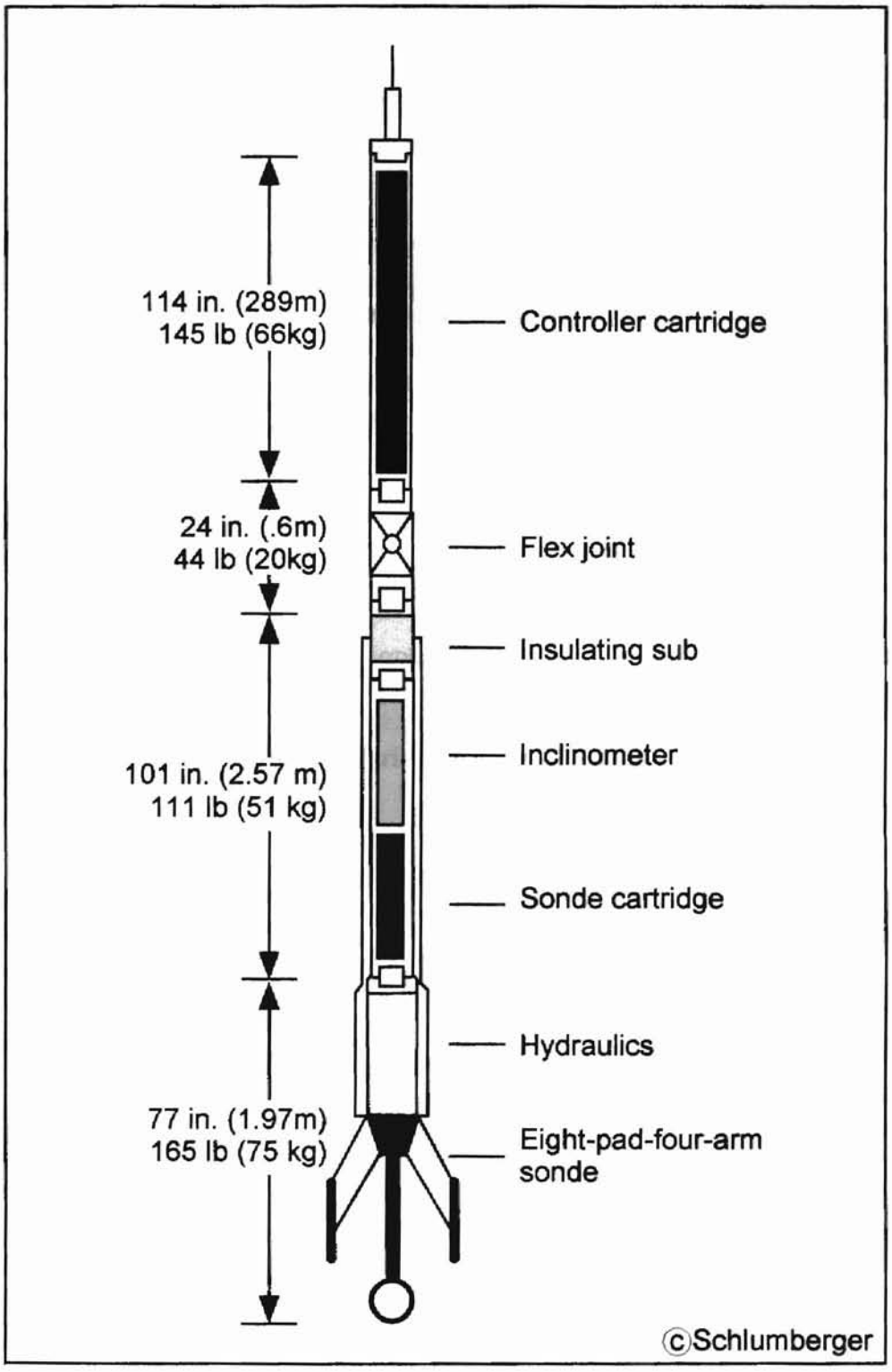

Figure 23. Schematic representation of FMI tool.

Imaging Filtering

Most micro-images are viewed in two forms, static and dynamic. The static view has a fixed resistivity scale over the logged interval so that beds with the same color shade have the same resistivity. The static view allows comparison of resistivities over depth. The dynamic view presentation uses a sliding resistivity scale that is applied at 1-ft intervals. This view enhances the visibility of small details by maximizing the contrast between features. Electrical images allow a different approach to sedimentary rock in boreholes. The data enhance sedimentological interpretations as well as reservoir characterizations. When these resistivities are core-calibrated, the micro-imager becomes a powerful tool for estimating rock properties.

Chromatic Variation in LR/LC Sandstones

Kerr-McGee Company provided static micro-imager views over two intervals that were cored. These cores were in the LR/LC section informally called the "9900 ft" sandstone. Lithologic heterogeneity provided ample bed boundaries to permit image to core correlation on an inch-scale. Once correlated, core sampling allowed the detailed analysis of the rocks to determine properties that were responsible for chromatic changes in the images.

Four basic color groups were identified on the micro-images: 1) dark gray to brown, 2) white, 3) yellow, and 4) orange. Mixing and transitional zones also occur.

Dark Gray to Brown Zones

Dark gray to brown-colored zones represent clay-rich rocks. Shale and claystone beds and laminae appear as dark bands on the static view. Some dark bands contain sand and/or silt-rich laminae, burrows, and flowage features that are more resistive (lighter color) and contrast with the clay-rich rocks (Figure 24).

White Zones

White zones represent the least conductive (most resistive) rocks. Thin section microscopy of this zone indicates resistivity is directly related to abundant cement (Figure 25). Calcite cement is predominant (Figure 25) and nearly occludes porosity in this zone. Silica cement is less pervasive, but gives the same white signature as the calcite. In some white zones, kaolinite is important cement (Figure 26).

Yellow Zones

Yellow zones are porous sandstones (Figure 25 and 27). They contain authigenic clay, but have significant moldic or enlarged moldic porosity that is relatively clay free (Figure 27).

Orange Zones

Orange image color is related to the abundance of authigenic clay in this zone (Figure 25 and 28). Clay-free moldic porosity is uncommon. Bound water associated with these clays reduces resistivity and gives the darker (orange) color characteristic of this zone.

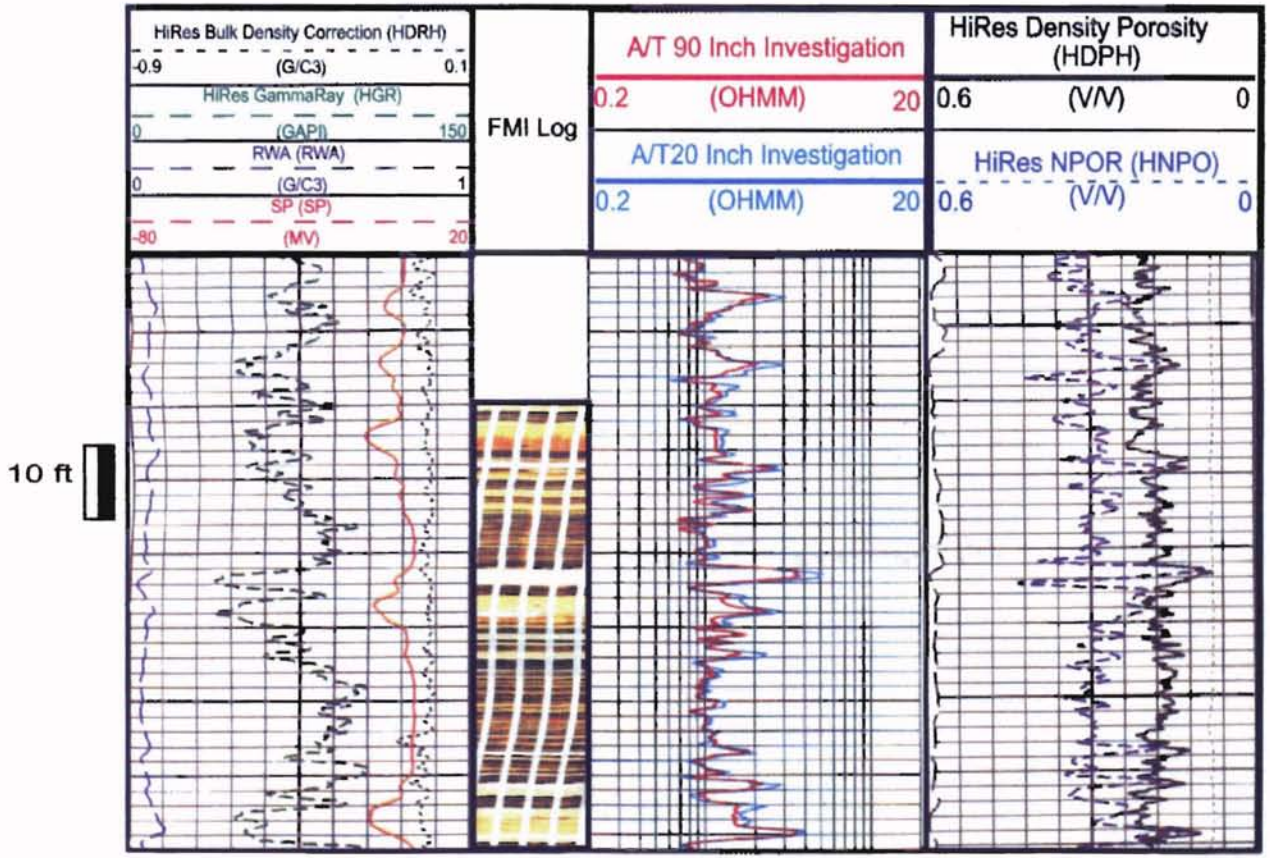

Figure 24. Static view micro-imaging log over a portion of the LR/LC 9900-ft Vicksburg reservoir. Four basic color groups that are correlated to lithologic properties are (1) dark gray to brown = shale or claystone, (2) white = tightly cemented sandstone, (3) yellow = porous and permeable sandstone, and (4) orange = porous, clay-rich sandstone. Mixed and transition zones are also evident.

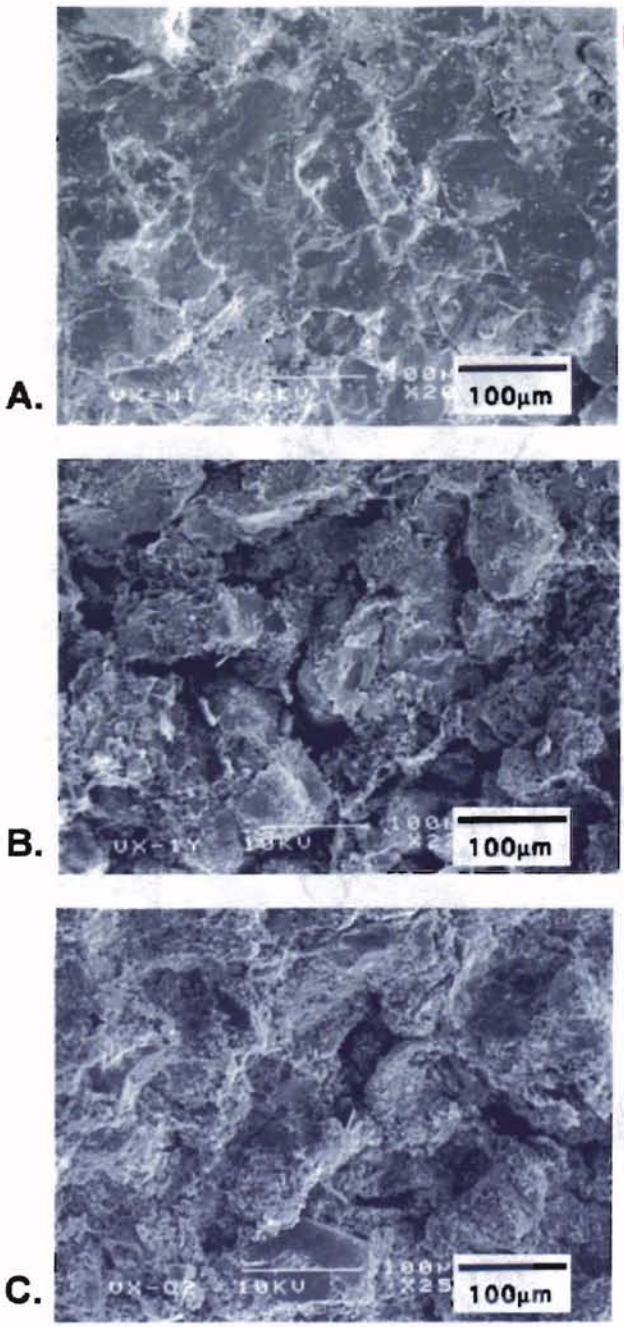

Figure 25. SEM photomicrographs with porosity and permeability data that illustrate the general petrographic and reservoir characteristics of sandstone.

(A) White zones (highest resistivity) are cemented and low porosity.

(B) Yellow zones (intermediate resistivity) are high porosity and permeability.

(C) Orange zones (lowest resistivity) are high porosity, but low permeability as the result of abundant pore-filling authigenic clays.

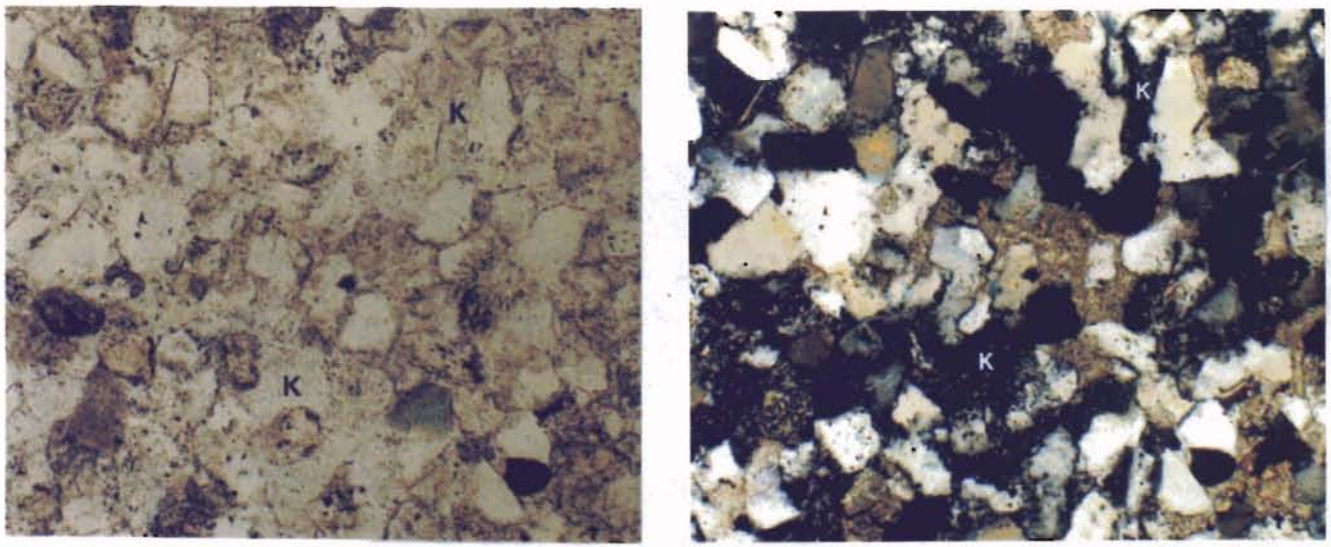

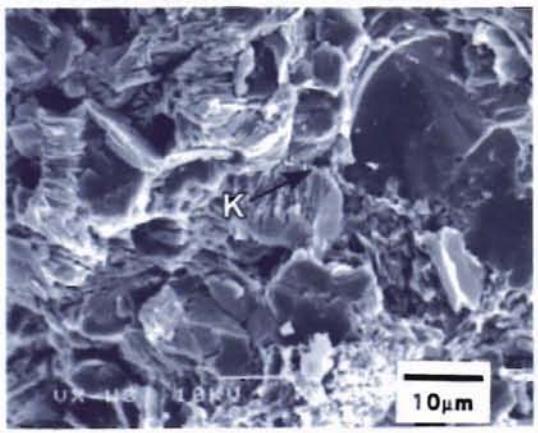

Figure 26. Petrographic characteristics of a white chromatic zone.

A. Photmicrograph indicates extensive calcite cement and scattered patches of kaolinite (K). PPL and CPL.

B. SEM photomicrograph of pore-filling kaolinite (K). Kaolinite-filled pores in calcite-cemented sandstone are an important component of white zone seals.

A.

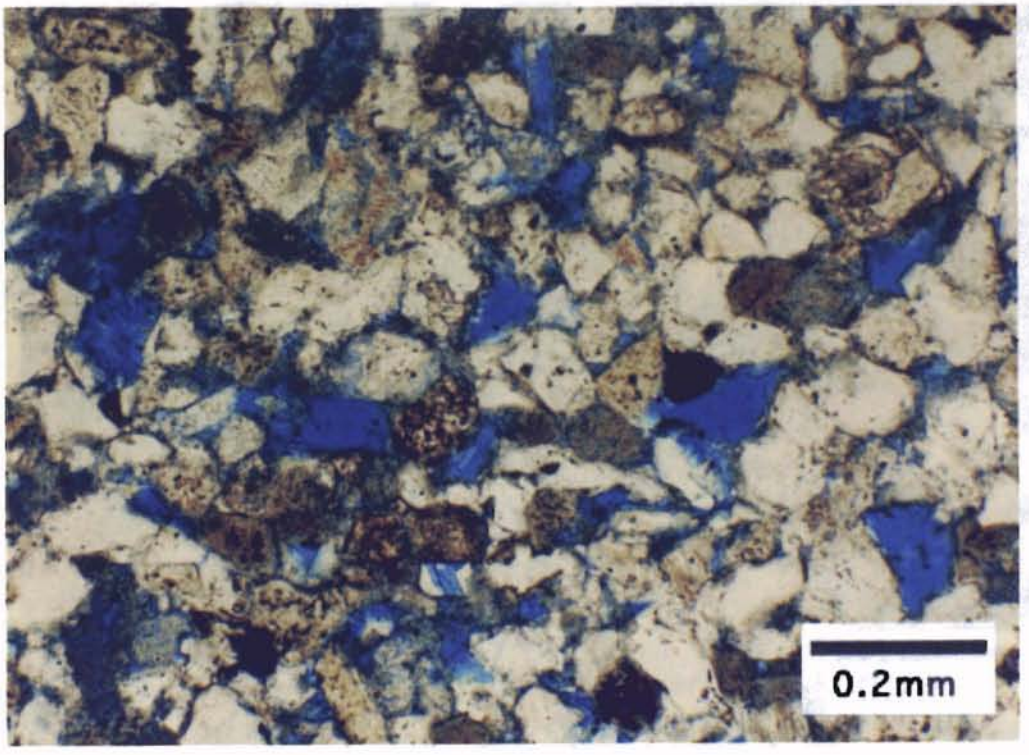

B.

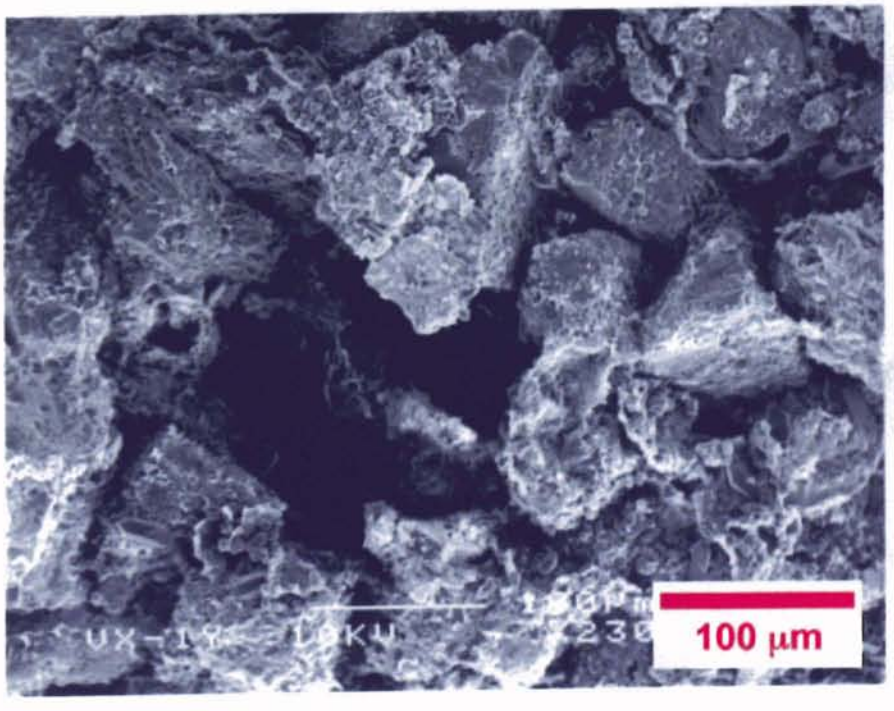

Figure 27. Petrographic characteristics of a yellow chromatic zone.

A. Photomicrograph of porous and permeable yellow zone with distinct blue-filled moldic porosity. PPL

B. SEM micrograph showing intergranular and moldic porosity common to yellow zones.

A.

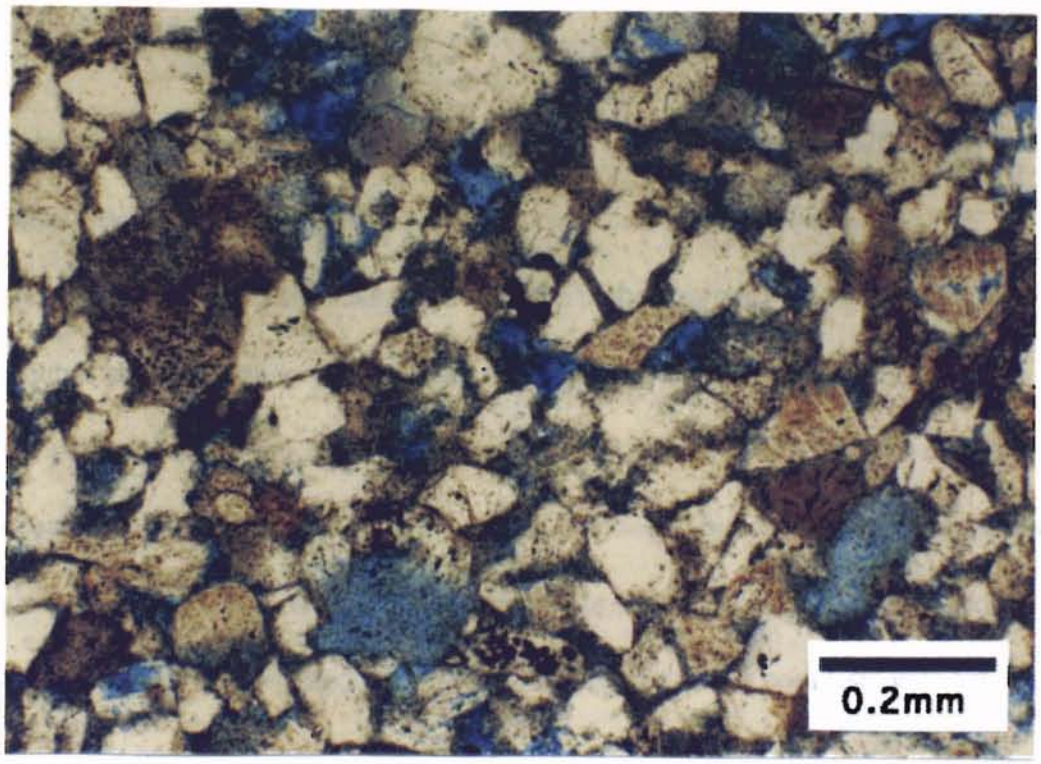

B.

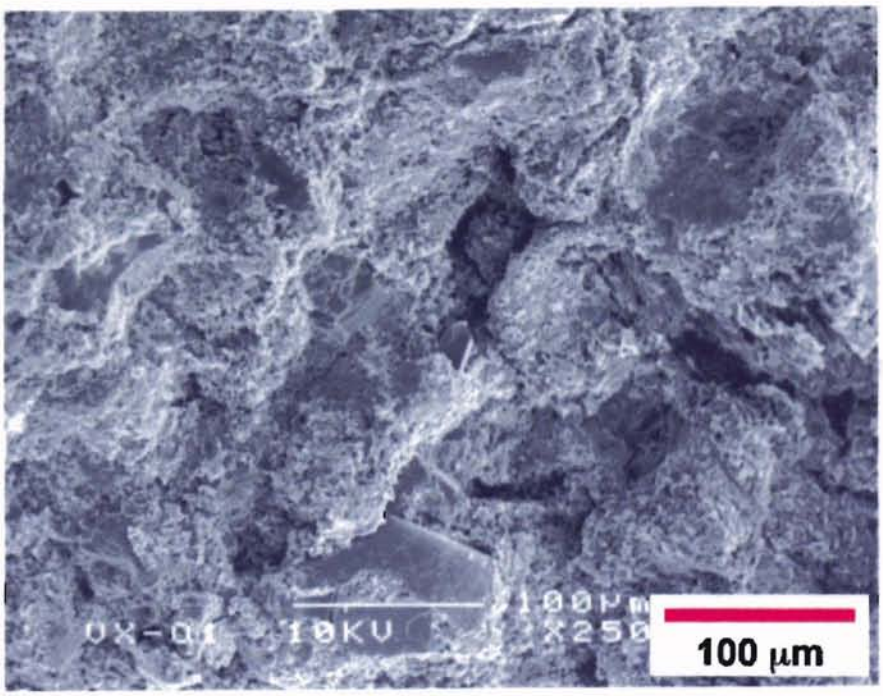

Figure 28. Petrographic characteristics of an orange chromatic zone, Vicksburg sandstone.

A. Photomicrograph of very fine grained sandstone with most pores partially filled with authigenic clays. Open moldic porosity is noticeable absent. PPL

B. SEM photomicrograph of extensive authigenic clay coating grains and filling pores.

Transition and Mixed Zones

Transition and mixed color zones are common in the Vicksburg LR/LC interval. Yellow zones frequently contain white areas that represent patches of cement. Alternately, white zones contain yellow areas where higher porosity was preserved. Orange patches are common in yellow zones, but are noticeably absent in white ones. Frequently, yellow and orange zones have transitional contacts as clay content changes across the sandstone. Yellow to white transitions also occur, but are less common. Many small-scale depositional, diagenetic and biogenic features are evident in the gray-brown zones. These features are detected because their higher resistivity contrasts with the adjacent clay-rich beds.

Reservoir and Seal Properties

All chromatic zones were sampled for core-plug analyses and capillary pressure measurements. In addition, mini-permeameter measurements were also available for one core. When possible, thin sections were made of core plugs to improve the visualization of rock architecture. Porosity values derived from core plug and thin-section analysis were compared to porosity log signatures of density and neutron porosity curves. Wire-line log characteristics were determined for each zone and used to develop a quick-look approach to log analysis. Figure (29) are shallow (20 inch) resistivity and micro-resistivity logs shown on track 2. This micro-resistivity log is derived using one pad from FMI tool. Gamma ray log is also displayed on track one. The spatial distribution of white, yellow, orange and brown chromatic zones were represented on this log.

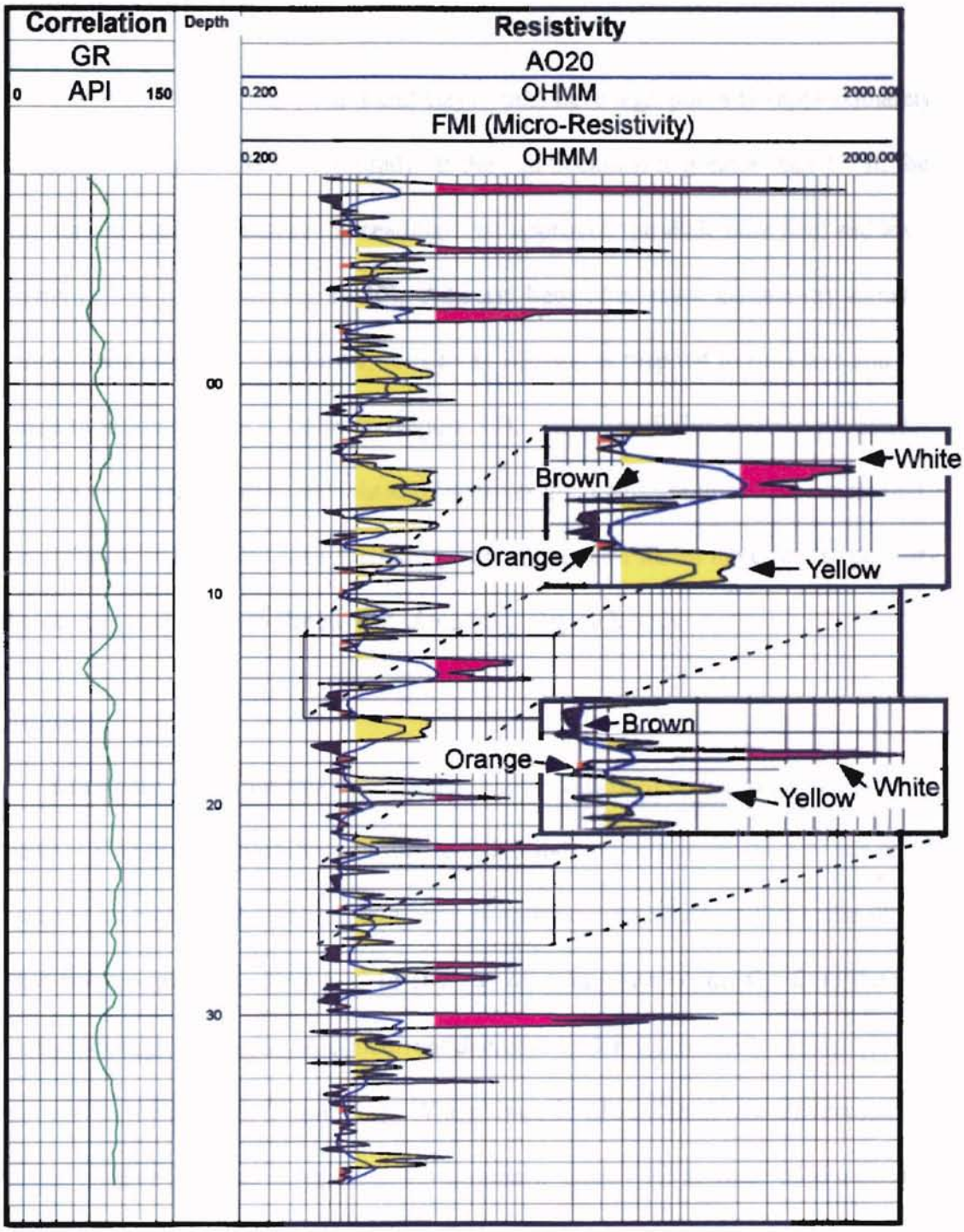

Figure 29. Micro-resistivity log of chromatic distribution in the LR/LC interval. In thicker beds (>1.5 ft) micro-resistivity and high resolution resistivity display similar patterns. In zones <1.5 ft thick, the microresistivity tool provides more accurate measurements by minimizing the effects of adjacent beds. Note that white chromatic zones are shaded pink in this illustration.

Dark Gray to Brown Zones

These clay-rich rocks (shales and claystones) have high porosity (approximately 18%) and low permeability (<0.005 md). If the bed thickness is greater than 1.5 ft, they exhibit normal high gamma-ray log readings that approach the shale base line, and low resistivity (0.5-0.7 ohm-m) (Figure 30). Adjacent beds often mask gamma-ray signatures of thinner units (<1.0 ft.). However, resisitivity signatures respond to the clays and decrease to around 0.5 to 0.7 ohm-m (Figure 30). High-resolution neutron porosity curves are very responsive to thin shales/claystones and delineate discrete beds around 1.0 ft thick (Figure 30). In this area, Vicksburg sandstones and shales have similar porosity, so the density tool was not effective in identifying clay-rich beds.

White zones

Core plug measurements indicate that highly cemented white zones have low porosity (<8%) and permeability (<0.001 to 0.003 md). White zones >1.5 ft. are readily recognized on high-resolution resistivity and porosity curves. Reduced smectite-illite content and low porosity cause a 12 to 18% decrease in neutron porosity from the values measured for adjacent beds. A concurrent decrease in density porosity of 6 to 10% occurs across these zones (Figure 31). White zones in LR/LC intervals are recognized by a marked relative increase in resistivity (3-4 ohmm). Beds >1.5 ft. thick have a deep invasion profile and a spike-like signature in which all resistivity curves have a similar form. Thinner beds (<1.5 ft.) have a similar spike-like signature, but the increase in resistivity is reduced as a result of the tool detecting porosity in adjacent porous beds (Figure 31). Gamma-ray logs indicate that white zones are less radioactive than adjacent

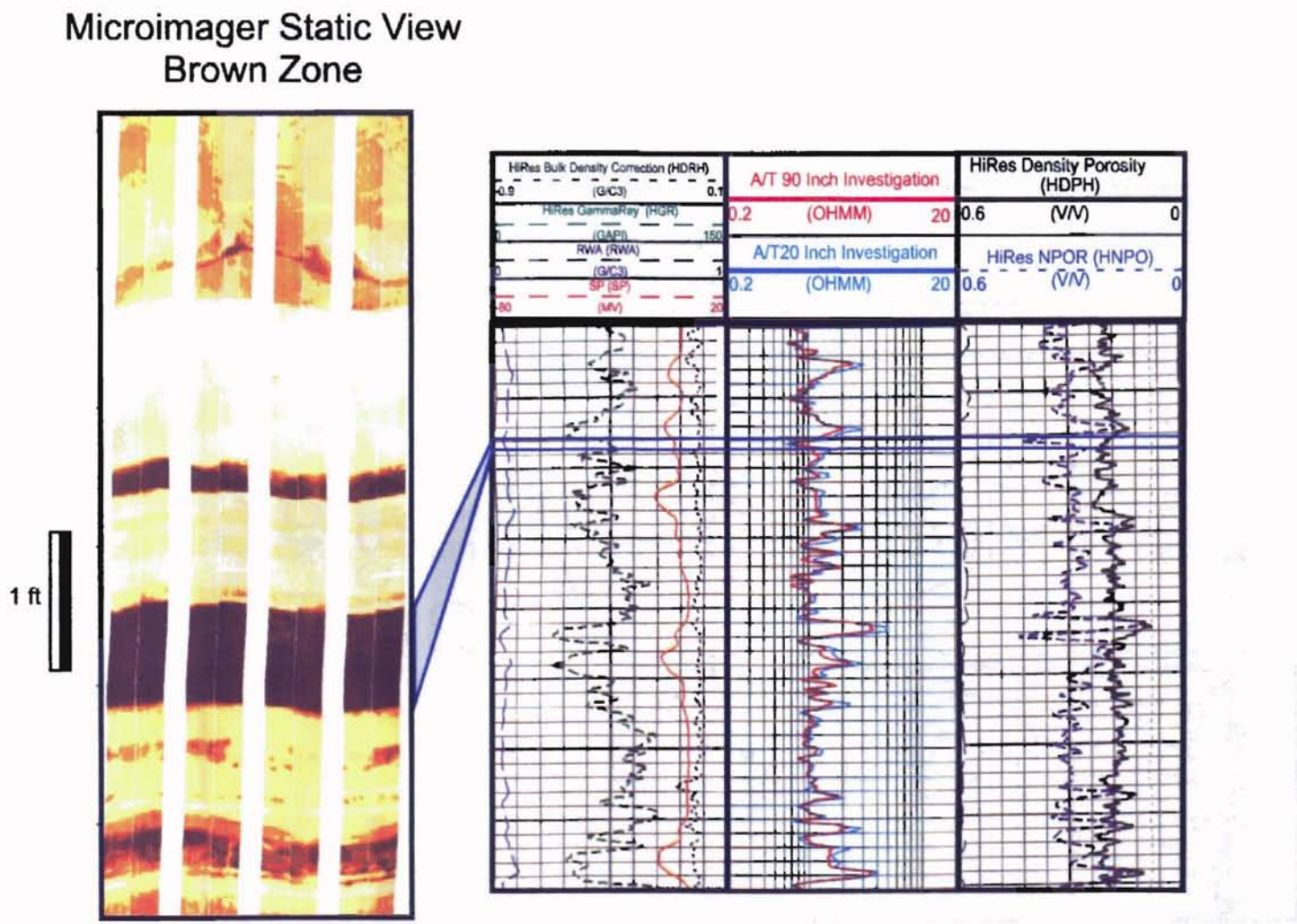

Figure 30. Wireline log characteristics of static view chromatic zone. Porosity and permeability measurements are from conventional core analysis. LR/LC 9900-ft sandstone, TCB field.

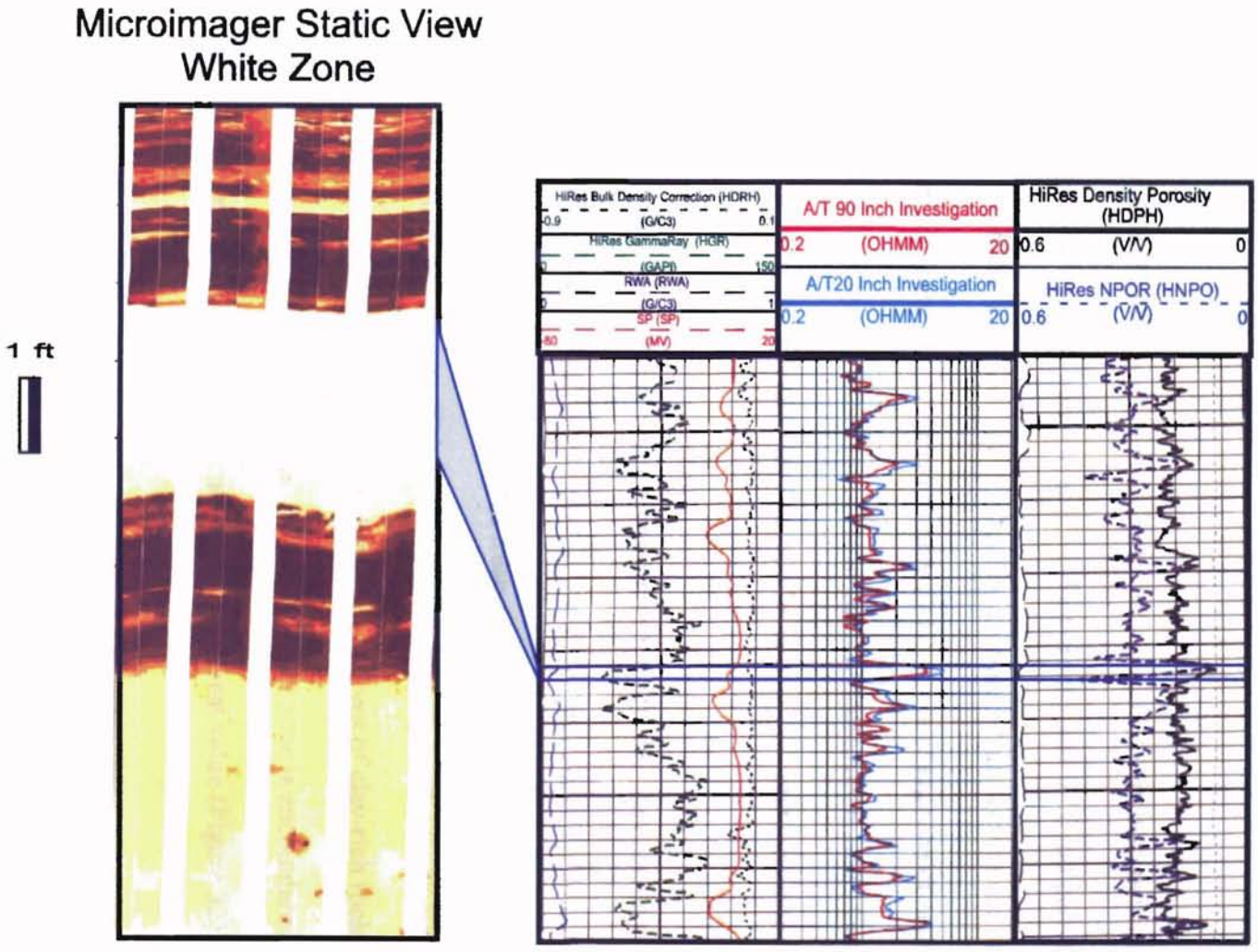

Figure 31. Wireline log characteristics of static view chromatic zone. Porosity and permeability measurements are from conventional core analysis. LR/LC 9900-ft sandstone, TCB field.

sandstones rich in smectite-illite. This cleaning affect becomes more apparent if the zone is >1.5 ft. thick.

Yellow Zones

Yellow bands are sandstones with high porosity and relatively high permeability. Core plug analyses indicate these zones average 21% porosity and 0.16 md permeability. The increased permeability in yellow zones is readily evident in thin section and scanning-electron microscopy (Figure 21). In thicker zones (>1.5 ft.) convergence of neutron and density porosity is also observed, however neutron-density crossover is rare. Gamma-ray response shows a decrease in radioactivity that results in a 45 API units deflection from the shale baseline.

A key to recognizing yellow zones is their invasion profile. Permeability in these sandstones is reflected in a separation between the deep (90, 60, 30, & 20 in) and shallow (10 in) resistivity curves. Separation indicates fresh-water filtrate invasion has increased resistivity adjacent to the wellbore. This profile is most evident when yellow zones are adjacent to shales or claystones (Figure 32). Resistivity curves of clay-rich rocks track one another and often appear as one curve. When a yellow zone is encountered, the resistivity curves separate and the 10 in.-curve has the highest value (Figure 32).

Orange Zones

Orange zones on the static micro-imager view are sandstones with relatively high porosity, but low permeability. Core plug measurements indicate orange zones average

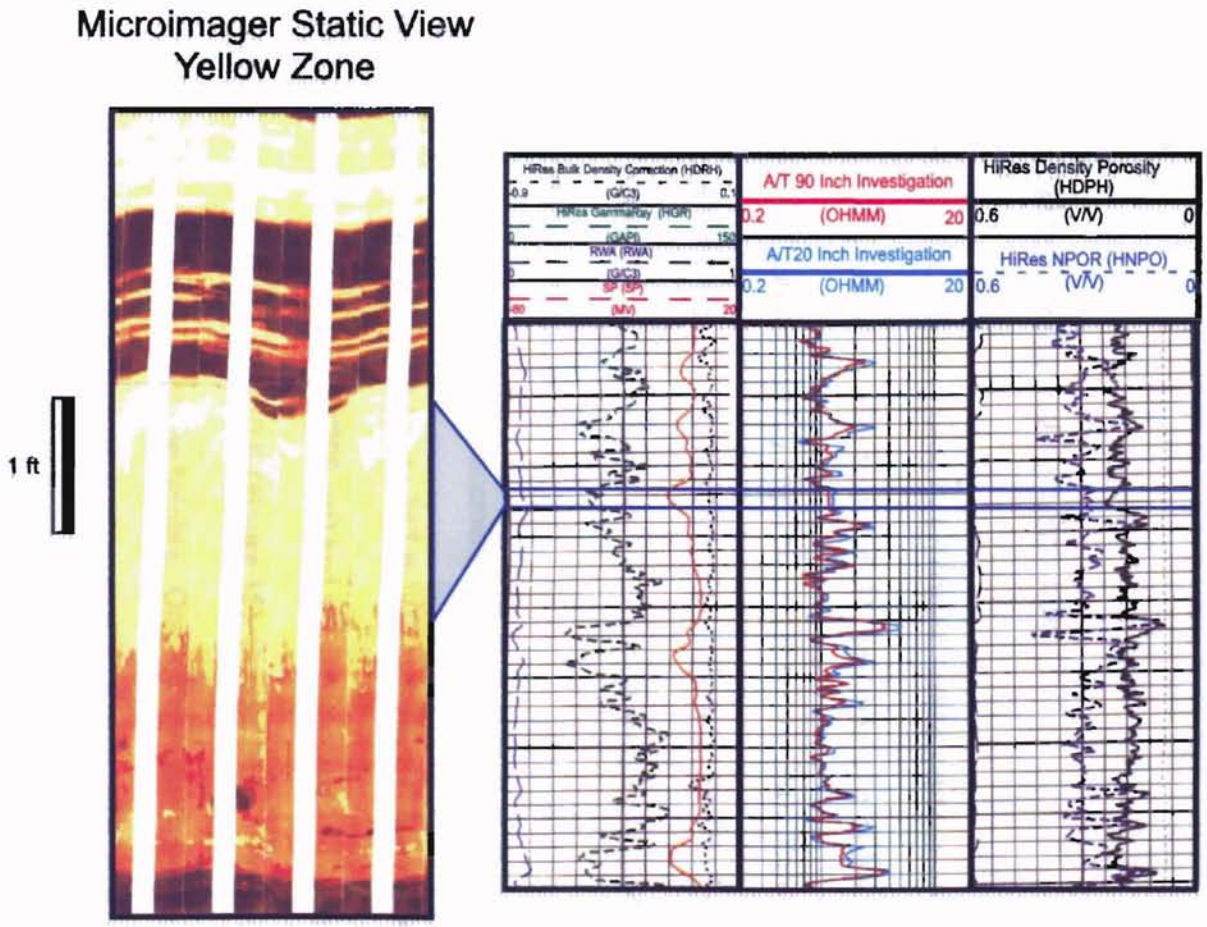

Figure 32. Wireline log characteristics of static view chromatic zone. Porosity and permeability measurements are from conventional core analysis. LR/LC 9900-ft sandstone, TCB field.

18% porosity and .06 md permeability. Thin-section and scanning-electron microscopy reveal the porosity in these sandstones is greatly reduced by pore-lining and filling authigenic clays. Log signatures resemble those of yellow zones. Resistivity curves separate as a result of filtrate invasion, but the spread is less than that of yellow zones (Figure 32 and 33). This pattern reflects the reduction of permeability and/or less gas content in this zone.

Capillary Pressure, Sealing Capacity and Pore Structure

Capillary pressure curves were used to determine sealing capacity and pore structure. Sealing capacity was defined in terms of (1) the height of a hydrocarbon column the rock will hold without leaking and (2) displacement pressure (Pd). Pore structure evaluation included size, sorting, and distribution of pore throats. Phillips Petroleum Company provided mercury injection measurements for core samples of sandstones representing all chromatic zones.

White zones have the highest displacement pressures (Pdma) (up to 2454 psi) and the highest gas column heights (Hpd) (up to 547 ft.) (Figure 34). Yellow zones have the lowest displacement pressures (Pdma <200 psi) and gas column heights at displacement pressure that are commonly less than 10 ft (Figure 35). Orange zones display a wide range of displacement pressures and gas column heights. One orange zone sample with microporosity, but no apparent moldic porosity (all pores were clay filled), had a displacement pressure of 682 psi and gas column height of 152 ft. A second orange sample exhibited typical values for displacement (Pdma = 171 psi) and gas column height (38 ft).

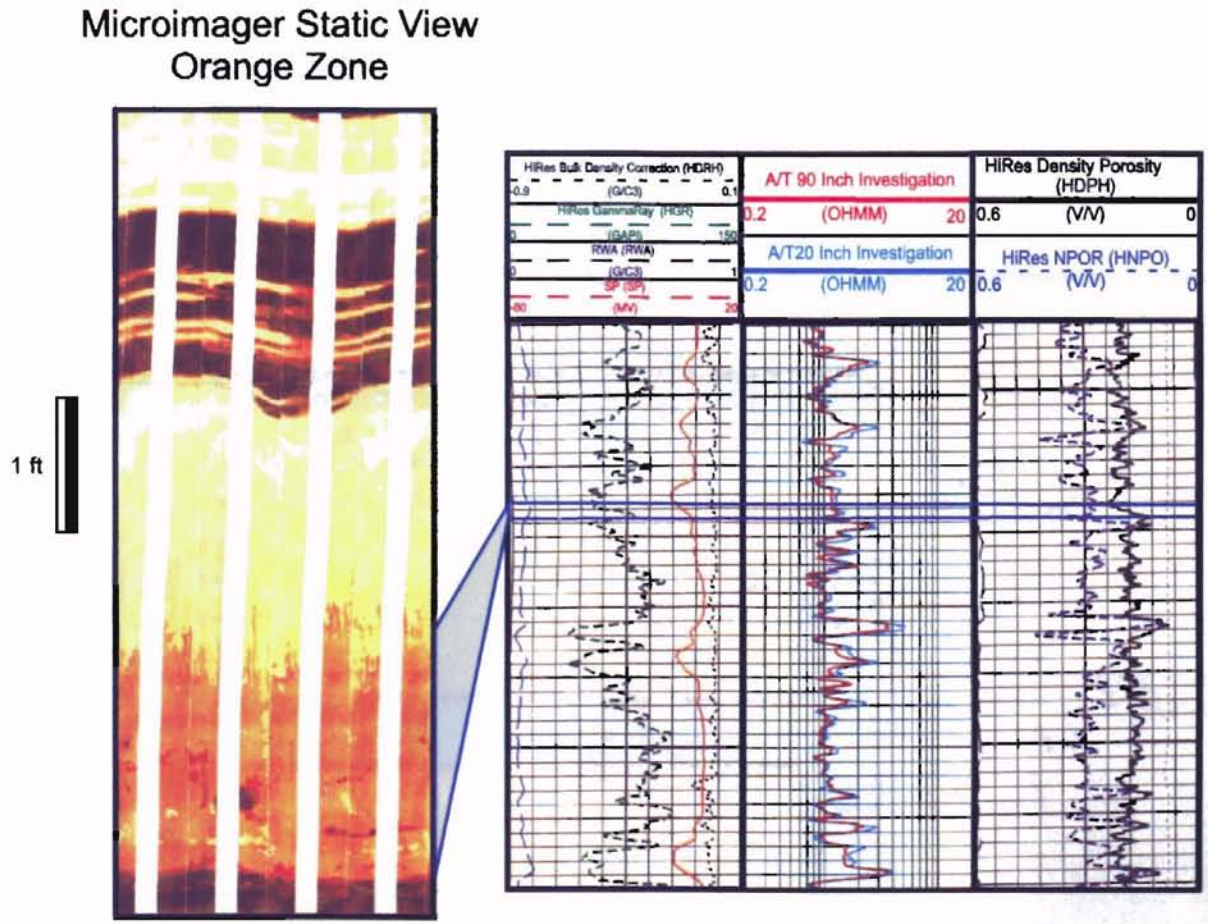

Figure 33. Wireline log characteristics of static view chromatic zone. Porosity and permeability measurements are from conventional core analysis. LR/LC 9900-ft sandstone, TCB field.

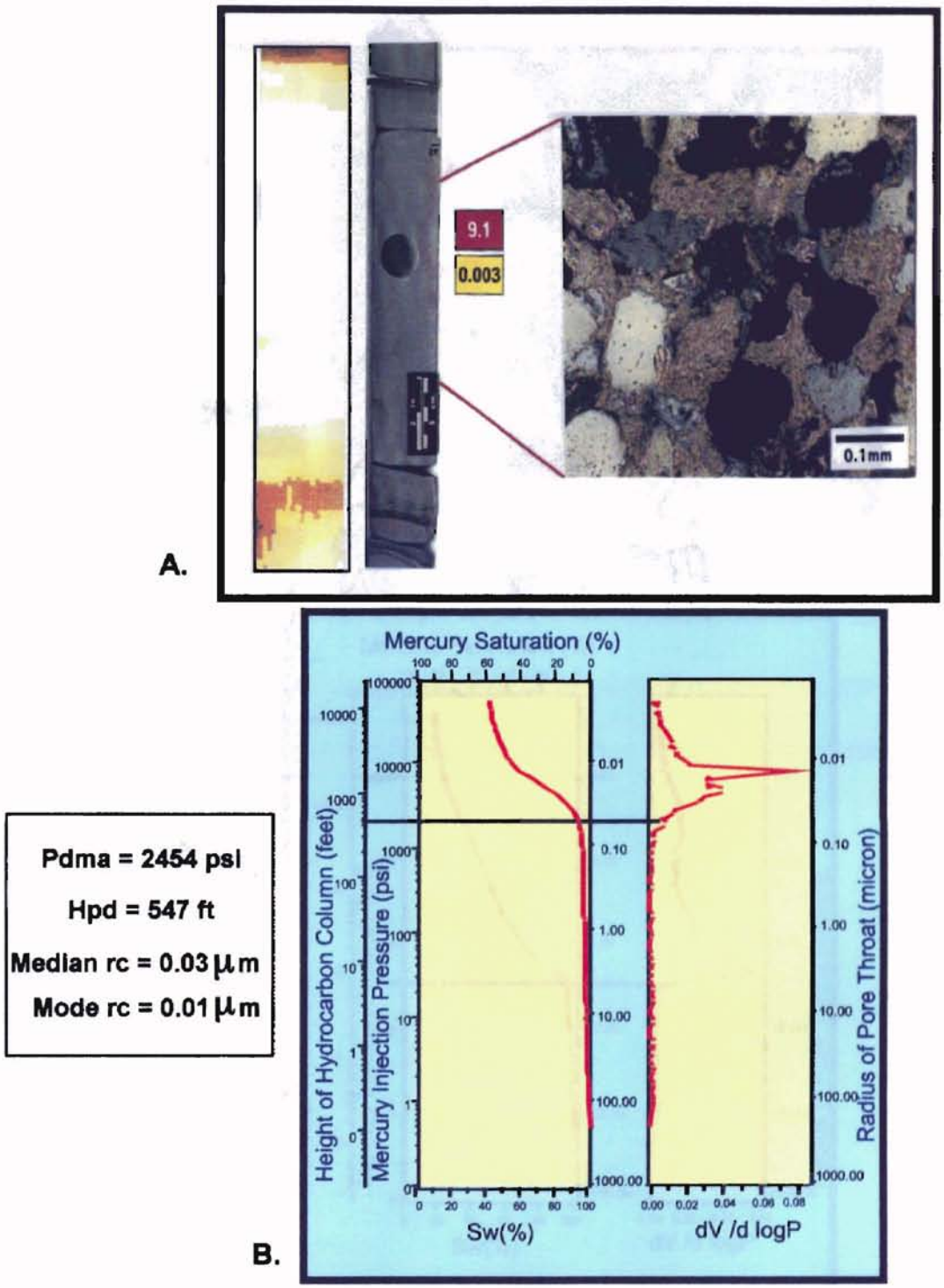

Figure 34. White zone

A. FMI, core photo, and photomicrograph of white zone demonstrates lo porosity and permeability due to high cementation.

B. White zone with high displacement pressure (Pdma), and highest gas column heights (Hpd).

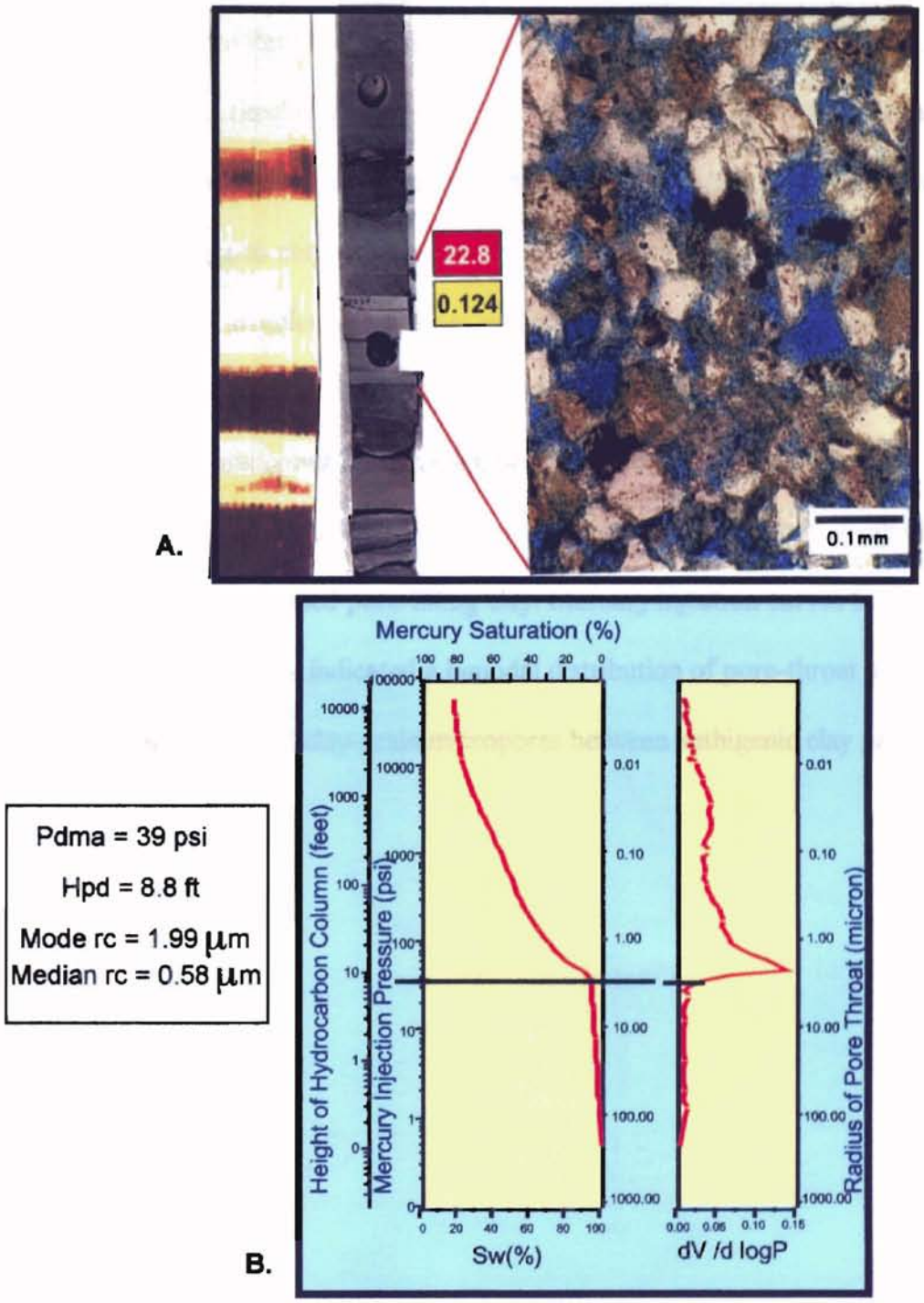

Figure 35. Yellow Zone

A. Photomicrograph of yellow zone with moldic porosity.

B. Capillary pressure data demonstrates low displacement pressures (Pdma), and low gas column (Hpd) height.

Pore throat size, sorting, and distribution were derived from capillary pressure curves. The sorting of pore throats reflects the rocks ability to accept hydrocarbons. Pore space in well sorted rocks rapidly saturate with hydrocarbons once a threshold buoyancy pressure is reached. Poorly sorted rocks saturate slower and require a pressure increase over a much broader range to obtain the same hydrocarbon saturation (Jennings, 1987). Pore throat sorting for all samples ranges from moderately to poorly sorted. Median pore-throat size ranges from 0.03 to 0.96 microns. Median pore throat size for white zones is less than 0.1 micron. Yellow zones have median pore throat apertures that range from 0.2 to 0.96 microns. Orange zones also have a wide range of median pore throat apertures that reflect the amount of dispersed pore-filling clay. Mercury injection curves for most yellow and orange zone samples indicated a bimodal distribution of pore-throat apertures between large moldic pores and clay-grain micropores between authigenic clay particles (Figure 36).

A.

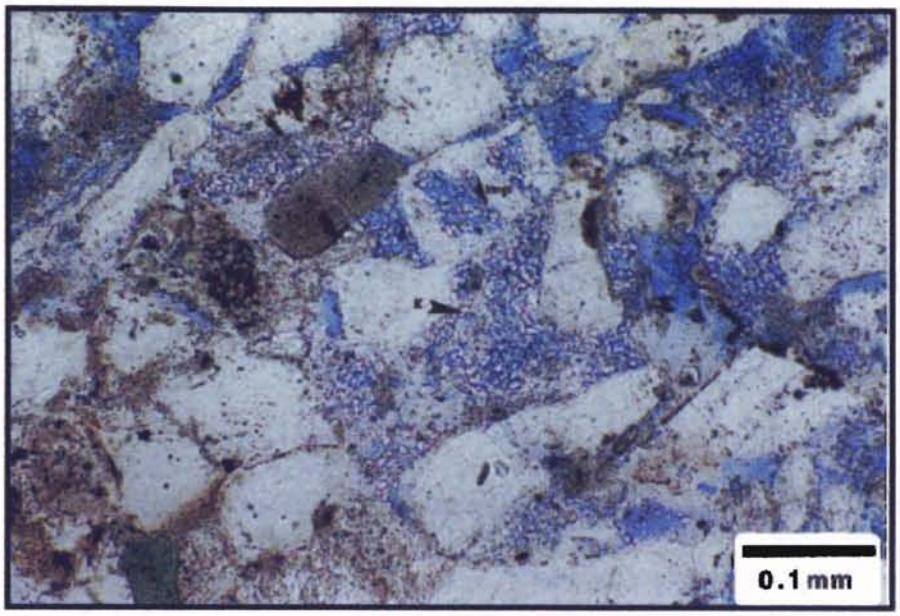

B.

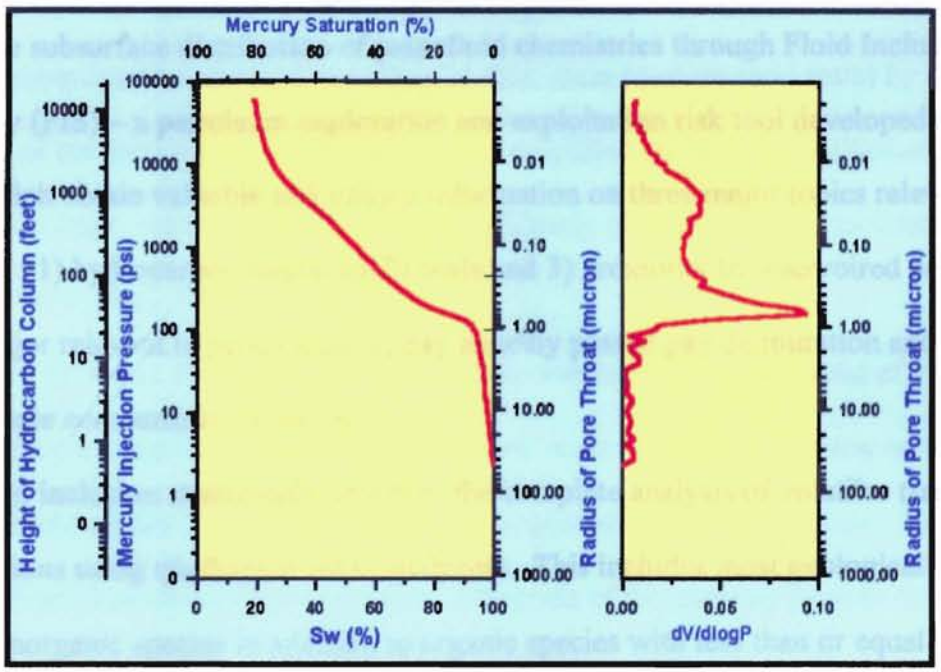

Figure 36. A. Photomicrograph of macro and micro-porosity.
B. Capillary pressure curves showing bimodal pore throat sizes.

CHAPTER V

FLUID INCLUSION STRATIGRAPHY RELATIONSHIP TO OVERPRESSURE

Introduction

The purpose of this chapter is to compare preserved fluid inclusions with the known over pressuring in the Gulf Coast Region. Fluid inclusions provide the only direct evidence of paleofluids existing in the subsurface, and as such have the potential to record conditions accompanying geologic processes, including petroleum migration. By studying the subsurface distribution of paleofluid chemistries through Fluid Inclusion Stratigraphy (FIS) – a petroleum exploration and exploitation risk tool developed at Amoco, which obtain valuable and unique information on three major topics relevant to exploration : 1) hydrocarbon migration 2) seals and 3) proximity to reservoired petroleum and two major relevant to production 1) pay zone\by passed pay delimitation and 2) reservoir-scale compartmentalization.

Fluid inclusion stratigraphy involves the complete analysis of volatiles trapped in fluid inclusions using quadrapole mass analyzers. This includes most geologically important inorganic species in addition to organic species with less than or equal to 13 carbon atoms. The resulting analysis of the petroleum fraction is comparable to the low-molecular weight fraction of a whole-gas chromatographic – mass spectrometer (GCM) analysis (Hall, 1999).

Procedure

Samples of rock cuttings are washed, picked and separated to remove drilling fluid, lost circulation materials and other metallic particles from the drillstring. Cleaned samples are loaded, together with appropriate standards, into 630-hole trays, covered with a metal impact slug and placed into a vacuum oven at elevated temperature for a minimum of 24 hours. This is done to remove remaining adsorbed organic and inorganic volatile material up to C_{13}. Sample trays are then placed into an ultra-high vacuum chamber and evacuated for approximately 8 hours. Bulk fluid inclusion volatiles are afterwards instantaneously released from each sample in a sequential manner by automated mechanical crushing. Volatile organic and inorganic species are dynamically pumped through four quadrupale mass analyzers where molecular species are ionized by electron bombardment, separated according to their mass to chare ratio (m/z) by application of combination of RF and DC fields, amplified by electron multipliers and recorded as voltage, where millivolts are approximately proportional to concentration in the ionized flow (Hall, 1999).

Fluid Inclusion Stratigraphy (FIS) analysis was carried out on a total of 403 cuttings and core samples composited from several wells to produce a nearly continuous section centered on the Vicksburg Formation, sampled at about 1 ft intervals. Samples span from depth intervals 5990-11616 feet. The goals of the analysis were to determine the distribution and chemical characteristics of hydrocarbons that have migrated through the penetrated section, to look for prominent seals that may correlate with known pressure cells and to establish whether or not nearby, undiscovered pay within potential reservoir intervals can be inferred. Additionally, FIS data was to be compared with FMI

data collected on the same section, to see if diagenetically controlled porosity bands can be correlated with fluid inclusion distribution.

Seal and Reservoir Identification

Fluid inclusion stratigraphy was carried out on a total of 403 cuttings and core samples from several wells to produce a nearly continuous composite section from the lower part of the Frio Formation, through the Vicksburg and into the Jackson Shale. These samples spanned a depth interval of 5990-11616 ft. The goals of this analysis were: (1) to determine the distribution and chemical characteristics of hydrocarbons that have migrated through the section, (2) identify zones of high inclusion frequency that might correlate to 1st and 2nd order seals and (3) establish the impact of these seals on migration paths and oil and gas accumulations. In addition, FIS data were compared with FMI data to determine if cemented bands and reservoirs could be identified at the core scale using fluid inclusion frequency distribution.

Pore fluids in the Gulf Coast are divided into two hydrologic regimes, hydropressure and geopressure. In the hydropressure zone, the pressure gradient is 0.465 psi/ft (normal hydrostatic), and rocks are under lithostatic pressure approximately 1.0 psi/ft. In the "soft" geopressure zone (pressure gradient 0.465 to 0.7psi/ft) the pore fluid supports part of the overburden load. Thus, the effective pressure on the rocks is less than the lithostatic pressure. At a pressure gradient of 0.7 psi/ft, the zone of "hard" geopressure is encountered. The 0.7 psi/ft value was chosen to define the top of the "hard" geopressure regime because it is at this value that resistivities increase

dramatically. Thus, this zone can easily be picked from electric logs (Loucks and others, 1981).

Fluids flow most readily through permeable units to areas of lower pressure, which are generally shallower in the section. Therefore, the distribution of sands and sandstones defines the major fluid flow path in the section. However, fluid also flow through shales but at diminished rates as a result of low permeabilities (10^{-6}md; Magara, 1978). Significant volumes of fluid may migrate through shales, given geologically significant periods of time. Hydrofractured shales at depth, may flow fluids through them more easily (Sharp, 1980).

Several sources were utilized to collect pressure data in the TCB field. The sources include calculated pressure data from initial well-head shut–in pressures, wire-line bottom hole pressure tests, wire-line formation tests and repeat formation tests. Overpressured Vicksburg Formation developed complex sealing patterns which reflect the deposition and compositional parameters of this formation. In general, these seals have a specific functional hierarchy and may be classified in three different categories.

1. 1st Order: 1st order seals are regional and separate normally pressured intervals from overpressured ones.
2. 2nd Order: These seals conform to various stratigraphic boundaries within the overpressured interval and subdivide it into reservoir-size compartments
3. 3rd Order: These are intra-reservoir seals that are relatively smaller scale. These seals further subdivide reservoir-sized compartments into smaller intra-reservoir ones and contribute to reservoir heterogeneity.

Figure (37) is pressure-depth profile of the data obtained from the TCB field. The 1st order seal separates the normally pressured to slightly overpressured Frio from the overpressured Vicksburg Formation. The 2nd order seals separate the high-stand system tract (Upper Vicksburg) from the lowstand system tract deposited (Lower Vicksburg). The 3rd order seals are intra-compartment seals. The seals are highly cemented containing abundant hydrocarbon fluid inclusions (Figure 38). During the cementation episode of a seal often entrapped pore fluid as inclusions. These inclusions contain a sample of the precipitating fluid and record a history of fluid migration in the basin. These seals are also represented as highest intensities of volatile responses on FIS pattern (Figure 39).

The FIS analysis indicated a marked change in the total volatile response that coincides with the regional seal that separates the Frio and Vicksburg Formations (Figure 39). This seal is recognized on the pressure-depth plot by an obvious shift in pressure values around 8000 ft deep (Figure 40). Furthermore, changes in the relative amounts of ionic species suggest different sources or migration pathways for hydrocarbons that filled reservoirs above and below this seal. Frio inclusions are relatively enriched in aromatics and naphthalene, while Vicksburg inclusion are enriched in lower molecular weight paraffins, including CH4 and C5 - C13.

FIS analysis of FMI-calibrated core samples indicate that white chromatic zones are richer in volatiles than adjacent orange and yellow zones (Figure 41). This response reflects an increased inclusion frequency in cements and suggests this tool is useful in identifying seals.

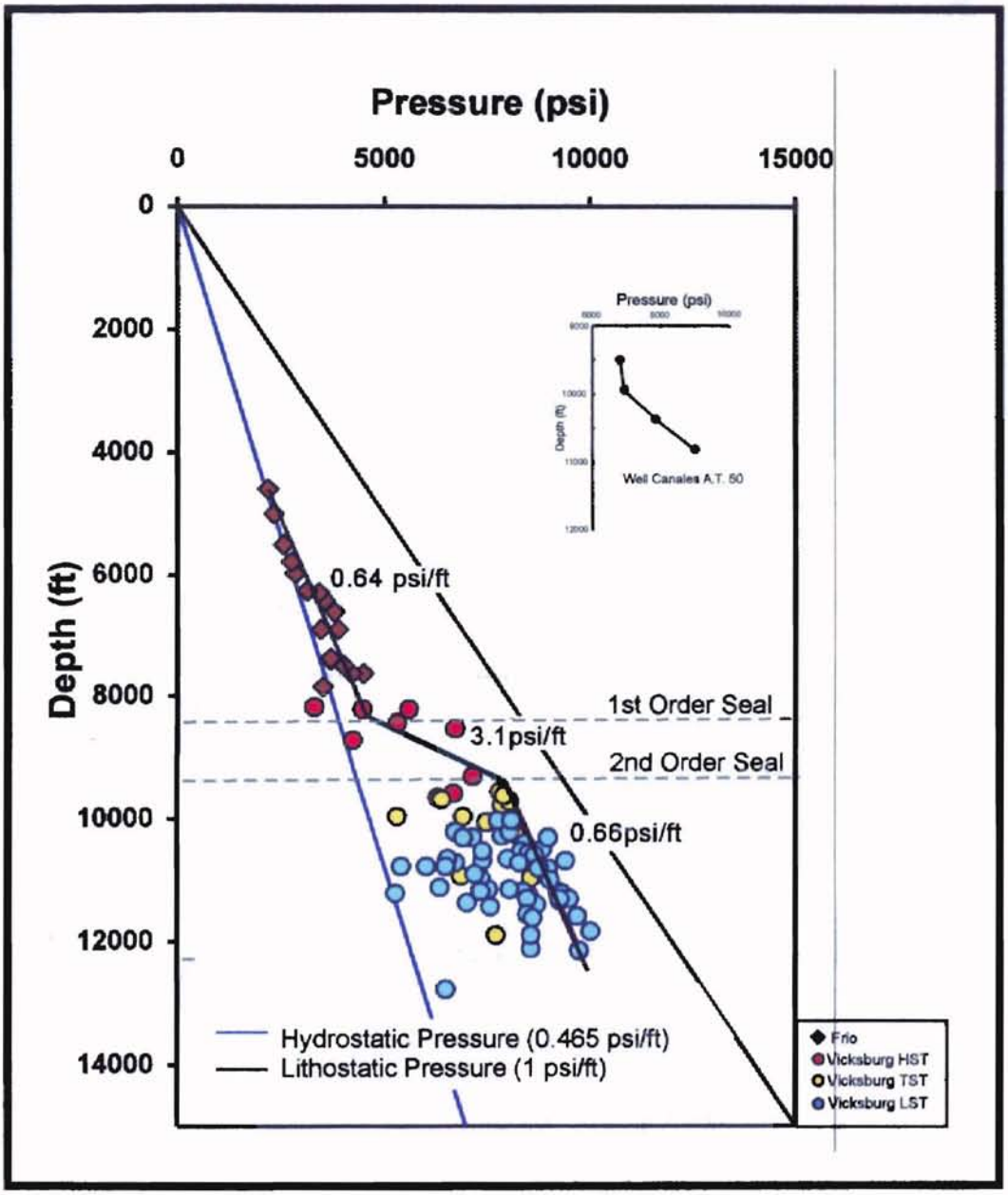

Figure 37. Compartmentalization of the Frio and the Vicksburg formations showing first and second order seals.

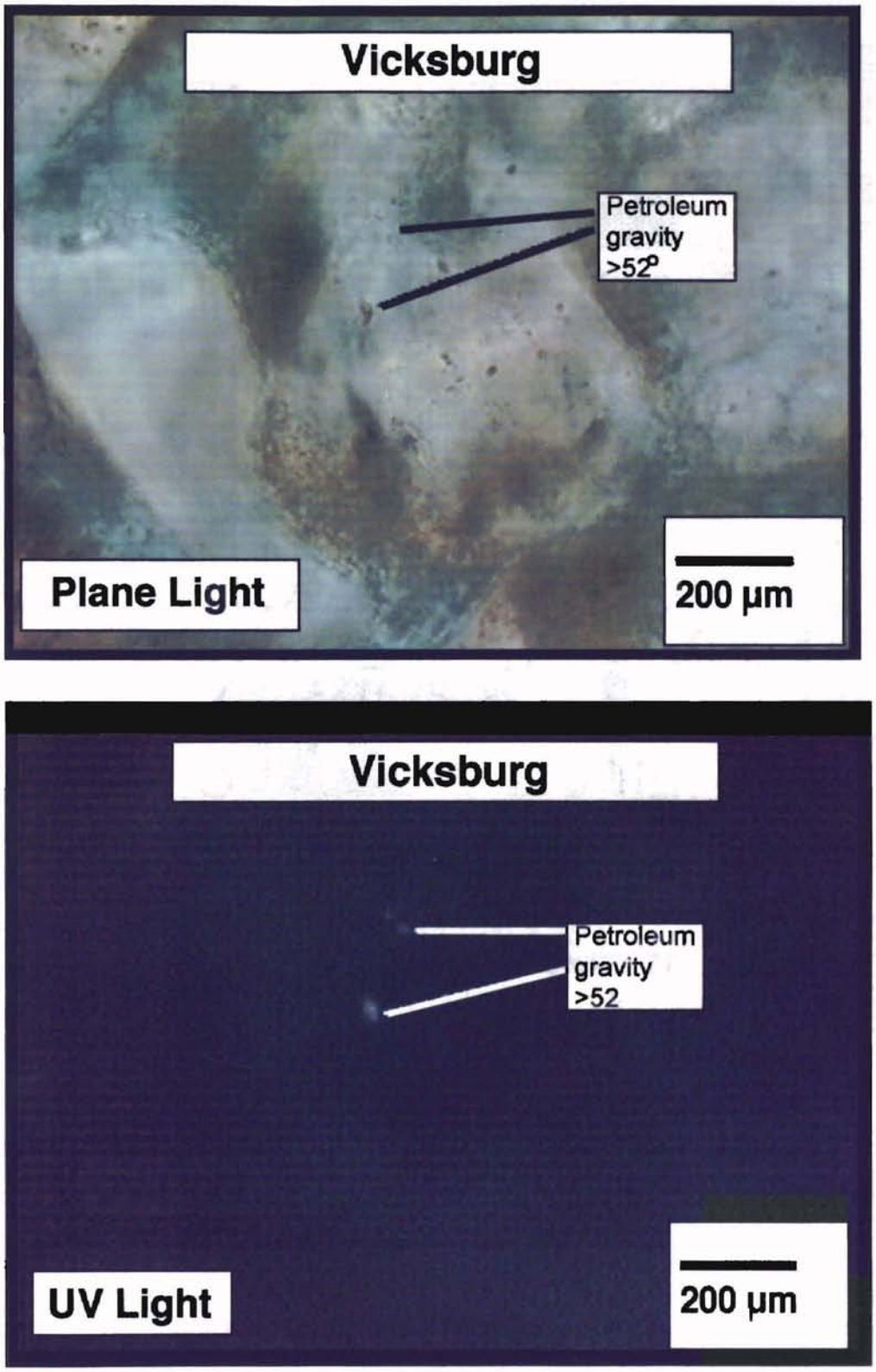

Figure 38. Photomicrograph of fluorescing petroleum inclusions.

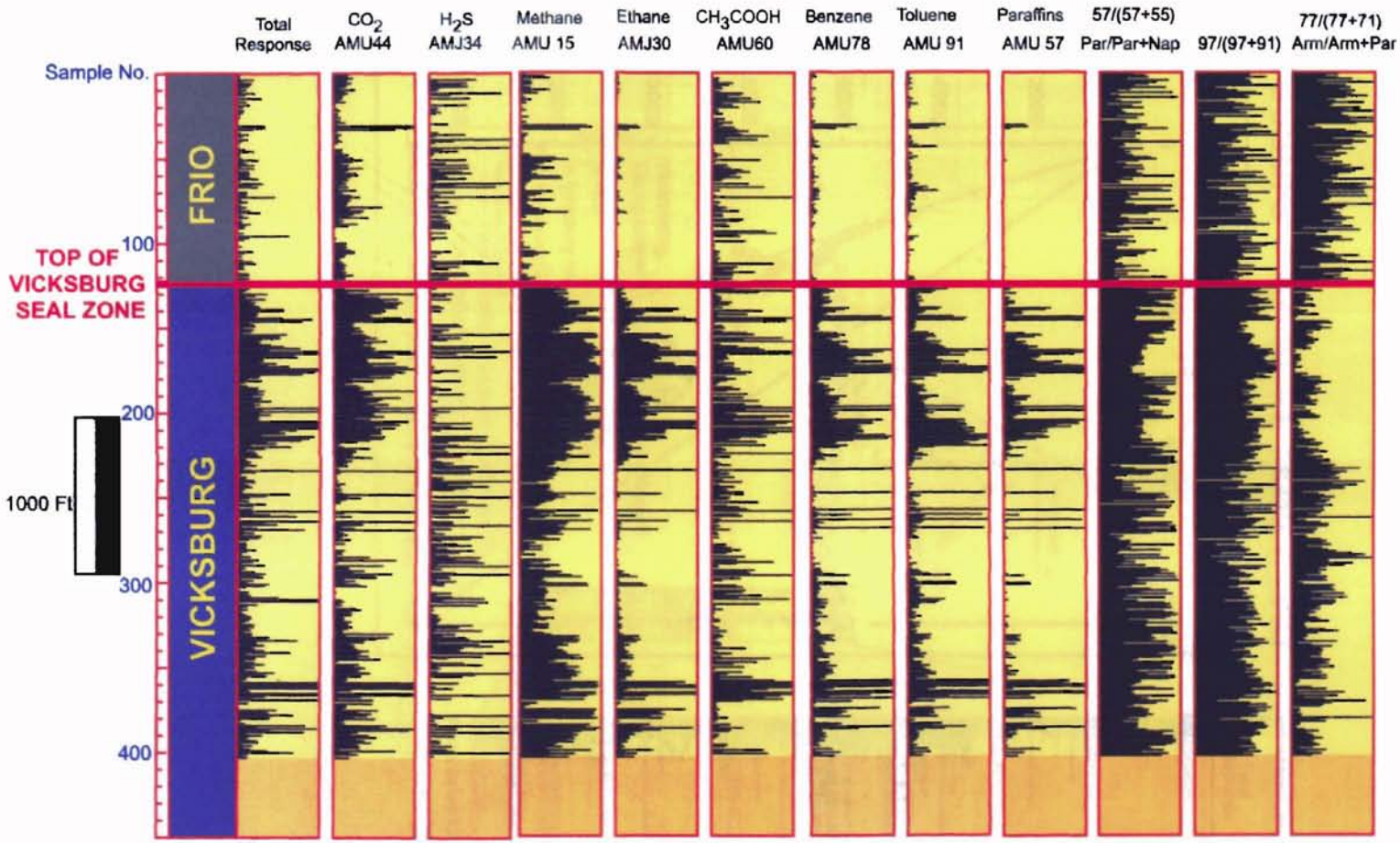

Figure 39. Changes in relative amounts of selected ionic species and ratios of ionic species. Peak intensity (relative amounts of species) increase to the right. Noticeable changes between responses in the Frio and Vicksburg sections suggest different sources and/or migration pathways on either side of the Vicksburg seal. Frio fluid inclusions are relatively enriched in aromatics (Arm) and naphthalene (Nap). Vicksburg inclusions are enriched in paraffins (Par), in particular, CH_4, C_2H_6, C_5 - C_{13} species, benzene and toluene.

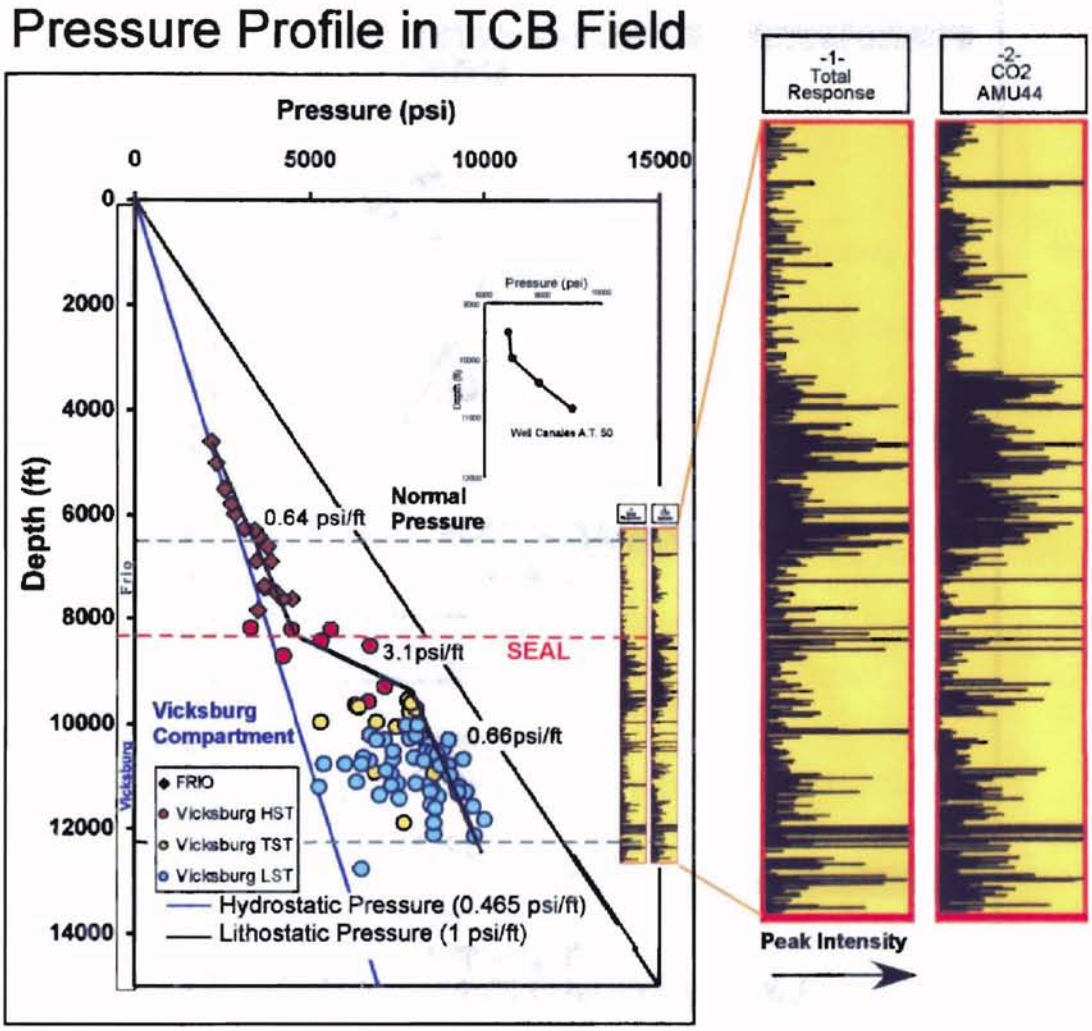

Figure 40. Correlation between pressure compartments, seals, and fluid inclusion stratigraphy (FIS) in TCB field, south Texas Gulf Coast. FIS indicates a marked change in total volatile response (increasing intensity to the right) that coincides with the regional pressure seal at the top of the Vicksburg Formation.

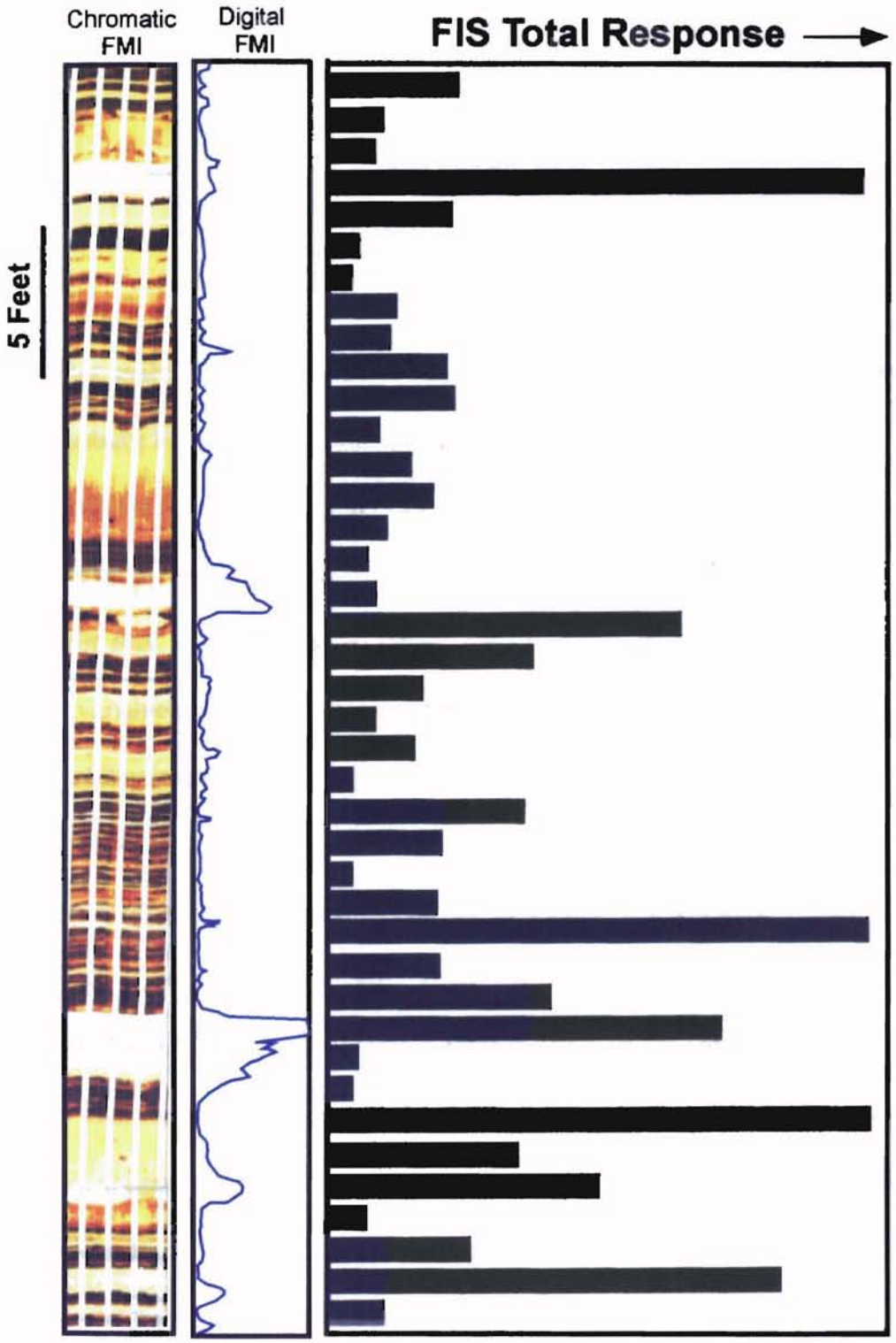

Figure 41. Relative intensities of volatile responses (increasing in the direction of the arrow) compared to chromatic and digital FMI data. FIS response to cement patches in mixed zones and white zones suggest the potential for using FIS to detect cement bands that contribute to reservoir heterogeneity.

CHAPTER VI

CONCLUSIONS

After analyzing various aspects of the low-contract/low-resistivity reservoir rocks in the Vicksburg Formation, several conclusions were made. These include:

1. Low resistivity/low contrast intervals in the Vicksburg Formation are composed of discrete thinly bedded reservoirs that are separated by seals. The reservoir beds are primarily silty, very fine-grained sandstones. Porosity values in the sandstones are highly variable as a result of presence of calcite, silica and clay minerals cements. Permeability is affected by the presence of various cements.
2. The Vicksburg Formation in the TCB is overpressured and compartmentalized. Highstand system tract reservoirs (Upper Vicksburg) and lowstand system tract reservoirs (Lower Vicksburg) are the two major compartments identified. The overpressured Vicksburg is separated from the Frio by 1st order seal. The upper and lower Vicksburg compartments exhibit different pressure regimes and are separated from each other by 2nd order seals. Intra-compartment seals are 3rd type seals which subdivide the major compartment into smaller ones.
3. Chromatic zones on FMI logs reflect specific petrographic and petrophysical properties. White color bands represent the highest relative resistivity rocks. These are calcite- and/or silica-cemented sandstone with low porosity (<8%) and

permeability (<0.003 md). Yellow bands represent sandstone with high porosity (average 21%) and higher permeability (average 0.16 md). Orange bands are sandstone with high porosity (average 18%) and lower permeability (0.06 md).

4. Capillary pressure measurements can be used to distinguish reservoirs from seal intervals. The yellow chromatic bands on FMI exhibit low displacement pressures (Pd) on capillary pressure curve. White chromatic bands that form intra-formation seals, can be identified by high injection, displacement pressures and sealing capacity.
5. Regional seals may be recognized in sample strings taken from well cuttings. Integration of high resolution logs, FMI, capillary pressure data and fluid inclusion stratigraphy may be the most suitable method in recognizing reservoirs and seal intervals.
6. Seal zones may be identified using fluid inclusion stratigraphy (FIS). Intra-reservoir seals usually contain abundant fluid inclusions, both aqueous and hydrocarbon due to extensive cementation.

REFFERENCES

Al-Shaieb, Z., J. Puckette, A. A. Abdalla, V. Tigert, and P. J. Ortoleva, The banded character of pressure seals: Basin Compartments and Seals AAPG Memoir, v. 61, 1994, p. 351-367.

Al-Shaieb, Z., J. Puckette, P. Blubaugh, P. Deyhim and H. Li, "Identification of reservoir and seal facies in the Vicksburg Formation, TCB field, Kleberg County, Texas", Topical Report to Gas Research Institute, Document No. GRI- 98/0240, 2000.

Al-Shaieb, Z., J. Puckette, P. Blubaugh, P. Deyhim and H. Li, Characterization of the low-contrast 9900-ft sandstone, Vicksburg Formation, TCB field, Kleberg County, Texas: Topical Report to Gas Research Institute, Document No. GRI-98/0240, 1998.

Coleman, J. M. C., Depositional systems and tectonic/eustatic history of the Oligocene Vicksburg episode of the Northern Gulf Coast: The University of Texas at Austin, Ph.D. dissertation, 1990.

Combes, J. M., The Vicksburg Formation of Texas: Depositional systems Distribution, Sequence Stratigraphy, and Petroleum Geology: AAPG Bull, v. 77, no. 11, 1993, p. 1942-1970.

Hall, D., Applying Fluid Inclusions to Petroleum Exploration and Production: Fluid Inclusion Technologies, Inc., 1999.

Halliburton, "Electrical Micro Imaging Service—Discover what you are missing", 1997.

Han, J. H., 1981, Genetic stratigraphy and associated growth structures of the Vicksburg Formation, South Texas: Ph.D. dissertation, University of Texas, Austin, Texas.

Hansen, S. M., T. Feet, Identification and evaluation of turbidite and other deepwater sands using open hole logs and borehole images, Fine-grained Turbidite Systems: AAPG Memoir v.72/SEPM Special Publication No. 68, 1999, p. 319-338.

International Oil Scouts Association, International Oil and Gas Development Yearbook, Review of 1995 Production, v. 66, 1997, 1071p.

Jennings, J. B., Capillary Pressure Techniques: Application to Exploration and Development: AAPG Bulletin v. 71, 1987, p. 1196-1209.

Loucks, R.G., D. L. Richmann and K. D. Milliken " Factors controlling Reservoir Quality in Tertiary Sandstones and Their Significance to Geopressured Geothermal Production", 1981, Bureau of Economic Geology—University of Texas at Austin.

Morton, Robert A., T. E. Ewing, and N. Tyler, "Continuity and Internal Properties of Gulf Coast Sandstones and Their Implication for Geopressured Fluid Production", Bureau of Economic Geology, University of Texas at Austin, 1983.

Nanz, R. H. Jr., "Genesis of Oligocene sandstone reservoirs, Seelingson Field, Jim Wells and Kelberg Counties, Texas", AAPG Bulletin, v. 38, 1954, p. 96-117.

Petroleum Information/Dwights, Natural Gas Well Production Histories, 1999.

Schlumberger, "FMI"—Fullbore Formation MicroImager", Pamphlet SMP-5145/M-090253. Houston: Schlumberger Wireline & Testing, 1992.

Shelton, J. W., "Models of sand and sandstone deposits: a methodology for determining sand genesis and trend", Oklahoma Geol. Survey Bulletin, v. 118, 1973, p. 30-32.

Sneider, R.M., and J. T. Kulha, Low-resistivity, low contrast productive sands, workshop, 1995.

Taylor, D. A., and Z. Al-Shaieb, Oligocene Vicksburg sandstones of the Tijerina-Canales-Blucher field: a south Texas jambalaya; Gulf Coast Association of Geological Societies Transactions, Vol. 36, 1986, p. 315-339.

Tigert, V., and Z. Al-Shaieb, Pressure seals: their diagenetic banding patterns: Earth-Science Reviews, v. 29, 1990, p. 227-240.

Williamson, J. D., Gulf Coast Cenozoic history: G.C.A.G.S. Transactions, v. 9, 1959, p. 15-29.

APPENDICES

APPENDIX A

CORE PETROLOGIC LOGS

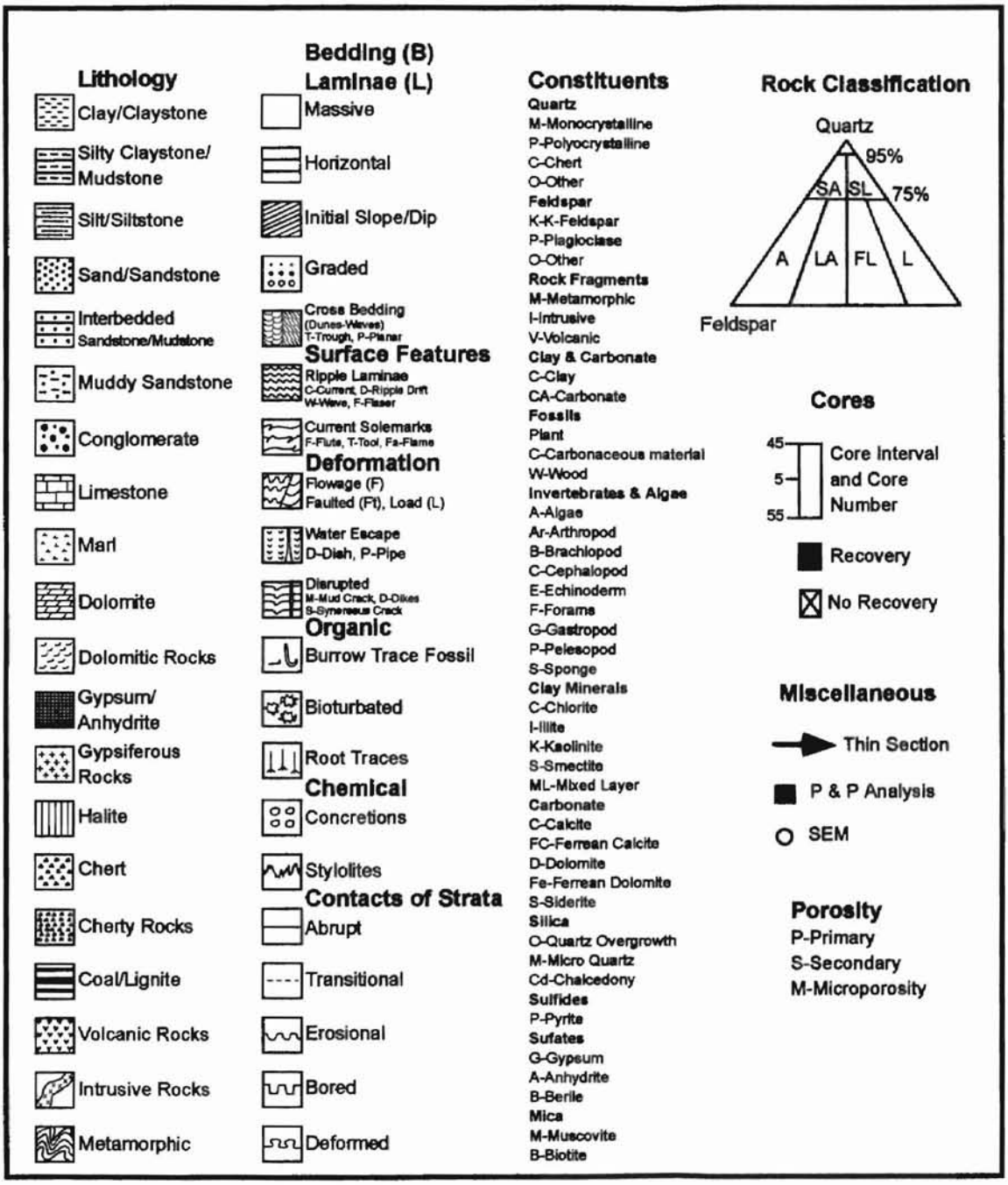
Lithology
Clay/Claystone
Silty Claystone/ Mudstone
Silt/Siltstone
Sand/Sandstone
Interbedded Sandstone/Mudstone
Muddy Sandstone
Conglomerate
Limestone
Marl
Dolomite
Dolomitic Rocks
Gypsum/ Anhydrite
Gypsiferous Rocks
Halite
Chert
Cherty Rocks
Coal/Lignite
Volcanic Rocks
Intrusive Rocks
Metamorphic
Bedding (B)
Laminae (L)
Massive
Horizontal
Initial Slope/Dip
Graded
Cross Bedding
(Dunes-Waves)
T-Trough, P-Planar
Surface Features
Ripple Laminae
C-Current, D-Ripple Drift
W-Wave, F-Flaser
Current Solemarks
F-Flute, T-Tool, Fe-Flame
Deformation
Flowage (F)
Faulted (Ft), Load (L)
Water Escape
D-Dish, P-Pipe
Disrupted
M-Mud Crack, D-Dikes
S-Synereses Crack
Organic
Burrow Trace Fossil
Bioturbated
Root Traces
Chemical
Concretions
Stylolites
Contacts of Strata
Abrupt
Transitional
Erosional
Bored
Deformed
Constituents
Quartz
M-Monocrystalline
P-Polyocrystalline
C-Chert
O-Other
Feldspar
K-K-Feldspar
P-Plagioclase
O-Other
Rock Fragments
M-Metamorphic
I-Intrusive
V-Volcanic
Clay & Carbonate
C-Clay
CA-Carbonate
Fossils
Plant
C-Carbonaceous material
W-Wood
Invertebrates & Algae
A-Algae
Ar-Arthropod
B-Brachiopod
C-Cephalopod
E-Echinoderm
F-Forams
G-Gastropod
P-Pelesopod
S-Sponge
Clay Minerals
C-Chlorite
I-Illite
K-Kaolinite
S-Smectite
ML-Mixed Layer
Carbonate
C-Calcite
FC-Ferroan Calcite
D-Dolomite
Fe-Ferroan Dolomite
S-Siderite
Silica
O-Quartz Overgrowth
M-Micro Quartz
Cd-Chalcedony
Sulfides
P-Pyrite
Sufates
G-Gypsum
A-Anhydrite
B-Berile
Mica
M-Muscovite
B-Biotite
Rock Classification
Quartz
95%
75%
SA
SL
A
LA
FL
L
Feldspar
Cores
45
5
55
Core Interval and Core Number
Recovery
No Recovery
Miscellaneous
Thin Section
P & P Analysis
SEM
Porosity
P-Primary
S-Secondary
M-Microporosity

COMPANY Oryx/Kerr-McGee

WELL NAME/ LOCATION A. T. Canales #85, Kleberg County, TX

PETROLOGIC LOG

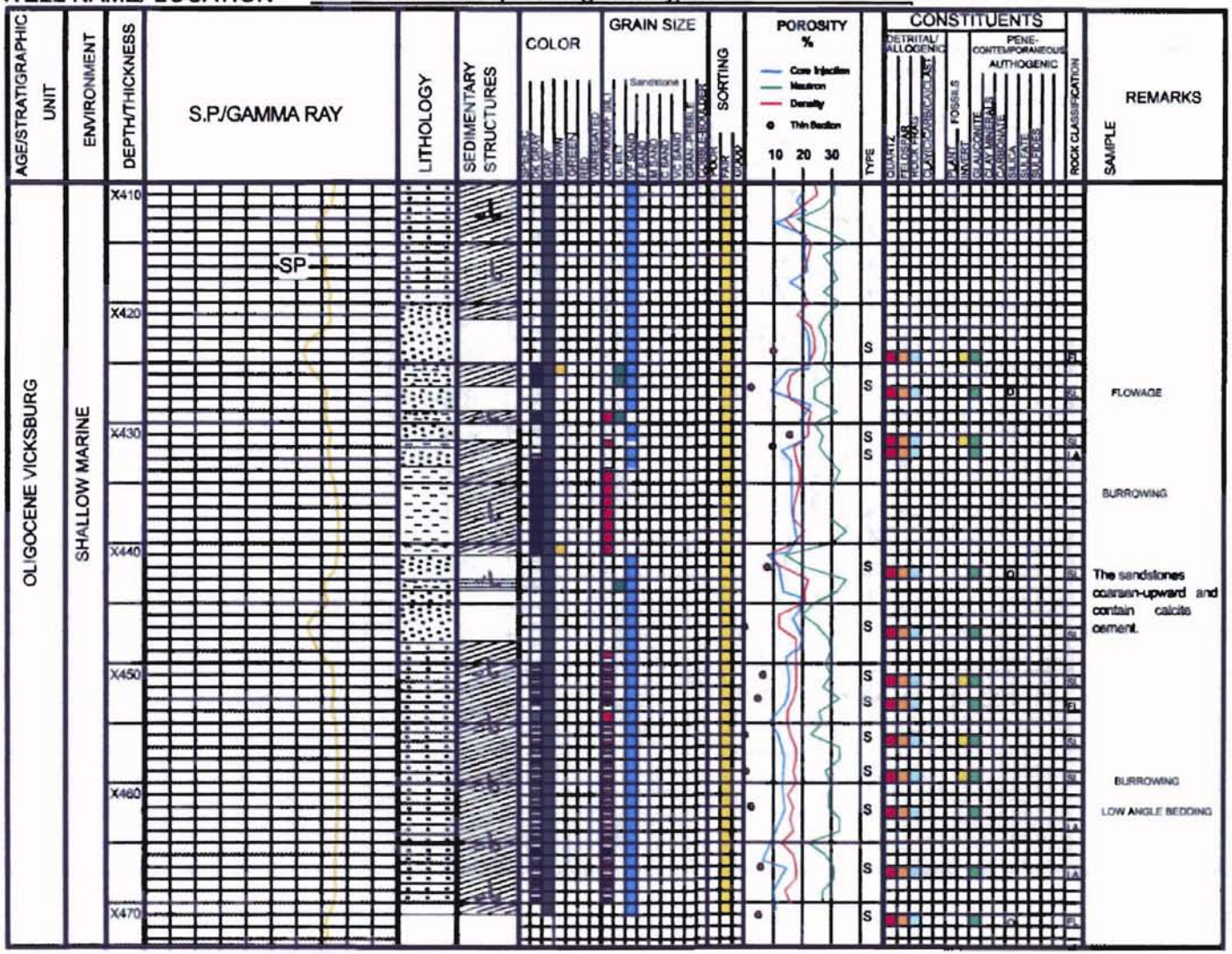

COMPANY Oryx/Kerr-McGee

WELL NAME/ LOCATION A. T. Canales #81, Kleberg County, TX

PETROLOGIC LOG

...PHIC	...ENT	...IESS				COLOR	GRAIN SIZE	...E	POROSITY %	CONSTITUENTS		
										DETRITAL/ ALLOGENIC	PENE- CONTEMPORANEOUS	

COMPANY Oryx/Kerr-McGee

WELL NAME/ LOCATION A. T. Canales #81, Kleberg County, TX

PETROLOGIC LOG

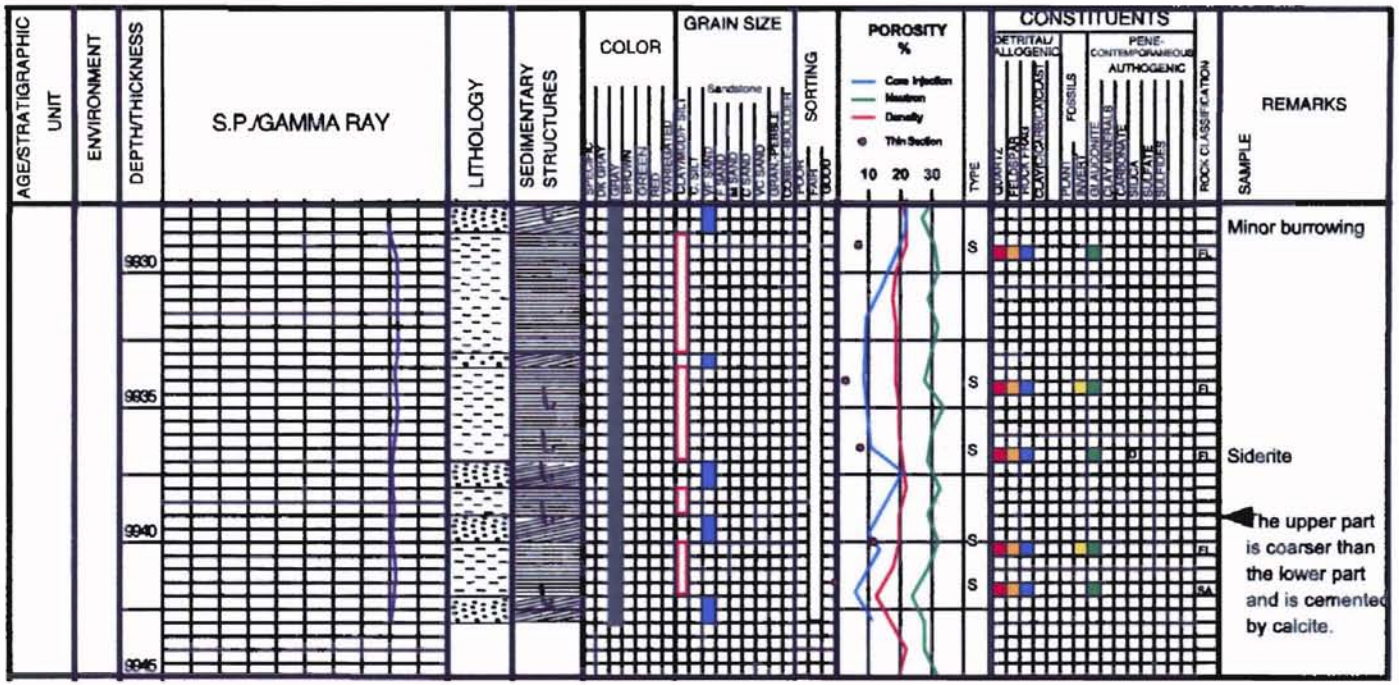

APPENDIX B

CORE PHOTOGRAPHS

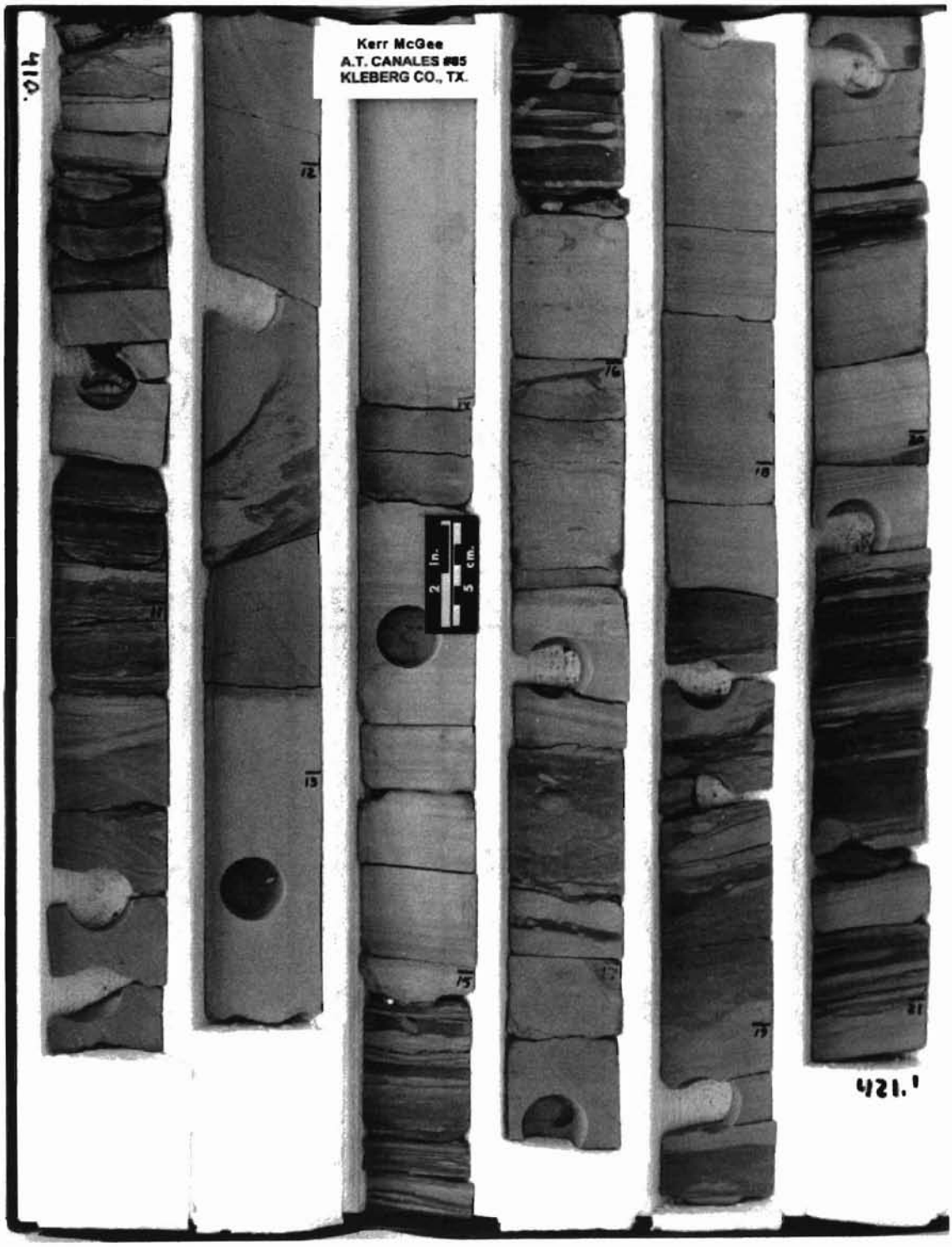
Kerr McGee
A.T. CANALES #85
KLEBERG CO., TX.
410.
421.'
2 in.
5 cm.

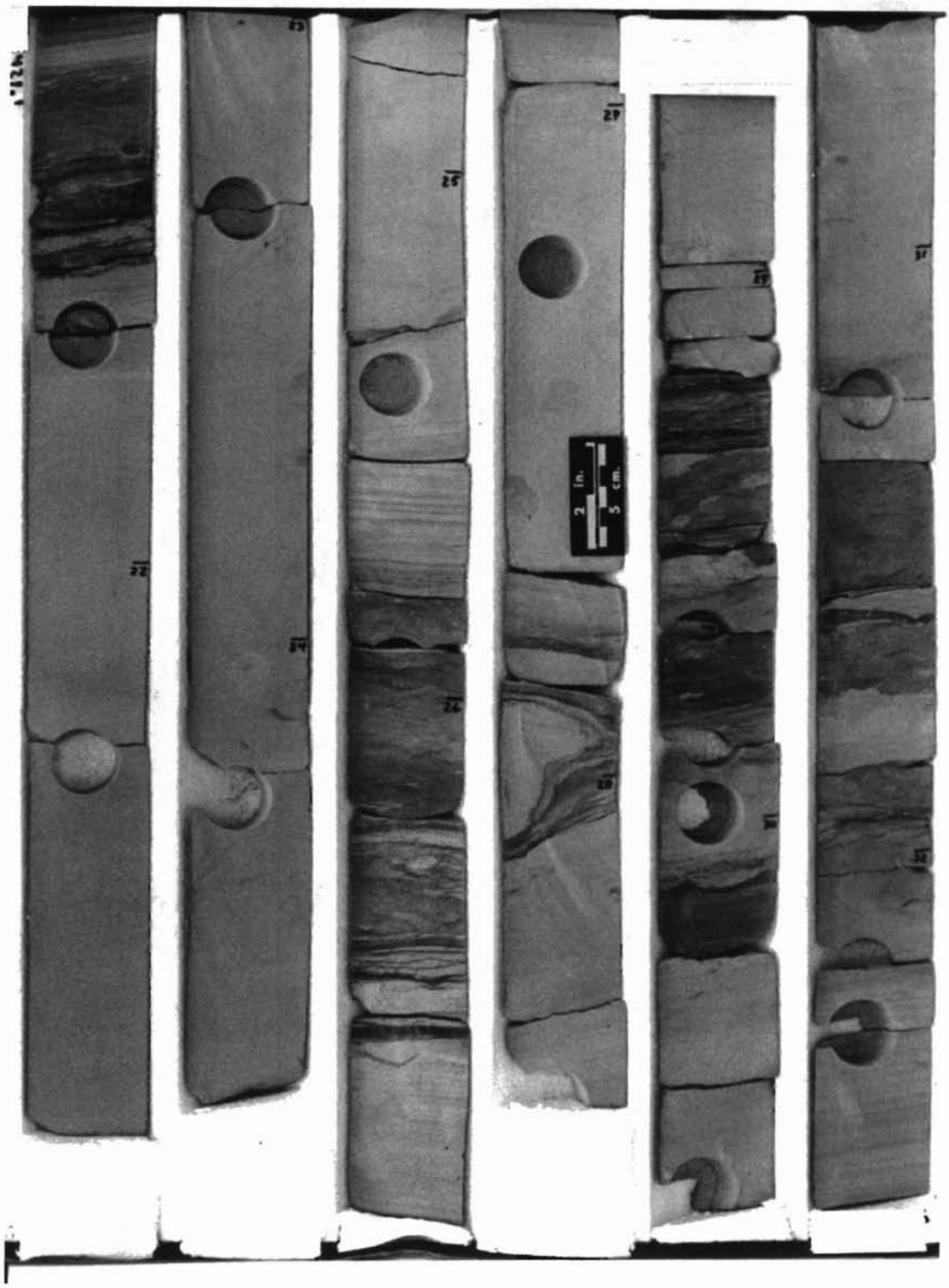
2 in.
5 cm.

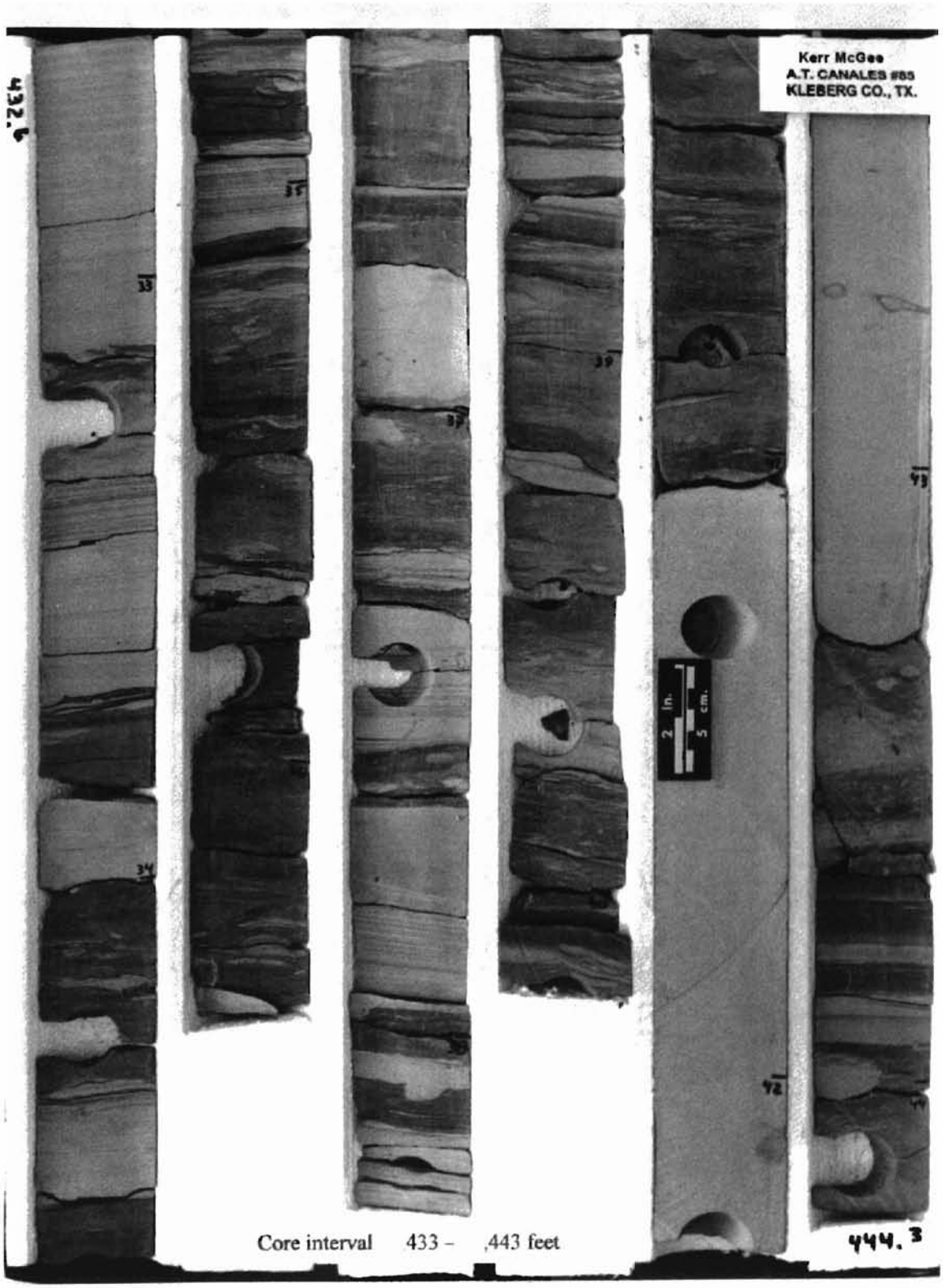
Kerr McGee
A.T. CANALES #85
KLEBERG CO., TX.
2 in.
5 cm.
Core interval 433 – ,443 feet
444.3

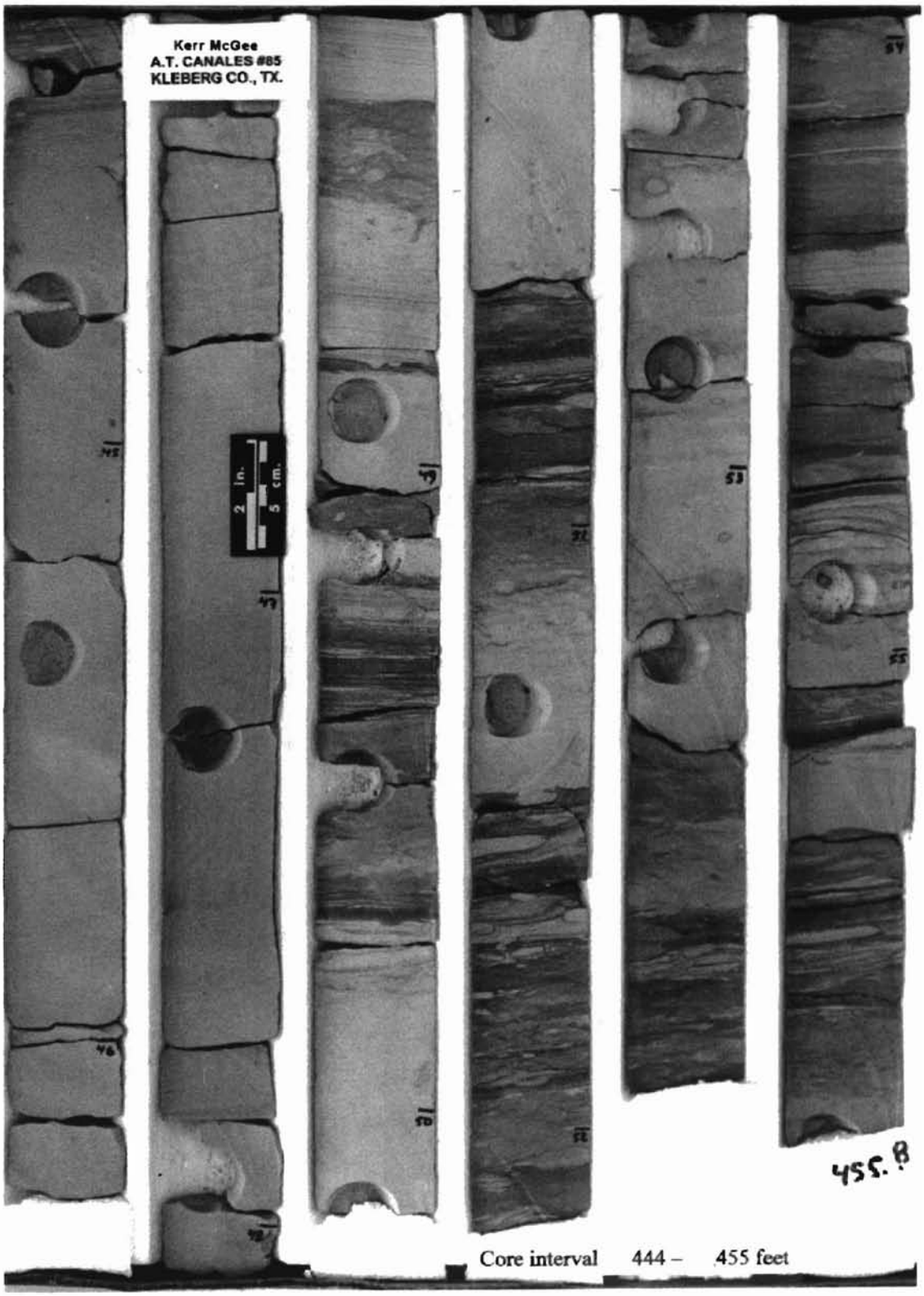

Core interval 444 – 455 feet

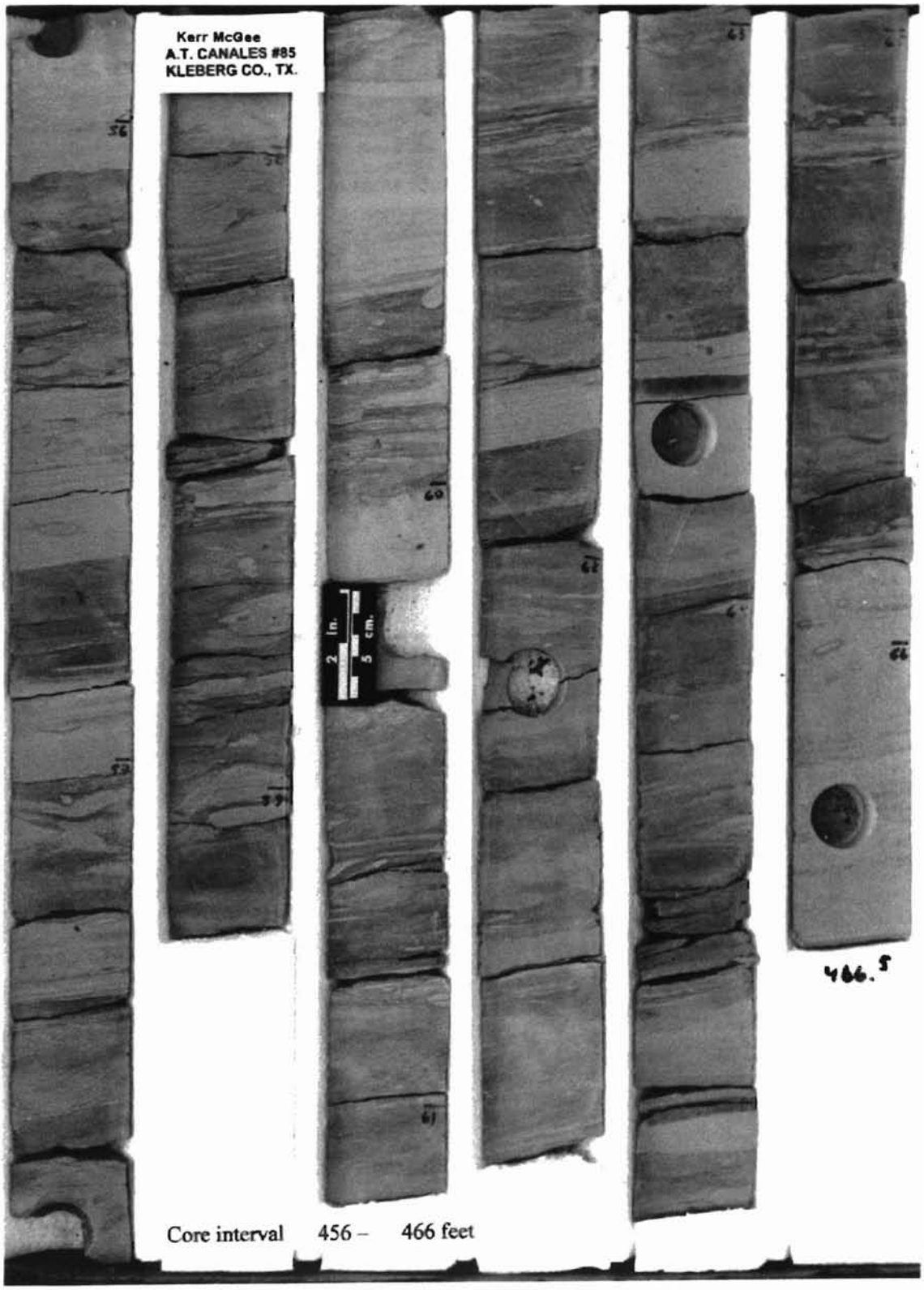
Kerr McGee
A.T. CANALES #85
KLEBERG CO., TX.
2 in.
5 cm.
466.5
Core interval 456 – 466 feet

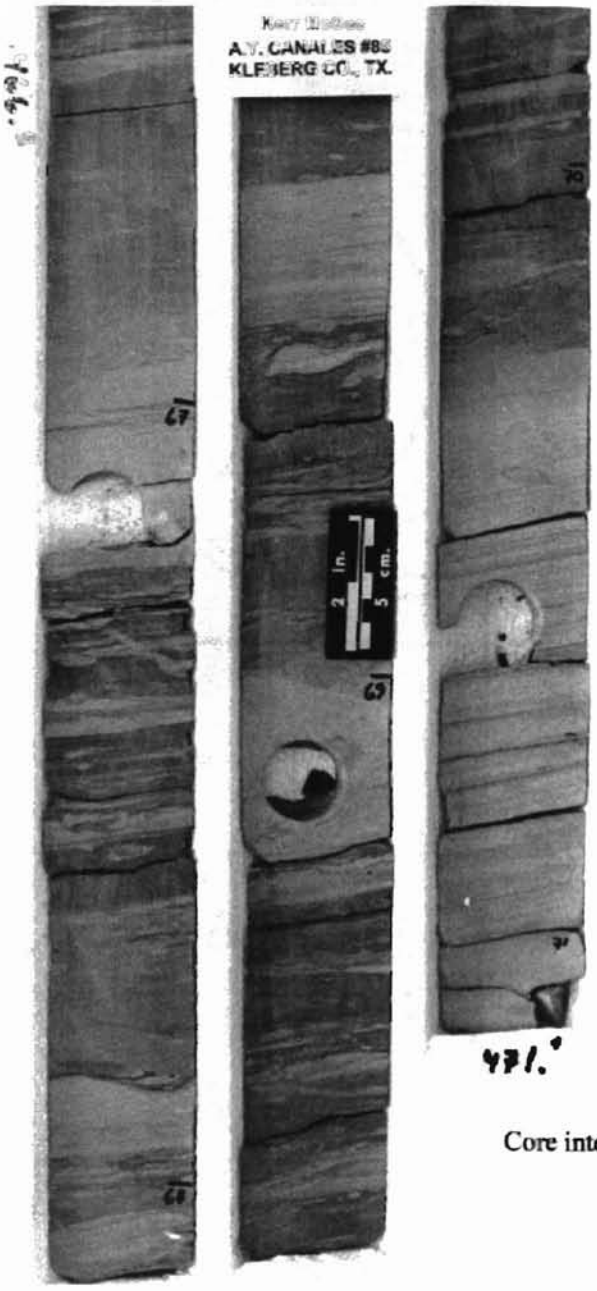

Core interval 467 – 471 feet

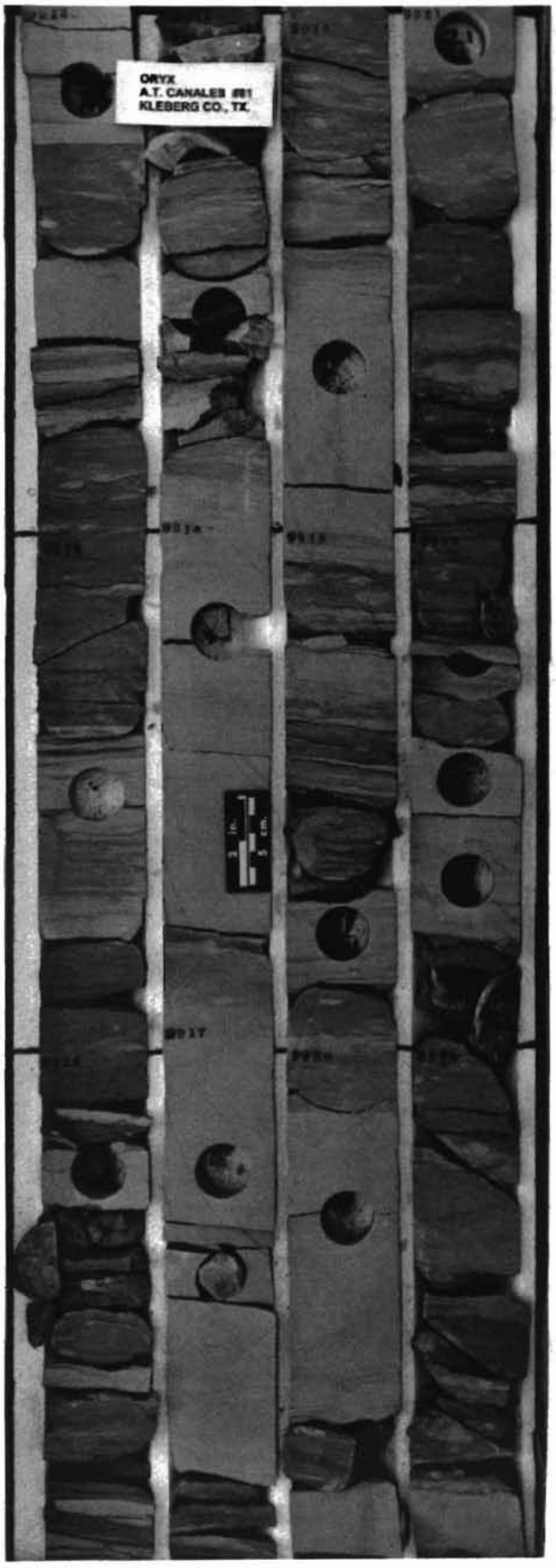

Core interval 9,912 – 9,923 feet

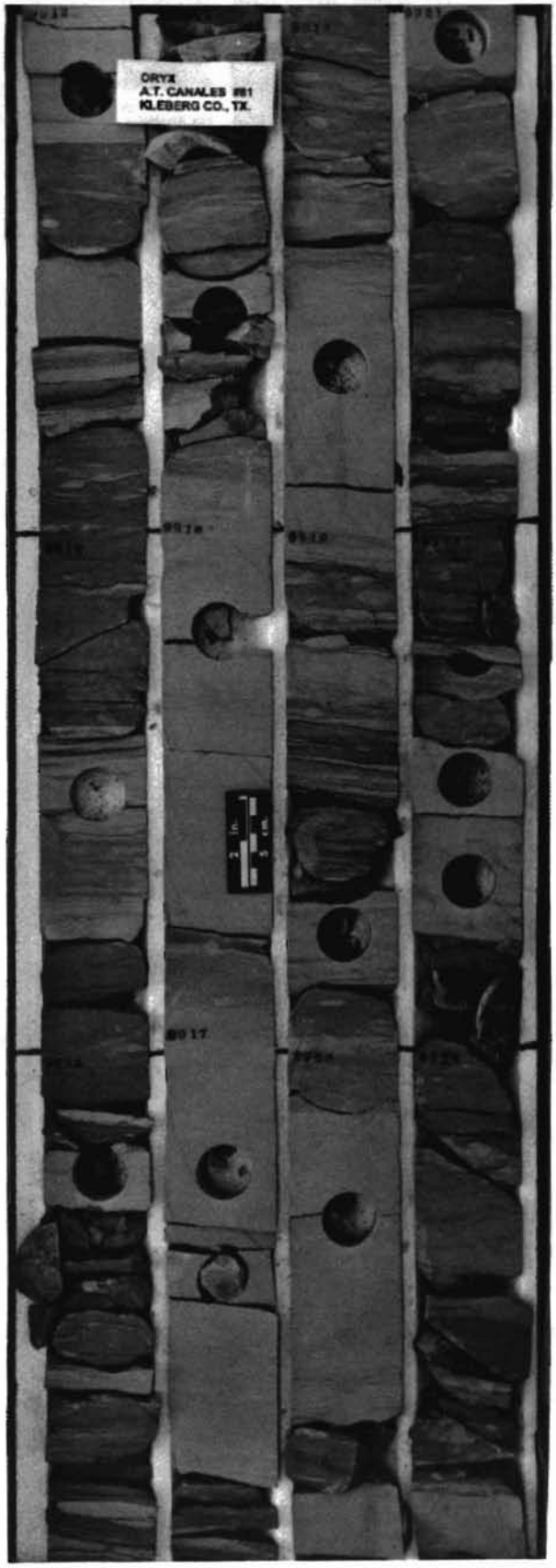

Core interval 9,912 – 9,923 feet

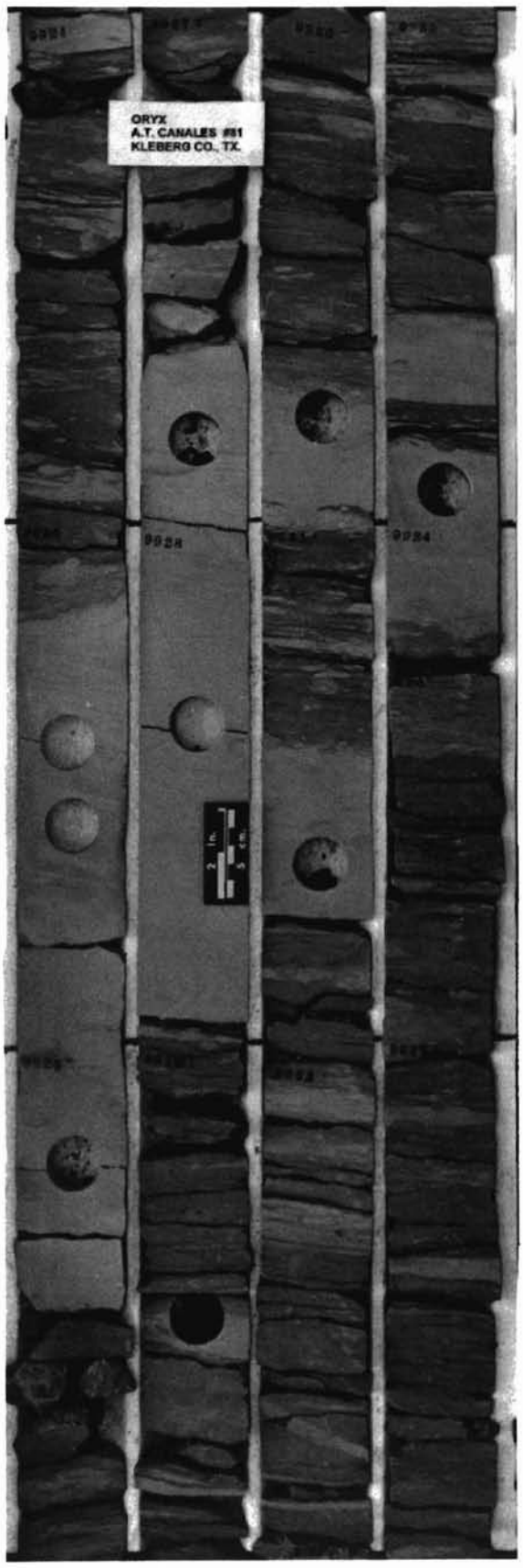

Core interval 9,924 – 9,935 feet

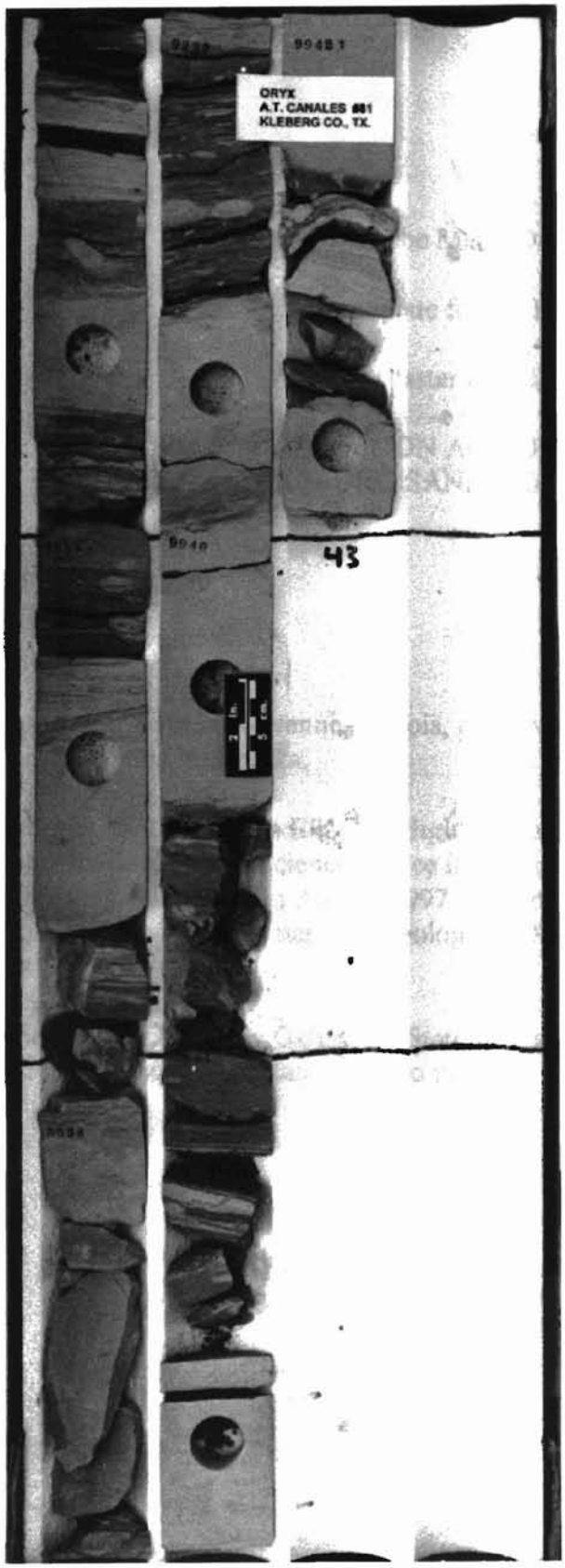

Core interval 9,936 – 9,942 feet

VITA

Phebe Marie Deyhim

Candidate for the Degree of

Master of Science

Thesis: COMPARTMENTALIZATION AND OVERPRESSURING OF THE OLIGOCENE VICKSBURG SANDSTONE, TCB FIELD, KLEBERG COUNTY, TEXAS

Major Field: Geology

Biographical:

Personal Data: Born in Kewenne, Illinois, on November 7, 1974, the daughter of Bruce and Rozanne Gruszeczka.

Education: Graduated from Elk City High School, Elk City, Oklahoma in May 1993; received Bachelor of Science degree in Geology from Oklahoma State University, Stillwater, Oklahoma in August 1997. Completed the requirements for the Master of Science degree with a major in Geology at Oklahoma State University in December 2000.

Experience: Employed by Oklahoma State University Department of Geology as a graduate research assistant, 1997 to present.